PACIFIC EARTHQUAKE ENGINEERING RESEARCH CENTER

Shear Wave Velocity as a Statistical Function of Standard Penetration Test Resistance and Vertical Effective Stress at Caltrans Bridge Sites

Scott J. Brandenberg
University of California, Los Angeles

Naresh Ballana
University of California, Los Angeles

Thomas Shantz
California Department of Transportation, Sacramento

PEER 2010/03
JUNE 2010

Technical Report Documentation Page

1. Report No.	2. Government Accession No.	3. Recipient's Catalog No.
PEER Report 2010/03		

4. Title and Subtitle	5. Report Date
Shear Wave Velocity as a Statistical Function of Standard Penetration Test Resistance and Vertical Effective Stress at Caltrans Bridge Sites	June 2010
	6. Performing Organization Code
7. Author(s) Scott J. Brandenberg, Naresh Bellana, and Thomas Shantz	8. Performing Organization Report No.
9. Performing Organization Name and Address Pacific Earthquake Engineering Research Center 325 Davis Hall MC 1792 University of California Berkeley, CA 94720	10. Work Unit No. (TRAIS)
	11. Contract or Grant No.
12. Sponsoring Agency Name and Address California Department of Transportation Engineering Service Center 1801 30th St., West Building MS-9 Sacramento, CA 95807	13. Type of Report and Period Covered Final technical report 1/1/2009–12/31/2009
	14. Sponsoring Agency Code

15. Supplementary Notes

This study was sponsored by the Pacific Earthquake Engineering Research Center's Program of Applied Earthquake Engineering Research of Lifelines Systems supported by the California Department of Transportation and the Pacific Gas and Electric Company.

16. Abstract

Shear wave velocity, V_s, is defined as a statistical function of SPT blow count, N_{60}, and vertical effective stress, σ_v', using a data set collected at various California bridge sites. At each site, V_s measurements were recorded by suspension logging in the same borehole in which N_{60} was measured. Regression analysis was used to derive statistical relations for sand, silt, and clay soil types. The relation between V_s and N_{60} is shown to depend strongly on σ_v', since V_s and N_{60} normalize differently with overburden, which has been mostly omitted in previously published correlations. A random effects regression model is used to separate the error into intra- and interboring terms. Interboring errors are shown to depend weakly on geologic age. The average shear wave velocity in the upper 30 m, V_{s30}, is computed directly from the suspension logs and compared with V_{s30} computed from the statistical relations. The relations are shown to provide unbiased estimates of V_{s30}, with standard deviation of the error equal to the standard deviation of the interboring error term. Ground motion prediction equations require V_{s30} as an input parameter, and the statistical relations may be useful for estimating V_{s30} at sites where only penetration resistance data are available. The proposed relations should not substitute for more accurate geophysical measurements when predicted ground motions are sensitive to the uncertainty in V_{s30}, but may be useful for identifying whether geophysical measurements should be performed to better refine the V_{s30} estimate.

17. Key Words	18. Distribution Statement		
Shear wave velocity, blow count, correlation, regression, effective stress	Unlimited		
19. Security Classif. (of this report)	**20. Security Classif. (of this page)**	**21. No. of Pages**	**22. Price**
Unclassified	Unclassified	84	

Form DOT F 1700.7 (8-72) **Reproduction of completed page authorized**

Shear Wave Velocity as a Statistical Function of Standard Penetration Test Resistance and Vertical Effective Stress at Caltrans Bridge Sites

Scott J. Brandenberg
Department of Civil and Environmental Engineering
University of California, Los Angeles

Naresh Bellana
Department of Civil and Environmental Engineering
University of California, Los Angeles

Thomas Shantz
Caltrans Division of Research and Innovation
California Department of Transportation, Sacramento

PEER Report 2010/03
Pacific Earthquake Engineering Research Center
College of Engineering
University of California, Berkeley

June 2010

ABSTRACT

Shear wave velocity, V_s, is defined as a statistical function of SPT blow count, N_{60}, and vertical effective stress, σ_v', using a data set collected at various California bridge sites. At each site, V_s measurements were recorded by suspension logging in the same borehole in which N_{60} was measured. Regression analysis was used to derive statistical relations for sand, silt, and clay soil types. The relation between V_s and N_{60} is shown to depend strongly on σ_v', since V_s and N_{60} normalize differently with overburden, which has been mostly omitted in previously published correlations. A random effects regression model is used to separate the error into intra- and interboring terms. Interboring errors are shown to depend weakly on geologic age. The average shear wave velocity in the upper 30 m, V_{s30}, is computed directly from the suspension logs and compared with V_{s30} computed from the statistical relations. The relations are shown to provide unbiased estimates of V_{s30}, with standard deviation of the error equal to the standard deviation of the interboring error term. Ground motion prediction equations require V_{s30} as an input parameter, and the statistical relations may be useful for estimating V_{s30} at sites where only penetration resistance data are available. The proposed relations should not substitute for more accurate geophysical measurements when predicted ground motions are sensitive to the uncertainty in V_{s30}, but may be useful for identifying whether geophysical measurements should be performed to better refine the V_{s30} estimate.

ACKNOWLEDGMENTS

This study was sponsored by the Pacific Earthquake Engineering Research Center's (PEER's) Program of Applied Earthquake Engineering Research of Lifelines Systems supported by the California Department of Transportation and the Pacific Gas and Electric Company. Any opinions, findings, conclusions or recommendations expressed in this material are those of the authors and do not necessarily reflect those of the sponsors.

The shear wave velocity data set was developed by Bill Owen, Geophysics and Geology Branch, California Department of Transportation, and Alan Yong, Geophysicist, United States Geological Survey. The authors would like to thank UCLA undergraduate student Barr Levy for helping to digitize the boring logs from the as-built drawings.

The report contains content from a paper accepted for publication in *Soil Dynamics and Earthquake Engineering.* The content is published with permission from Elsevier. The citation for the paper is Brandenberg, S.J., Bellana, N., and Shantz, T. (2010). "Shear wave velocity as function of standard penetration test resistance and vertical effective stress at California bridge sites." *Soil Dyn. Earthquake Eng.* Elsevier, doi: 10.1016/j.soildyn.2010.04.014. Accepted for publication on April 12, 2010; available online May 26, 2010.

CONTENTS

ABSTRACT .... **iii**

ACKNOWLEDGMENTS .... **iv**

TABLE OF CONTENTS .... **v**

LIST OF FIGURES .... **vii**

LIST OF TABLES .... **xi**

1 INTRODUCTION **1**

2 INFLUENCE OF OVERBURDEN STRESS **5**

3 DATA SET **9**

4 STATISTICAL REGRESSION **15**

4.1 Relative Influence of N_{60} and σ_v' on Regression 17

4.2 Overburden Scaling Parameters Implied by Regression Constants 18

4.3 Intraboring Residuals 19

4.4 Interboring Residuals 22

5 CALCULATION OF V_{S30} FROM BLOW COUNT DATA **23**

6 DISCUSSION **25**

6.1 Error Caused by Neglecting Overburden Influence 25

6.2 Comparison with Other Published Relations 27

6.3 Appropriate Use of Proposed Relations 28

7 CONCLUSIONS **29**

REFERENCES **31**

APPENDIX A: PROFILES OF N_{60}, σ_V', AND V_S USED IN REGRESSION STUDY

LIST OF FIGURES

Fig. 2.1 Example of influence of overburden scaling on relation between V_s and N_{60} 7

Fig. 3.1 Map of bridge locations to develop data set 10

Fig. 3.2 Distribution of soil type for recorded N_{60}, $\overline{V_s}$ pairs............11

Fig. 3.3 Example plots of V_s, N_{60}, weights, and $\overline{V_s}$ for a boring at the Noyo River Bridge....12

Fig. 4.1 Results of regression equations for (a) sand, (b) silt, and (c) clay, with trend lines corresponding to the mean and $\pm 1\sigma$ for σ_v' and N_{60}. 17

Fig. 4.2 Intraboring residuals, ε, versus N_{60} and σ_v' for (a) sand, (b) silt, and (c) clay. Plots of ε vs. σ_v' include lines showing $\pm 1\sigma$ for ε. 20

Fig. 4.3 Quantile-quantile plots showing degree to which intraboring residuals are normally distributed............21

Fig. 4.4 Interboring residuals, η, as function of surface geologic epoch............22

Fig. 6.1 Residuals, ε^*, versus σ_v' for ordinary least squares regression that neglects the influence of σ_v' on relation between V_s and N_{60}. Bias is evident based on the slope of the least squares regression lines............26

Fig. 6.2 Existing correlations from literature superposed on data set used in this study.........27

Fig. A.1 (a) Bridge no. 10-0298, boring no. 98-4 (abut.4), (b) Bridge no. 10-0298, boring no. 96-2, (c) Bridge no. 10-0298, boring no. 96-3............ A-2

Fig. A.2 (a) Bridge no. 10-0298, boring no. 98-10 (abut 1) (b) Bridge no. 28-0253R, boring no. 94B1R (Pier 9) (c) Bridge no. 28-0153R, boring no. 96-5 (Pier 8) A-3

Fig. A.3 (a) Bridge no. 28-1053R, boring no. 95B13R (Pier 7) (b) Bridge no. 28-1053R, boring no. 96-4 (Pier 7) (c) Bridge no. 28-1053R, boring no. 95-12 (Pier 5). A-4

Fig. A.4 (a) Bridge no. 28-0352L, boring no. 96B-29 (b) Bridge no. 28-0352L, boring no. 95-2 (Pier 3) (c) Bridge no. 28-0352L, boring no. 95-1 (Pier 4)............ A-5

Fig. A.5 (a) Bridge no. 28-0352L, boring no. 96B-37 (b) Bridge no. 28-0100, boring no. 96-2 (Piers 10 and 11) (c) Bridge no. 28-0100, boring no. 96-5 (Piers 31/32) A-6

Fig. A.6 (a) Bridge no. 28-0100, boring no. 96-7 (Pier 8) (b) Bridge no. 28-0100, 95-7 (Pier 21) (c) Bridge no. 28-0100, boring no. 95B4R (Pier 25)............ A-7

Fig. A.7 (a) Bridge no. 28-0100, boring no. 95B5R (Pier 35) (b) Bridge no. 28-0100, boring no. 95B2R (Pier 32/33) (c) Bridge no. 28-0100, boring no. 95B3R/95B9R (Pier 34) A-8
Fig. A.8 (a) Bridge no. 28-0100, boring no. 95-10 (Pier 47) (b) Bridge no. 28-0100, boring no. 95-11 (Pier 48) (c) Bridge no. 28-0100, boring no. 95B1R (Pier 58) A-9
Fig. A.9 (a) Bridge no. 33-0025, boring no. B6 (Pier E19) (b) Bridge no. 33-0025, boring no. B-7 (Pier E10) (c) Bridge no. 34-0003, boring no. 95-14 (Pier W6) A-10
Fig. A.10 (a) Bridge no. 34-0003, boring no. 95-12 (Pier W4) (b) Bridge no. 34-0003, boring no. 95-11 (Pier W3) (c) Bridge no. 34-0003, boring no. 95-10 (Pier W2) A-11
Fig. A.11 (a) Bridge no. 34-0003, boring no. 95-5 (Pier A) (b) Bridge no. 34-0003, boring no. 95-4 (c) Bridge no. 34-0003, boring no. 95-6........ A-12
Fig. A.12 (a) Bridge no. 34-0004, boring no. B95-2 (b) Bridge no. 34-0004, boring no. B95-3 (c) Bridge no. 34-0077, boring no. 01-B2. .... A-13
Fig. A.13 (a) Bridge no. 34-0077, boring no. 01-05 (b) Bridge no. 34-0077, boring no. 01-08 (c) Bridge no. 34-0077, boring no. 01-11........ A-14
Fig. A.14 (a) Bridge no. 37-0853, boring no.98-1 (Pier 4) (b) Bridge no. 38-0583, boring no. 98-4 (Bent 7) (c) Bridge no. 49-0014L, boring no.98-1 (Abut 1). A-15
Fig. A.15 (a) Bridge no. 51-0139, boring no. 98-1 (Abut 1) (b) Bridge no. 52-0443, boring no. 99-1 (c) Bridge no. 53-1471, boring no. 95B5R. A-16
Fig. A.16 (a) Bridge no. 53-1471, boring no. 95B4R (b) Bridge no. 53-1471, boring no. 95B1R (c) Bridge no. 53-1471, boring no. 95B2R........ A-17
Fig. A.17 (a) Bridge no. 53-1471, boring no. 95B3R (b) Bridge no. 53-2272, boring no. B-1 (c) Bridge no. 53-2790R, boring no. B-6........ A-18
Fig. A.18 (a) Bridge no. 53-2794R, boring no. B-1 (b) Bridge no. 53-2795F, boring no. 94-21 (c) Bridge no. 53-2796F, boring no. 94-30 .... A-19
Fig. A.19 (a) Bridge no. 54-1110R, boring no. 98-1 (Abut 1) (b) Bridge no. 54-1110R, boring no. 98-6 (Abut 8) (c) Bridge no. 57-0857, boring no. 96-52 (Bents R48 and 49) A-20
Fig. A.20 (a) Bridge no. 57-0857, boring no. 96-17 (Abut S48) (b) Bridge no. 57-0857, boring no. 95-2 (Pier 33) (c) Bridge no. 57-0857, boring no. 96-16 (Bent 41F,R) A-21

Fig. A.21 (a) Bridge no. 57-0857, boring no. 96-29 (b) Bridge no. 57-0857, boring no. 96-53R (c) Bridge no. 57-0857, boring no. 96-66 .... A-22

Fig. A.22 (a) Bridge no. 57-0857, boring no. 96-65 (b) Bridge no. 57-0857, boring no. 96-35 (Toll Plaza North West) (c) Bridge no. 57-0857, boring no. 96-34 (Toll Plaza South East). A-23

Fig. A.23 (a) Bridge no. 57-0857, boring no. 96-21 (b) Bridge no. 57-0857, boring no. 96-28 (c) Bridge no. 57-0857, boring no. 96-60.. A-24

Fig. A.24 (a) Bridge no. 57-0857, boring no. 96-68R (b) Bridge no. 57-0857, boring no. 96-56 (c) Bridge no. 57-0857, boring no. 96-67.. A-25

Fig. A.25 (a) Bridge no. 57-0857, boring no. 96-54 (b) Bridge no. 57-0857, boring no. 96-55 (c) Bridge no. 57-0857, boring no. 96-59.. A-26

Fig. A.26 (a) Bridge no. 57-0857, boring no. 96-58 (b) Bridge no. 57-0857, boring no. 96-57 (c) Bridge no. 57-0857, boring no. 96-64.. A-27

Fig. A.27 (a) Bridge no. 58-0335RL, boring no. B5-01. .... A-28

LIST OF TABLES

Table 1.1 Some existing correlations presenting V_s as a function of SPT blow count, N 3
Table 3.1 Bridge sites utilized to develop database in this study 9
Table 3.2 Rod length correction factors...11
Table 3.3 Unit weights based on soil type position relative to groundwater..............................11
Table 4.1 Regression parameters. 16

1 Introduction

A key property required to effectively estimate the dynamic response of soil is the small-strain shear modulus, G_{max}, which is most often computed by measuring the shear wave velocity, V_s, and mass density, ρ, where $G_{max} = \rho V_s^2$. The importance of G_{max} has been widely recognized in ground motion prediction equations by implementation of site factors that modify ground motion based on the difference between a site V_s and a reference V_s [typically for rock, e.g., Choi and Stewart (2005)], or by direct incorporation of a V_s term in the ground motion regression equations. For example, the Next Generation Attenuation relations [Abrahamson and Silva (2008); Boore and Atkinson (2008); Campbell and Bozorgnia (2008); Chiou and Youngs (2008)] include V_{s30} as a constant required for ground motion prediction, where V_{s30} is the average shear wave velocity in the upper 30m. Geophysical measurements are now commonplace for geotechnical projects where vibrations are anticipated. However, geophysical measurements were not always commonplace, and older site investigations often lack geophysical measurements and provide only the geologic setting, stratigraphy, and penetration resistance (i.e., SPT blow counts or CPT resistance). Lack of geophysical measurements from older site investigations is particularly pertinent for state departments of transportation. For example, Caltrans owns about 13,000 bridges, most of which were constructed before 1970. As ground motion prediction equations have advanced to include V_s values as inputs, there is a need to estimate V_s at the older bridges based on available information to guide retrofit evaluations. Correlations between shear wave velocity and blow count, geologic setting, and site stratigraphy are therefore potentially useful at least as a screening tool for identifying a subset of bridges where geophysical measurements would be the most beneficial.

Numerous relations between SPT blow count, N, and V_s exist in the literature (Table 1.1). Early efforts utilized laboratory results to develop relations, which were subsequently refined as field measurement of V_s became more routine and data became available. The early correlations based on field data often involved blow counts that were not corrected for energy, rod length, or sampler inside diameter. Hence, it is impossible to know whether bias is introduced by hammer efficiency, non-standard samplers, etc. Furthermore, various methods of measuring V_s were utilized in the correlations, including cross-hole, seismic CPT, spectral analysis of surface waves (SASW), and suspension logging. These different methods provide very different resolutions for V_s measurements at different depths. For example, SASW uses progressively lower-frequency surface waves to measure shear wave velocity deeper in a profile, resulting in high spatial resolution near the surface and poorer resolution deep in the profile where the low-frequency waves average the properties of a large volume of soil. Crosshole methods and suspension logging methods use higher-frequency waves that average the properties of a much smaller volume of soil, though measurements cannot often be made at shallow depths. Penetration resistance measurements are also spatially averaged within a small volume of soil near the sampler, since the sampler is driven through 0.3 m of soil to obtain the blow count, and because the failure mechanism extends some distance above and below the sampler tip. However, this volume of soil is small enough that SPT is often considered a point measurement, and involves a spatial scale that is more comparable to suspension logging than to other methods for estimating V_s.

Table 1.1 summarizes relations from 28 different studies, with nearly every relation utilizing the functional form $V_s = A \cdot N^B$, where the constants A and B were determined by statistical regression of a data set. The N-values are typically not corrected for overburden stress, but sometimes are corrected for hammer energy, rod length, and sampler inside diameter, in which case N is replaced by N_{60}. Jafari et al. (2002) summarized more than 20 such relations [e.g., Ohta et al. (1978), Ohta and Goto (1978)], and more recently, relations of the same form have been proposed by Hasancebi and Ulusay (2006), and Dikmen (2009). A few relations have explored using various combinations of overburden-corrected values. Sykora and Koester (1988) evaluated a relation between V_s and $(N_1)_{60}$, and found the correlation to be poorer than the relation directly between V_s and N_{60} because both V_s and N_{60} vary with overburden stress, whereas $(N_1)_{60}$ does not. Andrus et al. (2004) correlated the overburden-corrected shear wave velocity with overburden-corrected blow count values using a functional form $V_{s1} = \beta_0 \cdot (N_1)_{60}^{\beta_1}$ for Holocene clean sands. This functional form is superior because it removes the effect of overburden, since both V_{s1} and $(N_1)_{60}$ are theoretically independent of overburden stress.

Table 1.1 Some existing correlations presenting V_s as a function of SPT blow count, N.

Author(s)	I.D.	All soils	Sand	Silt	Clay
Shibata (1970)	A	-	$V_s = 31.7\ N^{0.54}$	-	-
Ohba and Toriuma (1970)	B	$V_s = 84\ N^{0.31}$	-	-	-
Imai and Yoshimura (1975)	C	$V_s = 76\ N^{0.33}$	-	-	-
Ohta et al (1972)	D	-	$V_s = 87.2\ N^{0.36}$	-	-
Fujiwara (1972)	E	$V_s = 92.1\ N^{0.337}$	-	-	-
Ohsaki and Iwasaki (1973)	F	$V_s = 81.4\ N^{0.39}$	-	-	-
Imai et al (1975)	G	$V_s = 89.9\ N^{0.341}$	-	-	-
Imai(1977)	H	$V_s = 91\ N^{0.337}$	$V_s = 80.6\ N^{0.331}$	-	$V_s = 80.2\ N^{0.292}$
Ohta and Goto (1978)	I	$V_s = 85.35\ N^{0.348}$	-	-	-
Seed and Idriss (1981)	J	$V_s = 61.4\ N^{0.5}$	-	-	-
Imai and Tonouchi (1982)	K	$V_s = 96.9\ N^{0.314}$	-	-	-
Sykora and Stokoe (1983)	L	-	$V_s = 100.5\ N^{0.29}$	-	-
Jinan (1987)	M	$V_s = 116.1\ (N+0.3185)^{0.202}$	-	-	-
Okamoto et al (1989)	N	-	$V_s = 125\ N^{0.3}$	-	-
Lee (1990)	O	-	$V_s = 57.4\ N^{0.49}$	$V_s = 105.64\ N^{0.32}$	$V_s = 114.43\ N^{0.31}$
Athanasopoulos (1995)	P	$V_s = 107.6\ N^{0.36}$	-	-	$V_s = 76.55\ N^{0.445}$
Sisman (1995)	Q	$V_s = 32.8\ N^{0.51}$	-	-	-
Iyisan (1996)	R	$V_s = 51.5\ N^{0.516}$	-	-	-
Kanai (1966)	S	$V_s = 19\ N^{0.6}$	-	-	-
Jafari et al (1997)	T	$V_s = 22\ N^{0.85}$	-	-	-
Kiku et al (2001)	U	$V_s = 68.3\ N^{0.292}$	-	-	-
Jafari et al (2002)	V	-	-	$V_s = 22\ N^{0.77}$	$V_s = 27\ N^{0.73}$
Hasancebi and Ulusay (2006)	W	$V_s = 90\ N^{0.309}$	$V_s = 90.82\ N^{0.319}$	-	$V_s = 97.89\ N^{0.269}$
Ulugergerli and Uyanık (2007)	X	$^{a}V_{SU} = 23.291\ \mathrm{Ln}(N)+405.61$	-	-	-
Ulugergerli and Uyanık (2007)	Y	$^{b}V_{SL} = 52.9\ e^{-0.011N}$	-	-	-
Dikmen (2009)	Z	$V_s = 58\ N^{0.39}$	$V_s = 73\ N^{0.33}$	$V_s = 60\ N^{0.36}$	$V_s = 44\ N^{0.48}$
Pitilakis et al. (1999)	AA	-	$V_s = 145(N_{60})^{0.178}$	-	$Vs = 132(N_{60})^{0.271}$
Hasancebi and Ulusay (2006)	AB	$V_s = 104.79(N_{60})^{0.26}$	$V_s = 131(N_{60})^{0.205}$		$V_s = 107.63(N_{60})^{0.237}$

This study utilizes a data set collected at various California bridge sites to define V_s as a statistical function of N_{60} and vertical effective stress, σ_v'. At each site, V_s measurements were recorded by suspension logging in the same borehole in which N_{60} was measured. Random effects regression analysis is used to derive statistical relations for sand, silt, and clay soil types, including median predictions and standard deviations of interboring and intraboring error terms. The proposed relations are used to compute V_{s30} values, which are subsequently compared with those computed directly from the suspension logs.

2 Influence of Overburden Stress

Vertical effective stress, σ_v', is known to affect V_s and N_{60}, and the effect is often removed using an overburden correction factor [e.g., Skempton (1986); Sykora (1987)]. The resulting stress-corrected quantities, V_{s1} and $(N_1)_{60}$, are often correlated with relative density for sands, and perhaps their most common use is for liquefaction evaluation [e.g., Youd et al. (2001)]. Equations 2.1 and 2.2 are common overburden correction equations for N_{60} and V_s, where the exponents n and m are empirical constants that depend on soil type, cementation, and plasticity index.

$$(N_1)_{60} = \left(\frac{P_a}{\sigma_v'}\right)^n \cdot N_{60} \tag{2.1}$$

$$V_{s1} = \left(\frac{P_a}{\sigma_v'}\right)^m \cdot V_s \tag{2.2}$$

Regarding SPT blow count corrections, typical values are n=0.5 for sand and n=1.0 for clay. Regarding V_s corrections, Yamada et al. (2008) found that the exponent m is 0.25 for clean sands and can be as high as 0.5 for cohesive soil, depending on plasticity index. A typical ratio is therefore n/m = 2, though there are many reasons why this ratio may not hold for a particular soil. For example, cementation has been observed to affect small-strain behavior (i.e., V_s) more than large-strain behavior (i.e., N_{60}). DeJong et al. (2006) tested loose sand specimens cemented using calcite precipitated by bacteria and found that V_s increased by as much as a factor of 4 due to cementation using small-strain bender element measurements. When the specimens were tested in undrained triaxial compression, the cemented specimens were stiffer initially but converged with the uncemented specimen behavior at large strains. Since the standard penetration test induces extremely large strains in the soil in the immediate vicinity of the sampler, and smaller strains with distance from the sampler, it would be expected to reduce the influence of age-induced cementation.

Since shear wave velocity and penetration resistance normalize differently with σ_v', it is surprising that nearly every existing published relation defines V_s directly as a function of N_{60} without quantifying the overburden effect. As an example of the potential error introduced by neglecting σ_v', consider a profile of uniform sand with $(N_1)_{60}$= 20 shown in Figure 2.1. Note that N_{60}=20 at a depth of 5 m, since this depth corresponds to $\sigma_v' = 1 atm$, and the N_{60} values at other depths were computed using Equation 2.1 with n=0.5. Based on the relation by Andrus et al. (2004) for Holocene clean sand, $V_{s1} = 87.8(N_1)_{60}^{0.253} = 187\ m/s$. Substituting (2.1) and (2.2) into the relation results in Equation (2.3).

$$V_s = 87.8 \cdot N_{60}^{0.253} \left(\frac{P_a}{\sigma_v'} \right)^{0.253n-m} \tag{2.3}$$

Notice that V_s depends on both N_{60} and σ_v' in Equation 2.3, since Andrus et al. included the effect of σ_v' by using stress-normalized $(N_1)_{60}$ and V_{s1}. Figure 2.1 contains two plots of V_s versus depth that show the bias introduced by neglecting the influence of overburden; one plot uses Equation 2.3 with $n=0.5$ and $m=0.25$ such that $0.253n\text{-}m = -0.124$, while the other neglects the overburden term by setting $0.253n\text{-}m = 0$. The two plots are clearly different with the latter overpredicting V_s at shallow depths and underpredicting deeper in the profile. The two curves in Figure 2.1 would be identical only in the special case when m/n = 0.253, but this ratio is not in the reasonable range of published relations. Hence, it is reasonable to conclude that neglecting the influence of σ_v' introduces errors in the relation between V_s and N_{60}. The influence of σ_v' can be included in two different ways: (1) the regression can represent V_{s1} in terms of $(N_1)_{60}$ for cases where n and m can be independently estimated to perform overburden corrections prior to regression [e.g., as done by Andrus et al. (2004)], or (2) the regression equations can include an overburden term that is solved in a least-squares sense to best fit the data sample. Independently estimating n and m may be difficult, particularly in cases when geophysical measurements are not available and V_s is being estimated from measured N_{60} values. Furthermore, using incorrect n and/or m values could introduce bias into the resulting relation with respect to σ_v'. Hence, approach (2) is adopted in this study.

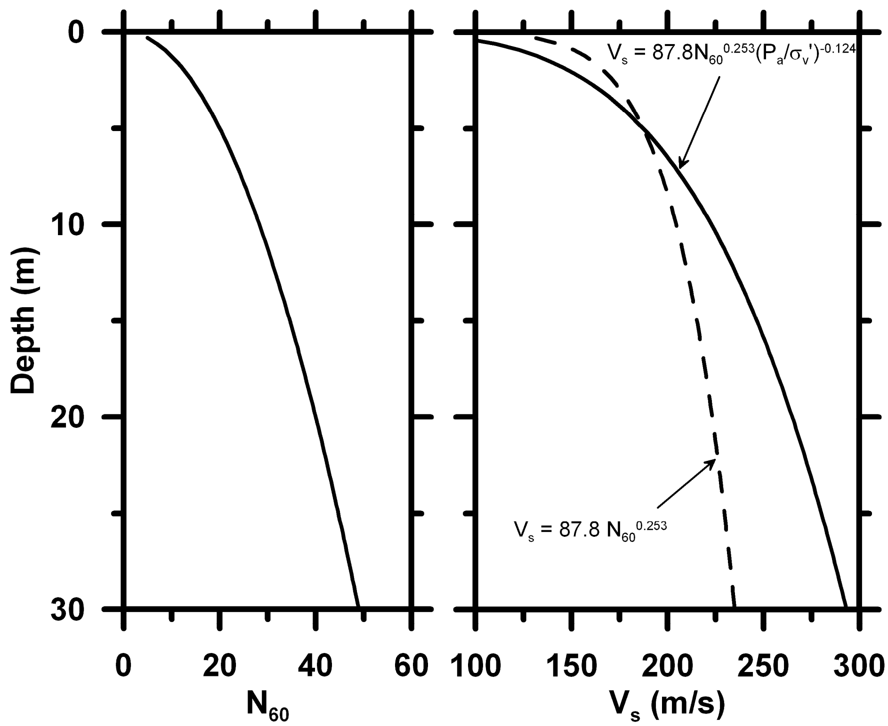

Fig. 2.1 Example of influence of overburden scaling on relation between V_s and N_{60}.

3 Data Set

This study utilized data from a set of boreholes at Caltrans bridge sites where SPT N-values and downhole suspension logs were obtained. A total of 21 bridges and 79 boring logs were identified where N_{60} and V_s measurements were available from the same borehole (Table 3.1).

Bridge Name	Bridge Number	Latitude	Longitude	Number of Borings with V_s measurements	Surface Geology Epoch
Noyo River Bridge	10-0298	39.429°	-123.807°	4	Pleistocene
Benicia-Martinez Bridge (Widen)	28-0153	38.023°	-122.072°	5	Pleistocene
Carquinez Straight Bridge	28-0352	38.066°	-122.226°	4	Holocene
Richmond-San Rafael Bridge	28-0100	37.942°	-122.476°	11	Holocene
San Francisco-Oakland Bay Bridge	33-0025	37.821°	-122.335°	2	Holocene
San Francisco-Oakland Bay Bridge	34-0003	37.801°	-122.375°	7	Holocene
San Francisco-Oakland Bay Bridge	34-0004	37.786°	-122.391°	2	Holocene
Central Viaduct	34-0077	37.771°	-122.423°	4	Holocene
Taylor Street Urban Interchange	37-0583	37.347°	-121.904°	2	Holocene
San Luis Obispo Creek Bridge	49-0014	35.184°	-120.702°	1	Holocene
Santa Rosa Creek Bridge	51-0139	34.632°	-120.288°	1	Holocene
Pleasant Valley Road Overcrossing	52-0443	34.166°	-119.143°	1	Holocene
San Pedro Terminal Island Bridge	53-1471	33.751°	-118.275°	5	Pleistocene
Fair Oaks Avenue Overcrossing	53-2272	34.152°	-118.151°	1	Pleistocene
Gavin Canyon Undercrossing	53-2790	34.350°	-118.540°	1	Pre-Quaternary
Bull Creek Canyon Channel Bridge	53-2794	34.269°	-118.487°	1	Holocene
Route 14/5 Separation & Overhead	53-2795	34.339°	-118.507°	1	Pre-Quaternary
Route 14/5 Separation & Overhead	53-2796	34.336°	-118.511°	1	Pre-Quaternary
Mojave River Bridge	54-1110	34.902°	-117.094°	2	Holocene
San Diego Coronado Bridge	57-0857	32.701°	-117.141°	22	Holocene
Rockwood Canal Bridge	58-0335	32.956°	-115.510°	1	Holocene

Locations of the bridges are shown in Figure 3.1. All of the data were collected between 1993 and 2001. Boring logs were provided in as-built drawings, and were digitized by recording blow count and soil type for each SPT measurement, and the site stratigraphy was also digitized based on the site geologist's or engineer's interpretation of layer contact elevations. Soil type was based on visual classification, and properties such as plasticity index and fines content that could help quantify soil behavior are not known. Corrections to the stratigraphy were often made so that transitions in the V_s profile better corresponded to interpreted layer boundaries. Elevation of the top of the borehole, ground water elevation, date, GPS coordinates, hammer type, and sampler type were recorded for each boring log. Shear- and p-wave velocity logs were provided as Excel files, and were recorded using the downhole suspension logging method explained by Owen (1996). In this method, a probe is lowered down the fluid-filled borehole and the source at the tip of the probe excites a wave that propagates through the boring fluid into the soil and is recorded by two receivers at 1 m spacing attached to the probe above the source. The data were subsequently evaluated for quality by Owen (1996), and poor quality data for which the recorded traces were difficult to evaluate were eliminated from the data set.

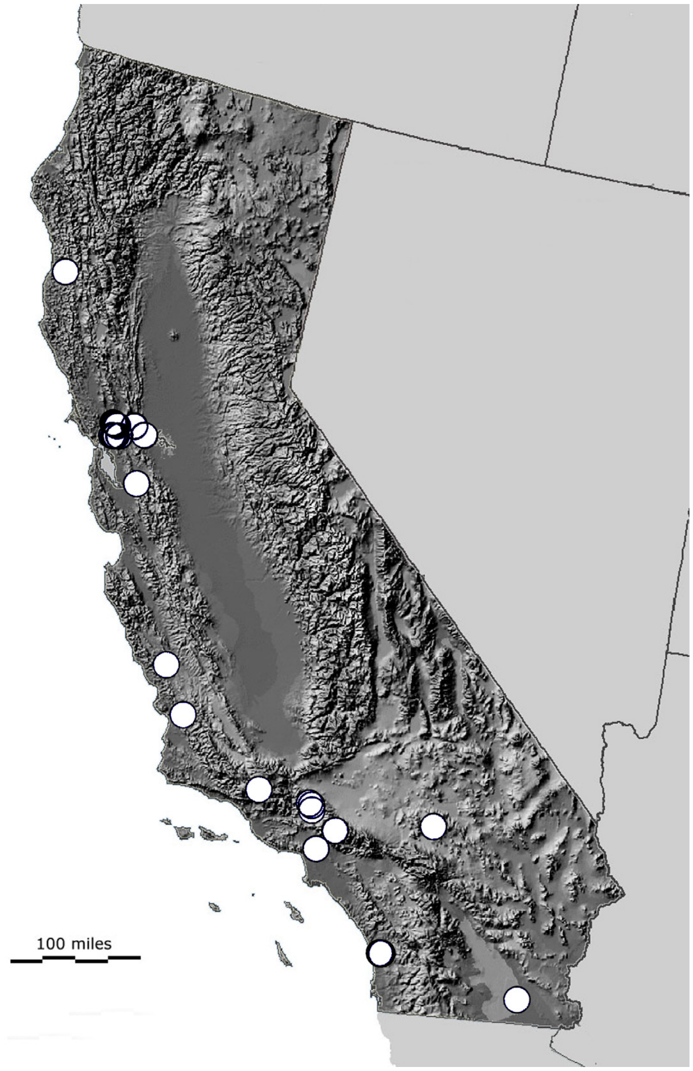

Fig. 3.1 Map of bridge locations to develop data set.

From the combination of boring logs and suspension logs, a total of 911 N_{60} values were available where V_s values were recorded at the same depth. Figure 3.2 shows the distribution of available data by soil type. For some boreholes V_s values were not recorded at shallow depths where N-values were available, and V_s values often were recorded deep in the profile where N_{60} was not recorded. Only the combinations where N-values and V_s-values were recorded at the same depth were included in the data sample. The standard SPT sampler was used for all of the borings and the hammer type was either a safety hammer with an estimated efficiency of 60%, or an automatic hammer with an estimated efficiency of 82% (Caltrans internal memorandum). A rod length correction factor was applied based on the information in Table 3.2, and a liner correction factor of 1.0 was applied for samplers with liners and 1.2 for samplers without liners [e.g., Youd et al. (2001)]. Caltrans does not utilize large-diameter borings for geotechnical site investigations; hence a borehole diameter correction was not needed. Some information was not included in every boring log. For example, groundwater elevation was sometimes not recorded for some borings, in which case the p-wave velocity profile provided in the downhole suspension logs was used to identify the approximate elevation of the ground water table. Typically an abrupt transition from p-wave velocity lower than 500 m/s to 1500 m/s or higher was apparent in the

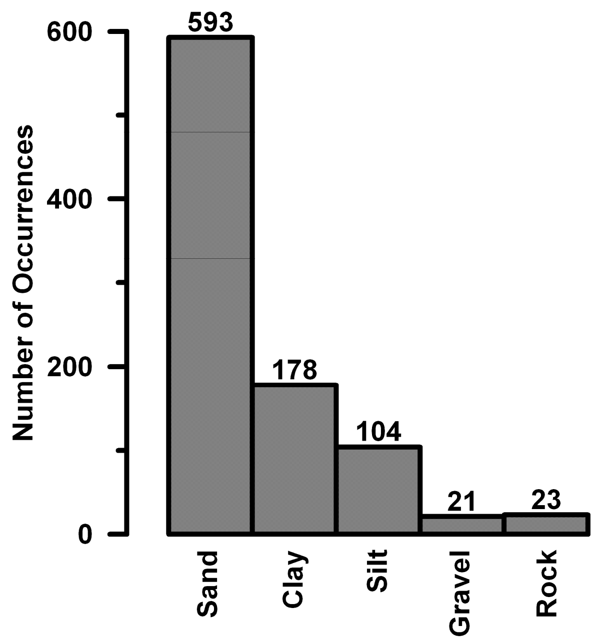

Fig. 3.2 Distribution of soil type for recorded N_{60}, $\overline{V_s}$ pairs.

Table 3.2 Rod length correction factors.

Rod Length (m)	Correction Factor
<3	0.75
3 – 4	0.8
4 – 6	0.85
6 – 10	0.95
>10	1

Table 3.3 Unit weights based on soil type position relative to groundwater.

Soil Type	Unit Weight Above Water Table (kN/m^3)	Unit Weight Below Water Table (kN/m^3)
Sand	18	20
Silt	19	17
Clay	16	18
Gravel	19	17

boring logs, clearly indicating the position of the groundwater table with approximately 1 m resolution. Whether the sampler was driven with liners was also not always available, in which case a liner correction of 1.0 was applied. Unit weights were recorded for only a small number of fine-grained soil samples (i.e., based on water content for saturated specimens), and unit weights for coarse-grained soils were assumed based on judgment. Table 3.4 presents unit weights used for the data sample depending on soil type and position relative to the ground water table.

Example data from the Noyo River Bridge are shown in Figure 3.3. The first two graphs show the V_s profile and N_{60} profile at the site. The V_s measurements were typically recorded at 0.5m intervals, whereas the N_{60} values were recorded at much coarser sampling intervals typically 1.5m or larger. A number of possible approaches were considered for selecting an appropriate V_s value to associate with each N_{60} value for statistical regression. The first possibility considered was to select the V_s value at the elevation that is nearest to the elevation where the N_{60} value was recorded. This approach was dismissed because high-frequency spatial variations in the V_s profiles could introduce errors in the regression. SPT *N*-values are not true point estimates, but rather average out soil properties over a finite region, and it is therefore important to obtain a V_s estimate that exhibits similar averaging.

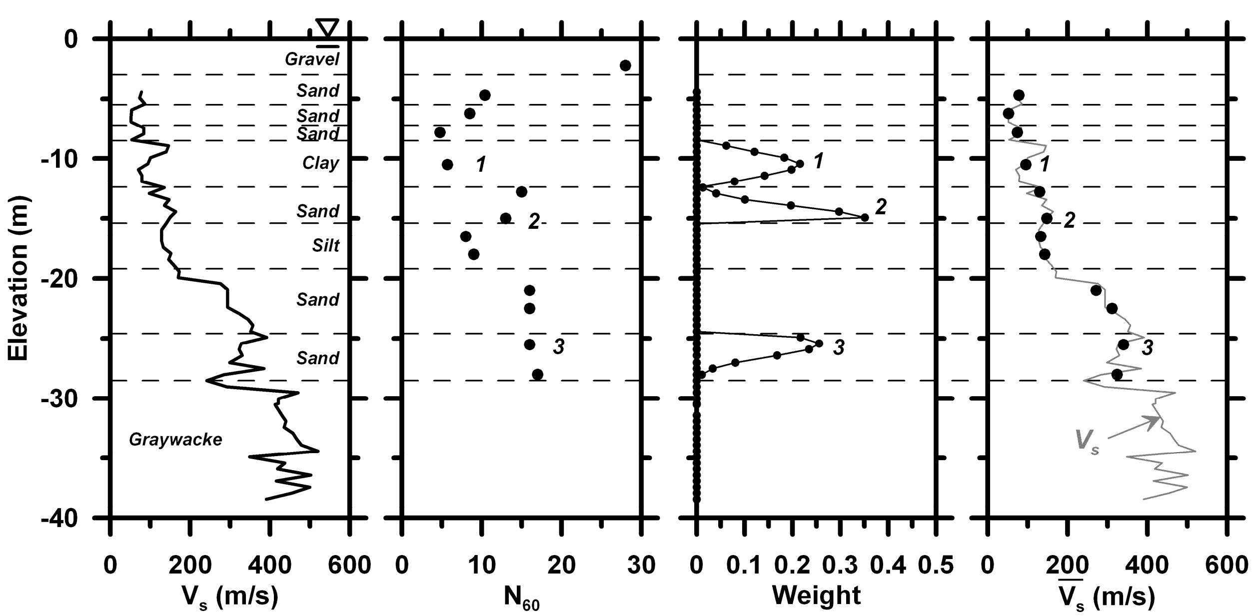

Fig. 3.3 Example plots of V_s, N_{60}, weights, and $\overline{V_s}$ for a boring at the Noyo River Bridge.

The approach adopted in this study utilized a weighted average of the V_s profile with the weighting values inversely proportional to the difference in elevation between the N_{60} measurement and the V_s measurements. The weights were based on a normal distribution centered at the N_{60} elevation with a standard deviation of 1m. This weighting scheme is intended to quantify the average shear wave velocity in a spatial region that may affect an SPT blow count value. The resulting averaged shear wave velocity values were not sensitive to the standard deviation of the weighting function. The probability density function was truncated at layer boundaries (i.e., weights were set to zero outside of the stratum containing the N_{60} value) and scaled to sum to unity. The weighted average shear wave velocity, $\overline{V_s}$ was computed using Equation 3.1.

$$\overline{V_s} = \sum_{i=1}^{rows(V_s)} w_i \cdot (V_s)_i \tag{3.1}$$

Figure 3.3 shows the weight functions and resulting $\overline{V_s}$ values for three different N_{60} values in the boring log. Point 1 shows an N_{60} value near the center of a stratum, where the weighting function is not significantly truncated at layer boundaries. Point 2 shows an N_{60} value near the bottom of a stratum that is truncated in the sand layer, and does not contain any influence of the underlying silt layer. Point 3 shows an N_{60} value near the top of a dense sand layer that is truncated so that the upper looser sand layer does not provide influence. Figure 3.3 also shows an N_{60} value in the upper gravel layer, which lies above the elevation where V_s measurements commenced. This N_{60} value is therefore not associated with a $\overline{V_s}$ value and was not included in the regression. Furthermore, the N_{60} values terminate when the underlying greywacke rock formation is reached, though V_s values continue into this formation. Values of $\overline{V_s}$ are therefore also not available in the greywacke formation and this layer is not included in the statistical regression. Layer corrections were not applied to the N_{60} or V_s values.

4 Statistical Regression

The form of statistical regression utilized in this study expresses $\overline{V_s}$ (in m/s) in terms of N_{60} (in blows/ft), σ_v' (in kPa), and regression constants, $\boldsymbol{\beta}$, using a random effects model as shown in Equation 4.1:

$$\ln\left(\overline{V_s}\right)_{ij} = \beta_0 + \beta_1 \ln\left(N_{60}\right)_{ij} + \beta_2 \cdot \ln\left(\sigma_v'\right)_{ij} + \eta_i + \varepsilon_{ij} \tag{4.1}$$

where η_i is the random effect for the i^{th} boring (i.e., the interboring variation) and ε_{ij} is the variation of the j^{th} measurement from the i^{th} boring (i.e., the intraboring variation). The η_i and ε_{ij} are assumed to be independent normally distributed variates with standard deviations τ and σ, respectively, and the standard deviation of the total error is $\sigma_T = \sqrt{\tau^2 + \sigma^2}$, since η and ε are presumed uncorrelated. Error was partitioned into two variables using the random effects model to permit the possibility that $\overline{V_s}$ might be systematically overpredicted for some borings and systematically underpredicted for others. Utilizing a single error term would neglect this important feature, which can be captured only by partitioning the error into interboring and intraboring terms. Random effects models are often applied in regression analysis of earthquake ground motions [e.g., Abrahamson and Youngs (1992)], wherein error is partitioned into intra-event and inter-event terms because an earthquake may produce ground motions that are systematically overpredicted or systematically underpredicted by ground motion prediction equations. The random effect is very important for estimating the variance of V_{s30}, the average shear wave velocity in the upper 30m, computed from the correlation as shown in detail later. Previously published regressions of V_s with N_{60} have not partitioned the error term into interboring and intraboring components, and it is therefore not possible to distinguish the two types of error.

The form of the regression equation used in this study also includes σ_v' as a regression variable and solves for β_2 that minimizes errors. The alternative approach would have involved estimating n and m for each sample and regressing on V_{s1} and $(N_1)_{60}$ without including a σ_v' term [i.e., as done by Andrus et al. (2004)]. However, n and m could not be accurately estimated for the data, since important properties such as plasticity index and fines content are not known. Including erroneous n and m terms could result in an expression for V_s that is biased with respect to σ_v', whereas Equation 4.1 eliminates this potential bias. The β_2 parameter provides a measure of the relative overburden scaling between V_s and N_{60} that minimizes residuals with respect to σ_v'.

Regression was performed for sand, silt, and clay soil types using the *lmer* function in R, the open-source software environment for statistical computing (Venables and Smith 2009). The number of data points for gravel was deemed insufficient for regression. The resulting regression parameters are summarized in Table 4.1, and trends are plotted in Figure 4.1 as $\overline{V_s}$ versus N_{60} and $\overline{V_s}$ versus σ_v'. Regression lines using Equation 4.1 and Table 1.1 are plotted through the data points corresponding to various σ_v' values for $\overline{V_s}$ versus N_{60} and for various N_{60} values for $\overline{V_s}$ versus σ_v'. All regression lines are the median values, with $\varepsilon=\eta=0$. Multiple trend lines are required, since the regression includes both N_{60} and σ_v', and the trend lines are useful for identifying the relative influence of N_{60} and σ_v' for the regression of each soil type. The trend lines correspond to the median and plus and minus one standard deviation for σ_v' and N_{60} so that a fair comparison can be made about their relative influence on the regression prediction.

Table 4.1 Regression parameters.

Soil Type	β_0	β_1	β_2	σ	τ
Sand	4.045	0.096	0.236	$0.57-0.07\cdot\ln(\sigma_v')$ if $\sigma_v'\leq 200$kPa 0.20 if $\sigma_v'>200$kPa	0.217
Silt	3.783	0.178	0.231	$0.31-0.03\cdot\ln(\sigma_v')$ if $\sigma_v'\leq 200$kPa 0.15 if $\sigma_v'>200$kPa	0.227
Clay	3.996	0.230	0.164	$0.21-0.01\cdot\ln(\sigma_v')$ if $\sigma_v'\leq 200$kPa 0.16 if $\sigma_v'>200$kPa	0.227

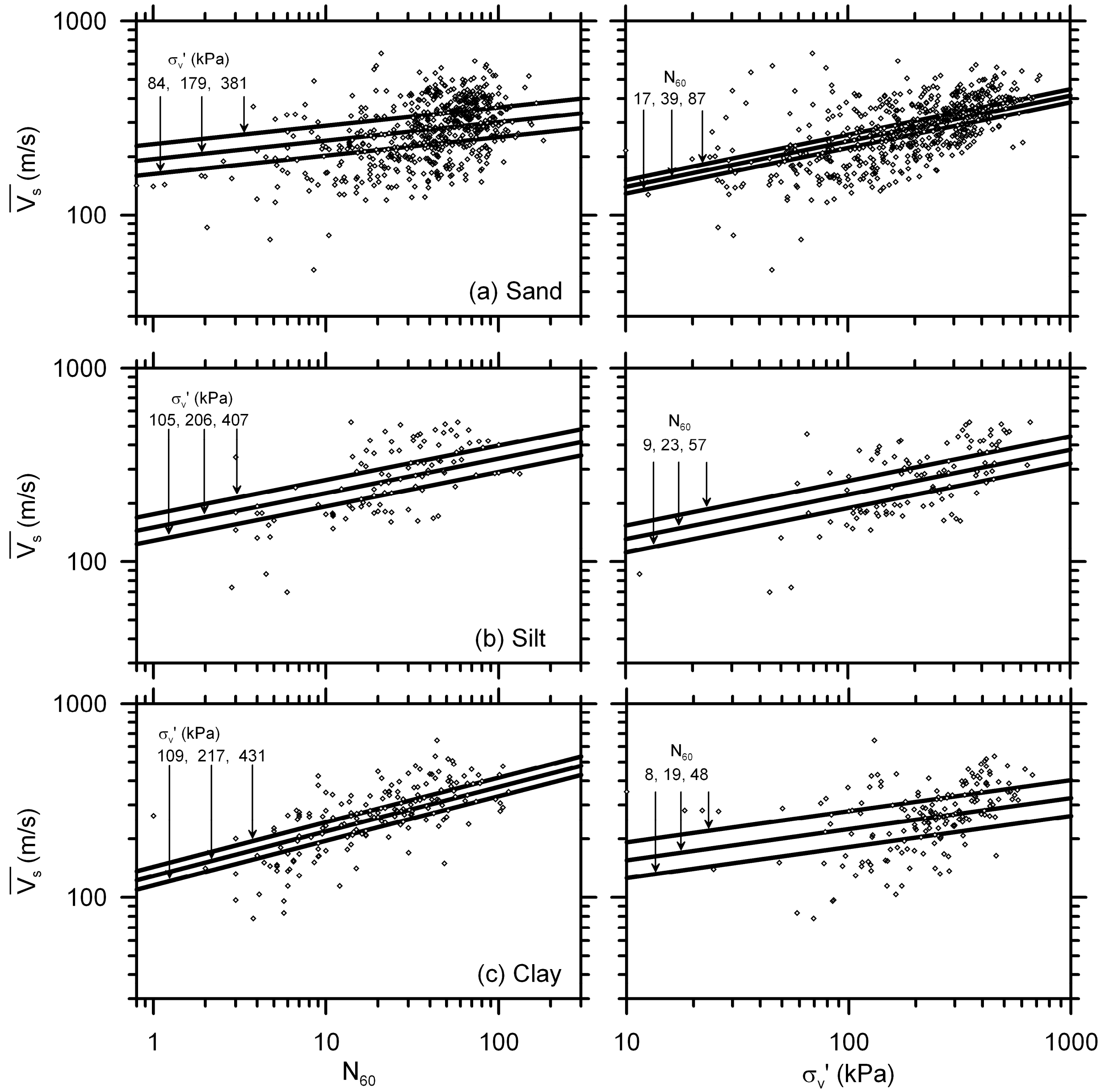

Fig. 4.1 Results of regression equations for (a) sand, (b) silt, and (c) clay, with trend lines corresponding to the mean and ±1σ for σ_v' and N_{60}.

4.1 RELATIVE INFLUENCE OF N_{60} AND σ_V' ON REGRESSION

For sand, $\overline{V_s}$ is more significantly related to σ_v' than to N_{60}. This trend is apparent by examining how closely spaced the trend lines are within a given plot. For example, the trend lines are further apart in the plot of $\overline{V_s}$ versus N_{60} than in the plot of $\overline{V_s}$ versus σ_v', which indicates that σ_v'

exerts a more significant influence than N_{60}. For example, considering sand with the median value N_{60}=39, the regression equation returns median values of $\overline{V_s}$ = 230, 275, and 329 m/s for σ_v' = 84, 179, and 381 kPa, respectively. On the other hand, for σ_v'=179 kPa, the regression equations return median values of $\overline{V_s}$ = 254, 275, and 297 m/s for N_{60} = 17, 39, and 87, respectively. This indicates that, in the range of common engineering interest, V_s is more strongly related to overburden stress than to blow count. Hence, knowing σ_v' alone would provide a statistically superior estimate of $\overline{V_s}$ than knowing N_{60} alone, though knowing both is better. This observation is significant, since the effect of overburden has not been directly quantified in nearly every previously published study, and may help explain the large differences among the numerous published relations.

The influence of σ_v' on the regression becomes smaller for silt and is the lowest for clay. For silt σ_v' and N_{60} exert approximately equal influence on $\overline{V_s}$, whereas for clay, N_{60} exerts more influence than σ_v'. For example, considering clay with the median value N_{60}=19, the regression equation returns median values of $\overline{V_s}$ = 227, 254, and 283 m/s for σ_v' = 109, 217, and 431 kPa, respectively. On the other hand, for σ_v'=217 kPa, the regression equations return median values of $\overline{V_s}$ = 208, 254, and 314 *m/s* for N_{60} = 8, 19, and 48, respectively. Hence, $\overline{V_s}$ is more strongly related to blow count than overburden stress in the range of engineering interest for clay, which is opposite to the trend for sand. However, in all cases V_s was influenced by σ_v', and neglecting the overburden effect would introduce bias into the results.

4.2 OVERBURDEN SCALING PARAMETERS IMPLIED BY REGRESSION CONSTANTS

The statistical regression parameters provide information about the relative overburden scaling for V_s and N_{60}. Individual values of n and m cannot be solved from the regression, but a linear relation between n and m can be defined by rearranging terms in Equations 2.1, 2.2, and 4.1 to obtain $\beta_2 = m - n \cdot \beta_1$, and values of m can be computed for assumed values of n. For example, if we assume n=0.5 for sand, then m=0.28, which is reasonably close to the commonly assumed value of 0.25. If we assume n=1.0 for clay, then m=0.39, which is reasonably close to m=0.5 suggested for clay by Yamada et al. (2008). The range of n for silt would be anticipated between

0.5 and 1.0, since silt could vary from non-plastic to highly plastic, which corresponds *m* in the range 0.32 to 0.41. The overburden scaling implied by the regression constants is therefore reasonably consistent with observations from other published studies.

4.3 INTRABORING RESIDUALS

Intraboring residuals defined as $\varepsilon_{ij} = ln(\overline{V_s})_{ij} - [\beta_0 + \beta_1 ln(N_{60})_{ij} + \beta_2 ln(\sigma_v')_{ij} + \eta_i]$ are plotted versus N_{60} and σ_v' in Figure 4.2. The mean value of the residuals is zero, and there is no trend in the residuals with either N_{60} or σ_v', which indicates that the regression has removed bias with respect to these input variables. The standard deviation of the intra-event residuals decreases as σ_v' increases, indicating a weaker relationship at low confining stress (i.e., at shallow depths). The cause of the decreased correlation at low σ_v' is unclear, but could be an indication of reduced measurement accuracy at shallow depths in the suspension logging. Since the standard deviation term depends on σ_v', the residuals are heteroscedastic. The variation in σ with σ_v' was quantified by (1) sorting the residuals in order of increasing σ_v', (2) selecting a subsample of data points with the lowest confining stress values, (3) computing the standard deviation of the subsample, (4) computing the mean σ_v' for the subsample, (5) shifting the subsample window by one data point and repeating (3) and (4), and (6) repeating (5) until the subsample window reached the last residual value with the highest σ_v'. The subsample standard deviations were then plotted versus the natural logarithm of the subsample mean σ_v' values, and a linear trend was fit to the data. The subsample standard deviations were observed to be fairly constant when σ_v'>200kPa, as reflected in the equations for σ in Table 3.1. The sand residuals exhibit the most pronounced heteroscedasticity, whereas the standard deviation of the residuals for silt and clay depend only weakly on σ_v'. Trend lines corresponding to $\pm 1\sigma$ are included in Figure 4.2.

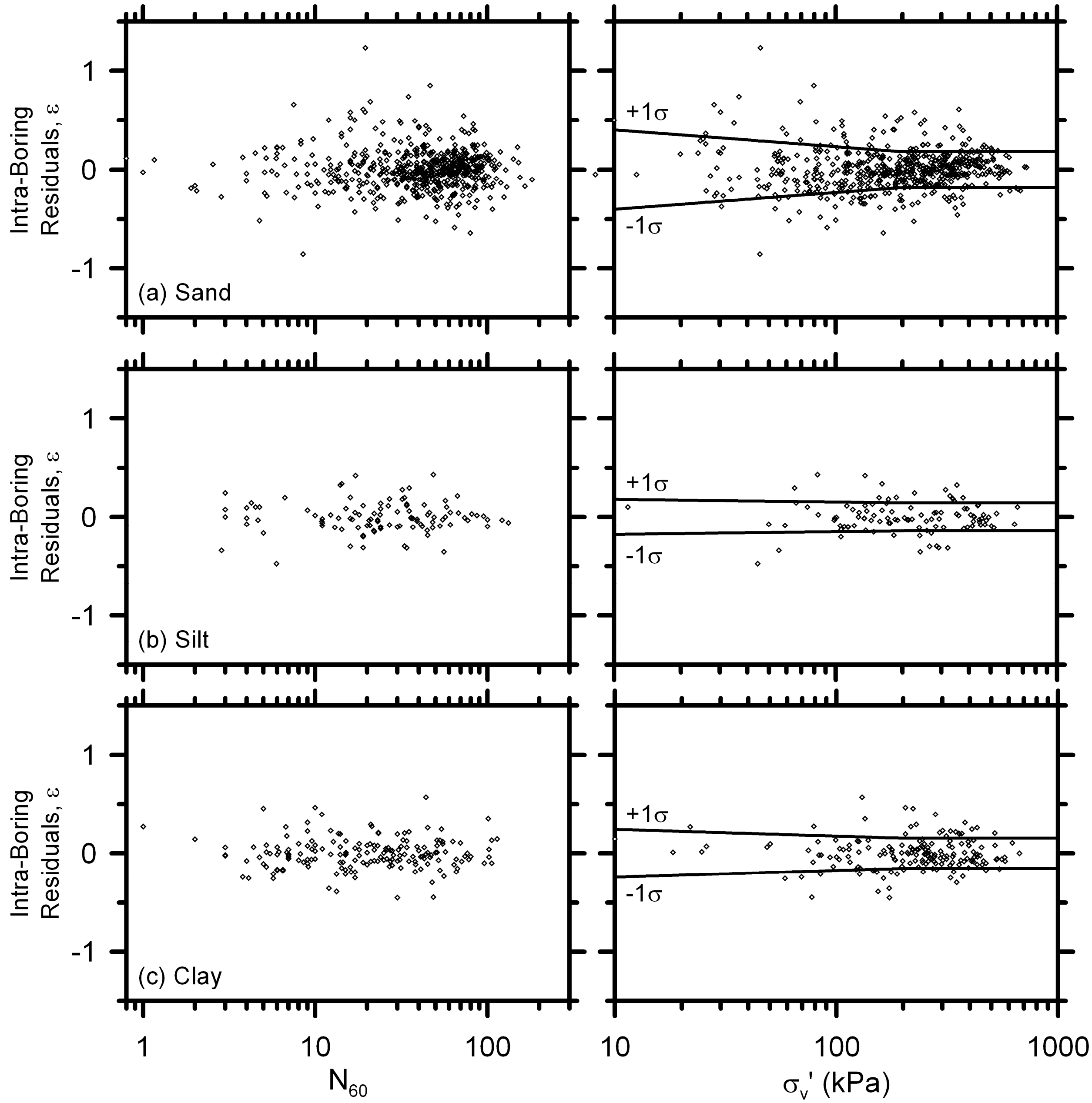

Fig. 4.2 Intraboring residuals, ε, versus N_{60} and σ_v' for (a) sand, (b) silt, and (c) clay. Plots of ε vs. σ_v' include lines showing $\pm 1\sigma$ for ε.

Normality of the intraboring residuals is examined using the quantile-quantile (Q-Q) plots in Figure 4.3. The Q-Q plots represent the sorted residuals (i.e., the quantiles) versus the theoretical residuals that would be anticipated if the error term were normally distributed. When measured quantiles are plotted against theoretical quantiles, a normally distributed variable exhibits a linear Q-Q plot with a slope of unity, whereas deviation from normality is manifested by data points that do not lie along the 1:1 line. Some deviations at the ends of the Q-Q plots are anticipated based on sampling variability, since the tails of distributions are often not well-characterized by the sample. In this case, residuals for sand and clay deviate from normality at the tails of the distribution, dropping below the 1:1 line. This indicates that the distributions are more peaked than a normal distribution, with more probability density lying near the mean and less at the tails. Indeed, kurtosis of the intraboring residuals were 3.9, 1.1, and 1.5 for sand, silt, and clay, respectively. For reference, a normal distribution has kurtosis of zero, and a distribution that is more peaked than a normal distribution has a positive kurtosis, while flatter distributions have negative kurtosis. Despite these deviations from normality, the normal distribution is a convenient model for quantifying distribution of the intraboring residuals, and the authors suggest that the residuals can be considered normally distributed for practical implementation.

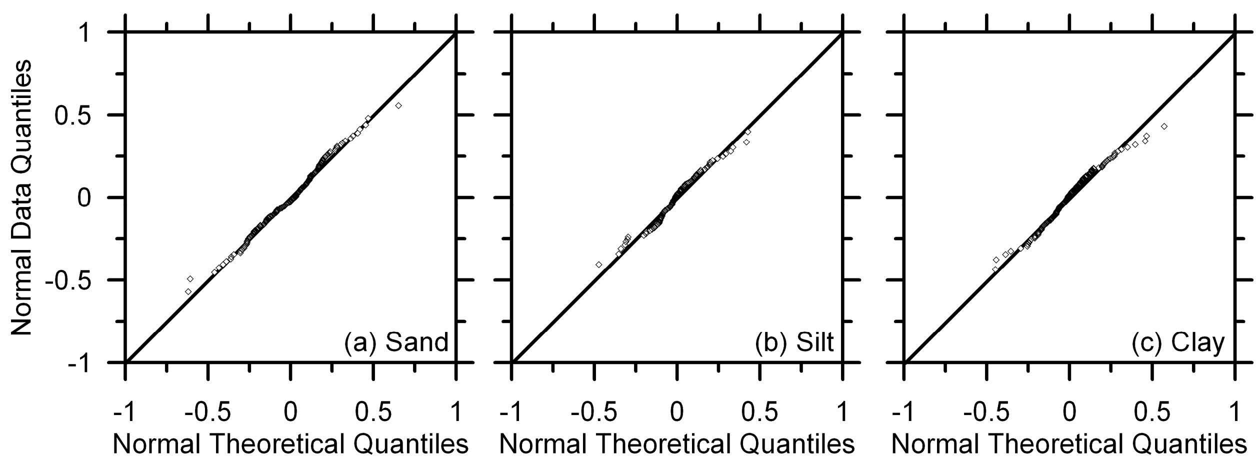

Fig. 4.3 Quantile-quantile plots showing degree to which intraboring residuals are normally distributed.

4.4 INTERBORING RESIDUALS

Figure 4.4 plots inter-event residuals, η_i, corresponding to Holocene, Pleistocene, and Pre-Quaternary surface geology epochs. Surface geology mapping was based on a study by Knudsen et al. (2009) who reported the surface geologic epoch at all Caltrans bridge sites. A positive η value indicates that the median value of $\overline{V_s}$ predicted using Equation 4.1 would underpredict the measured value. A weak trend is apparent in which the η values decrease with geologic age, which implies that for a given N_{60} the corresponding V_s value decreases as age increases. This is contrary to the expectation that age-induced cementation would have a larger effect on V_s than on N_{60}. However, the trend is weak and the number of data points is insufficient (particularly for Pleistocene and pre-Quaternary epochs) to confidently propose age-dependent inter-event residuals. Furthermore, sites with a Holocene surface geology may transition to older epochs deeper in the profile, such that some data points in the Holocene epoch may actually arise from older geologic units. Sykora and Koester (1988) also found that geologic age had little effect on the correlation between V_s and N_{60}. Inter-event error should be presumed normally distributed with zero mean and a constant standard deviation specified in Table 3.3.

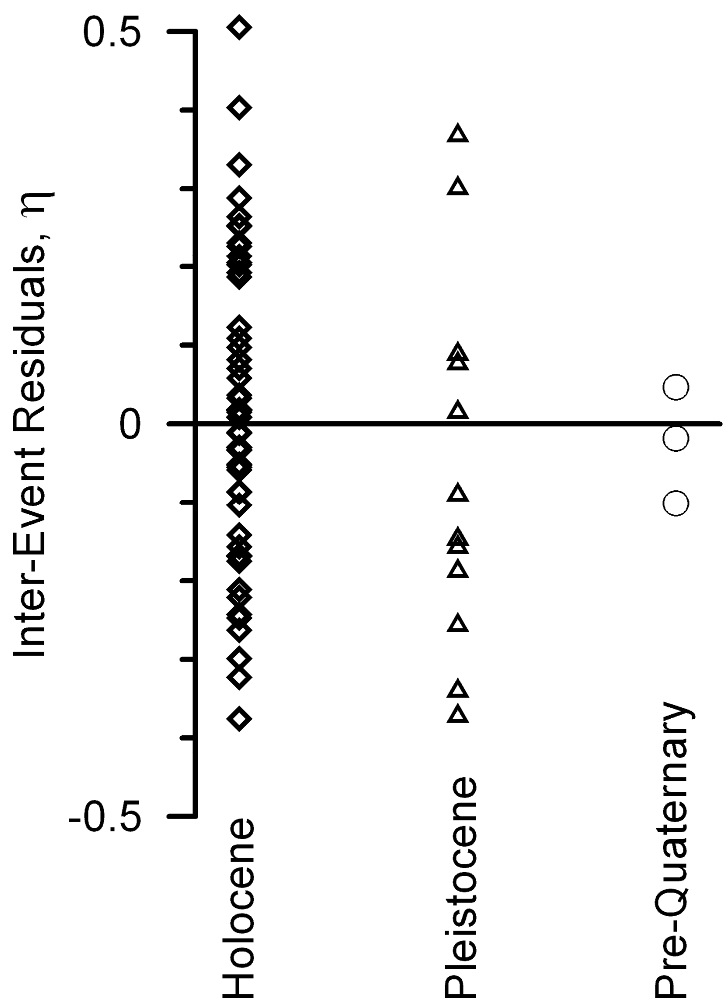

Fig. 4.4 Interboring residuals, η, as function of surface geologic epoch.

5 Calculation of V_{s30} from Blow Count Data

A likely application of the correlations presented in this paper is the calculation of the thirty-meter shear wave velocity, V_{s30}, which is defined as 30 m divided by the travel time of a vertically propagating shear wave in the upper 30 m. The Next Generation Attenuation ground motion prediction models utilize V_{s30} as a required input, and it is therefore required for seismic hazard evaluation. Geotechnical site investigations at many older sites contain boring logs, but no geophysical measurements. Obtaining a rough estimate of V_{s30} based on the recorded boring logs could therefore be useful for assessing seismic hazard at sites with that lack geophysical measurements, and for identifying whether geophysical measurements are necessary to further refine the estimate of V_{s30}. The authors are not advocating the use of correlations as an accurate substitute for geophysical measurements; rather the goal is to quantify errors that may arise so that better-informed decisions can be made regarding which data to collect from a site.

The set of boring logs was screened to identify borings for which adequate spatial coverage in the upper 30 m was provided for the shear wave velocity suspension log and the recorded blow counts to obtain a reasonable estimate of V_{s30}. Borings were excluded when fewer than 6 blow counts were recorded in the upper 30 m, when V_s was not recorded in the upper 5 m, or when large gaps were present in the V_s logs or the recorded blow counts. A total of 30 borings were identified for which accurate V_{s30} measurements could be made. A $\widehat{V_s}$ value was estimated for each N_{60} value using the median relation in Equation 4.1, and V_{s30} was computed for the V_s values recorded directly in the suspension logs (V_{s30}) and for the V_s values computed from Equation 4.1 ($\overline{V_{s30}}$) using Equation 5.1 [e.g., Dobry et al. (2000)], where dx is the tributary length assigned to each V_s value, and N is the number of V_s values in the upper 30 m.

$$V_{s30} = \frac{30m}{\sum_{i=1}^{N} \frac{dx_i}{(V_s)_i}} \tag{5.1}$$

Residuals were computed as $\ln(V_{s30}) - \ln(\overline{V_{s30}})$. The mean of the residuals was found to be 8.6×10^{-3} which is very low and indicates that the proposed correlation between V_s and N_{60} and σ_v' (see Eq. 4.1) produces an unbiased estimation of V_{s30}. This is not surprising, since the data being evaluated to compute V_{s30} are a subset of the same data that were used to develop the relation.

The standard deviation σ_{Vs30} was 0.221, which is less than the total standard deviation $\sqrt{\sigma^2 + \tau^2}$. For a given site, the intraboring residuals, ε, are presumed uncorrelated, and the averaging in Equation 5.1 therefore reduces uncertainty in V_{s30} contributed by the ε's. However, the interboring error is not reduced by averaging. Stated differently, for a given boring log, errors in the estimated V_s values can be divided into the average error for that boring log (i.e., the interboring error), and the scatter of the data points about this average error (i.e., the intraboring error). When a sufficient number of data points are available, the influence of the scatter about the average error has little influence on V_{s30} because some data points are overestimated while others are underestimated, and the errors cancel each other. However, the influence of the average error is preserved in the V_{s30} estimate. The fact that the σ term contributes little to σ_{Vs30} can be verified by noting that the computed σ_{Vs30} value from the 30 borings in this study is 0.221, which is consistent with the τ values in Table 4.1. The standard deviation of V_{s30} should therefore be taken as equal to τ. For sites with multiple soil types, τ should be based on the predominant soil type at a particular site using the values in Table 4.1.

6 Discussion

6.1 ERROR CAUSED BY NEGLECTING OVERBURDEN INFLUENCE

The most fundamental observation in this paper is the influence of σ_v' on the correlation between V_s and N_{60}, hence exploring errors associated with neglecting σ_v' is justified to demonstrate the importance. An ordinary least-squares regression was performed using the form in Equation 6.1, and residuals, ε^*, are plotted versus σ_v' in Figure 6.1 for sand, silt, and clay data types.

$$\ln\left(\overline{V_s}\right) = \beta_0^* + \beta_1^* \ln\left(N_{60}\right) + \varepsilon^* \tag{6.1}$$

For simplicity, the error term was not divided into inter- and intraboring terms, hence Figure 6.1 displays the total error for each data point in the regression. Bias is clearly evident with respect to σ_v', with negative residuals at low overburden stress and positive residuals at high overburden, which is consistent with the trend that was demonstrated in Figure 3.1 (a negative residual indicates an underprediction of V_s, whereas positive residuals indicate overprediction). Neglecting the influence of σ_v' on the relation between V_s and N_{60} results in statistically significant error. Such relations can be used accurately only in rare cases where the overburden stresses used to develop the relation match the overburden stresses for a particular problem. However, this is a stringent constraint that is not likely to be satisfied for practical problems that involve a range of different overburden stresses.

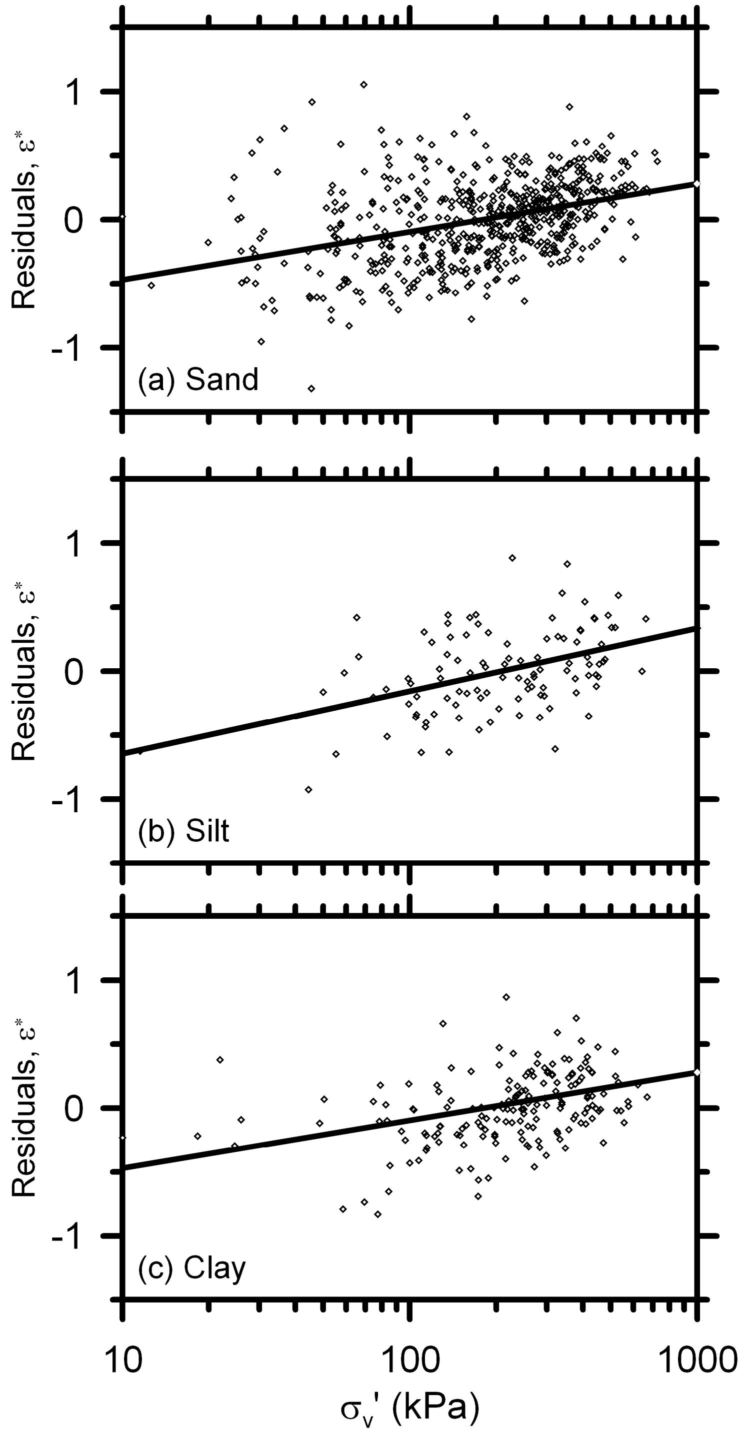

Fig. 6.1 Residuals, ε^*, versus σ_v' for ordinary least squares regression that neglects the influence of σ_v' on relation between V_s and N_{60}. Bias is evident based on the slope of the least squares regression lines.

6.2 COMPARISON WITH OTHER PUBLISHED RELATIONS

Some of the correlations from Table 1.1 are plotted against the data in Fig 6.2. Some of the correlations fit the data points reasonably well, though there is tremendous difference in the various predictions. It is unclear how much of these deviations are caused by natural variability in soil deposits, how much are caused by errors in measurements of N and V_s, and how much is caused by exclusion of overburden correction in the existing relations. For example Kanai (1966) may have utilized data recorded primarily at shallow depths, which could largely explain why their relation is lower than the others. Future efforts should aim to reduce the variability in these relations by utilizing only high-quality measurements of N and V_s, and properly incorporating the influence of overburden. This effort would involve reinterpretation of the data available in published relations, which is beyond the scope of this report.

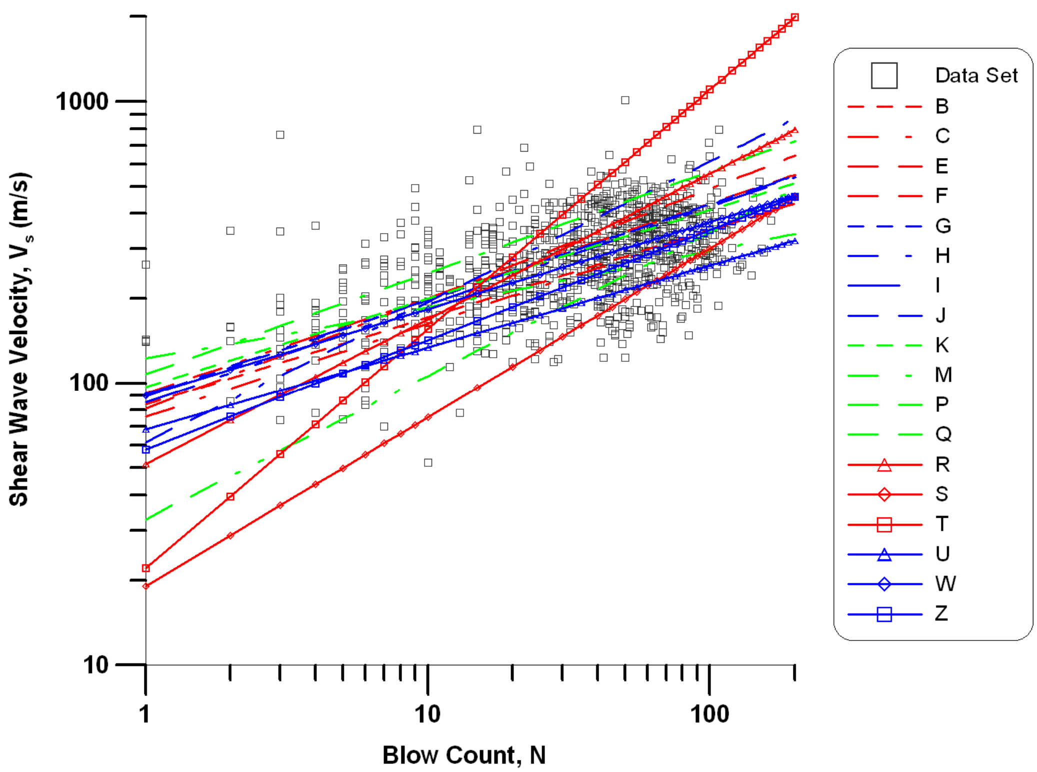

Fig. 6.2 Existing correlations from literature superposed on data set used in this study.

6.3 APPROPRIATE USE OF PROPOSED RELATIONS

The proposed relations are intended to be used to obtain a rough estimate of V_s given N_{60} and σ_v' values at sites where geophysical measurements are not available. The relations are not an accurate substitute for geophysical measurements, and estimates from the relations contain significant uncertainty. The primary intended user is the California Department of Transportation, who owns about 13,000 bridges and geophysical measurements have often not been made at the bridge sites. Making geophysical measurements at every bridge site would be economically unfeasible, and the relations provide a simple but crude method of estimating site stiffness for the purpose of ground motion prediction. The relations should never be used at a site where geophysical measurements are available because the geophysical measurements provide a direct measurement of V_s that contains far less uncertainty. The relations should also never be used as a substitute for projects where making geophysical measurements would be feasible.

The proposed relations are not intended to be used in soft clay deposits. Often, soft clays exhibit very low blow counts (i.e., 1 or push), and the standard penetration test is known to be a very poor predictor of the engineering properties of soft clay as a result of its poor resolution at low blow count. Just as a competent geotechnical engineer would never rely on SPT N-values to predict undrained shear strength in soft clay, one should also never rely on SPT N-values to predict V_s in soft clay using the proposed relations. Very few soft clay data points are included in the correlations, with only four points at N_{60}<3. Hence, the proposed relations are not a valid indicator of V_s for soft clays with N_{60}<3, and other methods should be used to estimate V_s in such layers.

The proposed relations pertain only to blow counts measured using the standard penetration test sampler. Blow counts obtained from non-standard samplers (e.g., the Modified California Sampler) should not be used in combination with the proposed relations. It is the authors' opinion that geotechnical engineers should never use the Modified California Sampler because the recorded blow counts are different from those recorded using the standard penetration test sampler, and the samples obtained from the Modified California Sampler are so badly disturbed that they cannot possibly be used to measure accurate strength properties in the laboratory.

7 Conclusions

Shear wave velocity has been defined as a statistical function of standard penetration resistance and vertical effective stress. Nearly every previously published statistical relation represented V_s as a function of N_{60} alone, without considering the influence of σ_v'. Statistically significant errors arise from neglecting the influence of σ_v' on the relation between V_s and N_{60}, and such relations should not be used except in rare cases when the overburden stresses for the data used to develop a particular relation match the overburden stresses anticipated at a particular site. Data from previously published studies should be reinterpreted to include the effect of overburden to remove bias and reduce uncertainty.

Uncertainty in V_{s30} computed using the proposed relations is much larger than the uncertainty associated with geophysical measurements of V_{s30}. For example, Moss (2008) estimates the coefficients of variation on the order of only 1% to 3% for downhole measurements compared with 22% from the proposed relations. This additional uncertainty in the proposed relations will increase dispersion in ground motion predicted from V_{s30} compared with directly measuring V_{s30} using geophysical measurements. Hence, the proposed relations should not be used at sites where accurate geophysical measurements are available or can readily be obtained.

REFERENCES

Abrahamson, N., and Silva, W. (2008). "Summary of the Abrahamson & Silva NGA ground-motion relations." *Earthquake Spectra*, 24(1), 67-97.

Abrahamson, N. A., and Youngs, R. R. (1992). "A stable algorithm for regression analyses using the random effects model." *Bulletin of the Seismological Society of America*, 82(1), 505-510.

Andrus, R. D., Piratheepan, P., Ellis, B. S., Zhang, J., and Juang, C. H. (2004). "Comparing liquefaction evaluation methods using penetration-Vs relationships." *Soil Dynamics and Earthquake Engineering*, 24(9-10), 713-721.

Athanasopoulos, G. A. (1995). "Empirical correlations *Vs*-NSPT for soils of Greece: a comparative study of reliability," *Proc. 7th Int. Conf. on Soil Dynamics and Earthquake Engineering (Chania, Crete)* ed. A. S. Cakmak (Southampton: Computational Mechanics), 19–36.

Boore, D. M. and Atkinson, G. M. (2008). "Ground-motion prediction equations for the average horizontal component of PGA, PGV, and 5%-damped PSA at spectral periods between 0.01 s and 10.0 s." *Earthquake Spectra*, 24(1), 99-138.

Campbell, K. W., and Bozorgnia, Y. (2008). "NGA ground motion model for the geometric mean horizontal component of PGA, PGV, PGD and 5% damped linear elastic response spectra for periods ranging from 0.01 to 10 s." *Earthquake Spectra*. 24(1), 139-171.

Chiou, B. S.-J. and Youngs, R. R. (2008). "An NGA model for the average horizontal component of peak ground motion and response spectra." *Earthquake Spectra*, 24(1), 173-215.

Choi, Y. and Stewart, J. P. (2005). "Nonlinear site amplification as function of 30 m shear wave velocity," *Earthquake Spectra*, 21 (1), 1-30.

DeJong, J. T., Fritzges, M. B., and Nusslein, K. (2006). "Microbially induced cementation to control sand response to undrained shear." *J. Geotech. Geoenviron. Eng.*, 132(11), 1381-1392.

Dikmen, U. (2009). "Statistical correlations of shear wave velocity and penetration resistance for soils." *Journal of Geophysics and Engineering*. 6(1), 61-72.

Dobry, R., Borcherdt, R. D., Crouse, C. B., Idriss, I. M., Joyner, W. B., Martin, G. R., Power, M. S., Rinne, E. E., and Seed, R. B., (2000). "New site coefficient and site classification system use in recent building code provisions." *Earthquake Spectra*, 16 (1), 41-67

Fujiwara, T. (1972). "Estimation of ground movements in actual destructive earthquakes," *Proc. 4th European Symp. Earthquake Engineering (London),* 125–32.

Hasancebi, N. and Ulusay, R. (2006). "Empirical correlations between shear wave velocity and penetration resistance for ground shaking assessments." *Bulletin of Engineering Geology and the Environment.* 66(2), 203-213.

Idriss, I. M. (2008). "An NGA empirical model for estimating the horizontal spectral values generated by shallow crustal earthquakes." *Earthquake Spectra*. 24(1), 217–242.

Imai, T. (1977). "P-and S-wave velocities of the ground in Japan," *Proc. 9th Int. Conf. on Soil Mechanics and Foundation Engineering,* vol. 2, 127–32.

Imai, T. and Tonouchi, K. (1982). "Correlation of N-value with S-wave velocity and shear modulus," *Proc. 2nd European Symp. Of Penetration Testing (Amsterdam),* 57–72.

Imai, T. and Yoshimura, Y. (1975). "The relation of mechanical properties of soils to P and S-wave velocities for ground in Japan," *Technical Note,* OYO Corporation.

Iyisan, R. (1996). "Correlations between shear wave velocity and in-situ penetration test results," *Tech. J. Chamber Civil Eng. Turkey,* 7**,** 1187–99 (in Turkish).

Jafari, M. K., Shafiee, A. and Ramzkhah, A. (2002). "Dynamic properties of the fine grained soils in south of Tehran," *J. Seismol. Earthq. Eng.,* 4**,** 25–35.

Jafari, M. K., Asghari, A. and Rahmani, I. (1997). "Empirical correlation between shear wave velocity (*Vs*) and SPT-*N* value for south of Tehran soils," *Proc. 4th Int. Conf. on Civil Engineering (Tehran, Iran)* (in Persian).

Jinan, Z. (1987). "Correlation between seismic wave velocity and the number of blow of SPT and depth," *Chin. J. Geotech. Eng. (ASCE),* 92–100 (selected papers).

Kanai, K. (1966). "*Conf. on Cone Penetrometer The Ministry of Public Works and Settlement (Ankara, Turkey),"* (presented by Y Sakai 1968).

Kiku, H., Yoshida, N., Yasuda, S., Irisawa, T., Nakazawa, H., Shimizu, Y., Ansal, A. and Erkan, A. (2001). "In-situ penetration tests and soil profiling in Adapazari, Turkey," *Proc. ICSMGE/TC4 Satellite Conf. on Lessons Learned from Recent Strong Earthquakes,* 259–65.

Knudsen, K. L., Bott, J. D. J., Woods, M. O., and McGuire, T. L. (2009). "Development of a liquefaction hazard screening tool for Caltrans bridge sites." TCLEE 2009 Conference: 7th International Conference on Lifeline Earthquake Engineering. Oakland, CA.

Lee, S. H. (1990). "Regression models of shear wave velocities," *J. Chin. Inst. Eng.,* 13**,** 519–32.

Moss, R.E.S. (2008) "Quantifying measurement uncertainty of thirty-meter shear-wave velocity." *Bulletin of the Seismological Society of America*, 98(3), 1399-1411.

Ohba, S. and Toriuma, I. (1970). "Dynamic response characteristics of Osaka Plain," *Proc. Ann. Meeting AIJ (in Japanese).*

Ohsaki, Y. and Iwasaki, R. (1973). "On dynamic shear moduli and Poisson's ratio of soil deposits," *Soil Found.,* 13**,** 61–73.

Ohta, Y. and Goto, N. (1978). "Empirical shear wave velocity equations in terms of characteristic soil indexes," *Earthq. Eng. Struct. Dyn.,* 6**,** 167–87.

Ohta, Y., Goto, N., Kagami, H., and Shiono, K. (1978). "Shear wave velocity measurement during a standard penetration test." *Earthquake Engineering and Structural Dynamics*. 6(1), 43-50.

Ohta, T., Hara, A., Niwa, M. and Sakano, T. (1972). "Elastic shear moduli as estimated from N-value," *Proc. 7th Ann. Convention of Japan Society of Soil Mechanics and Foundation Engineering,* 265–8.

Okamoto, T., Kokusho, T., Yoshida, Y. and Kusuonoki, K. (1989). "Comparison of surface versus subsurface wave source for P–S logging in sand layer," *Proc. 44th Ann. Conf. JSCE,* vol. 3, 996–7 (in Japanese).

Owen, W. (1996). "Interim report of PS velocity log for borehole 96-2, SFOBB East Viaduct seismic retrofit." Department of Transportation, Engineering Service Center, Office of Structural Foundations. 3 p.

Pitilakis, K., Raptakis, D., Lontzetidis, K. T., Vassilikou, T. and Jongmans, D. (1999). "Geotechnical and geophysical description of Euro-Seistests, using field and laboratory tests, and moderate strong ground motions," *J. Earthq. Eng.,* 3, 381–409.

Seed, H. B. and Idriss, I. M. (1981). "Evaluation of liquefaction potential sand deposits based on observation of performance in previous earthquakes," *ASCE National Convention (MO),* 81–544.

Sisman, H. (1995). "The relation between seismic wave velocities and SPT, pressuremeter tests," *MSc Thesis,* Ankara University (in Turkish).

Skempton, A. W. (1986), "Standard penetration test procedures" *Geotechnique*, vol. 36, no. 3, pp. 425-557.

Sykora D. W., Koester J. P. (1988). "Review of existing correlations between shear wave velocity or shear modulus and standard penetration resistance in soils." Proceedings, Earthquake Engineering and Soil Dynamics II Conference, pp. 389-404, Park City, UT.

Sykora, D. W. (1987). "Creation of a data base of seismic shear wave velocities for correlation analysis." *Geotech. Lab. Miscellaneous Paper GL-87-26,* U.S. Army Engineer Waterways Experiment Station, Vicksburg, Miss.

Sykora, D. E., and Stokoe, K. H. (1983). "Correlations of in-situ measurements in sands of shear wave velocity," *Soil Dyn. Earthq. Eng.,* 20**,** 125–36.

Ulugergerli, U. E. and Uyanik, O. (2007). "Statistical correlations between seismic wave velocities and SPT blow counts and the relative density of soils," *J. Test. Eval.,* 35**,** 1–5.

Venables and Smith (2009). "An introduction to R, Notes on R: a programming environment for data analysis and graphics." Version 2.10.1. 108 p.

Yamada, S., Hyodo, M., Orense, R. P., Dinesh, S. V., and Hyodo, T. (2008). "Strain-dependent dynamic properties of remolded sand-clay mixtures." *J. Geotech. Geoenviron. Eng.*, 134(7), 972-981.

Youd, T. L. et al. (2001). "Liquefaction resistance of soils: summary report from the 1996 NCEER and 1998 NCEER/NSF workshops on evaluation of liquefaction resistance of soils." *J. Geotech. Geoenviron. Eng.*, 127(10), 817-833.

Appendix A: Profiles of N_{60}, σ_v', and V_s Used in Regression Study

This appendix includes plots of vertical effective stress, SPT blow count (N_{60}), measured shear wave velocity (V_s), and median predicted shear wave velocity, $\overline{V_s}$ versus elevation for all boring logs utilized in this study.

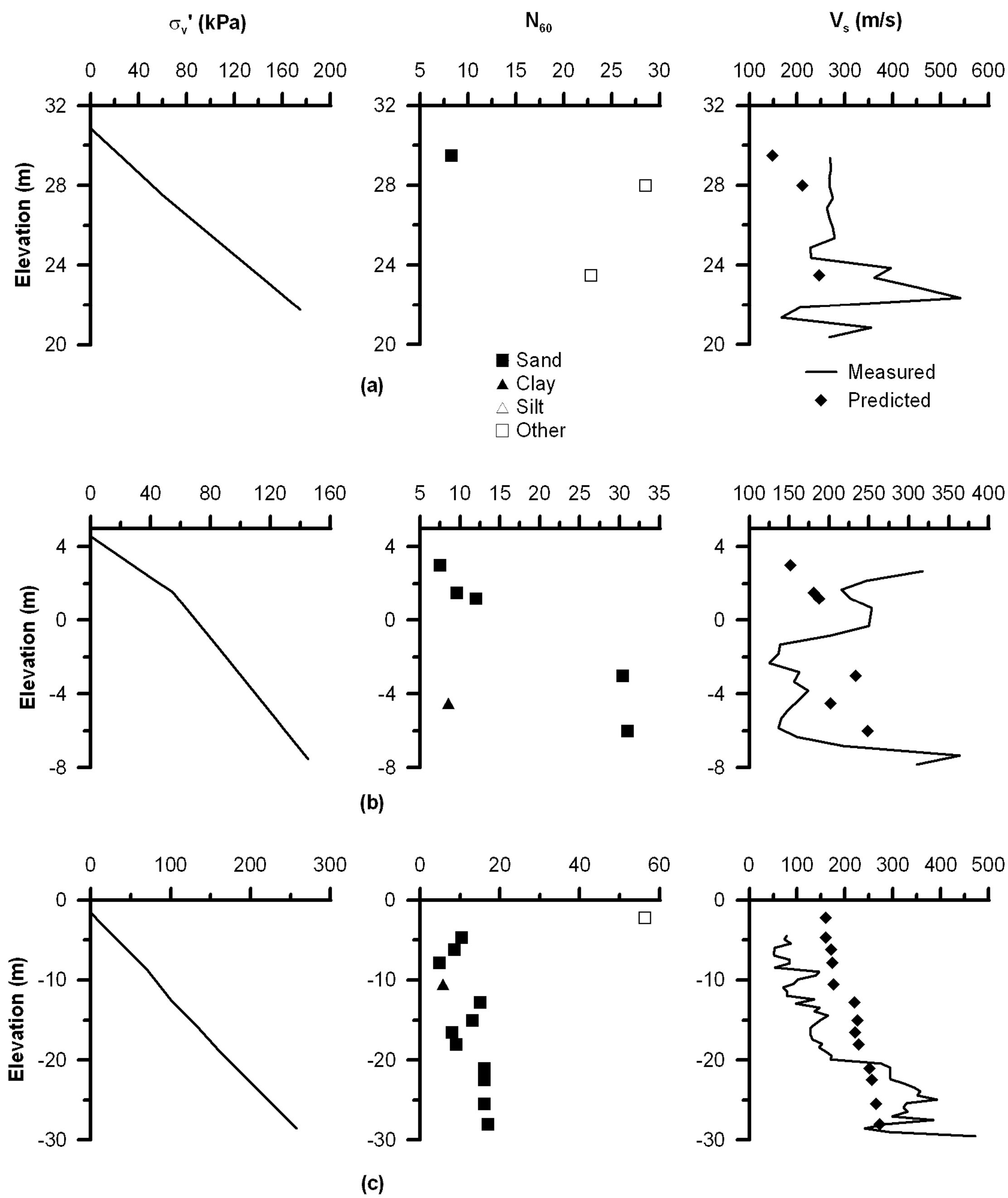

Fig. A.1 (a) Bridge no. 10-0298, boring no. 98-4 (abut.4), (b) Bridge no. 10-0298, boring no. 96-2, (c) Bridge no. 10-0298, boring no. 96-3.

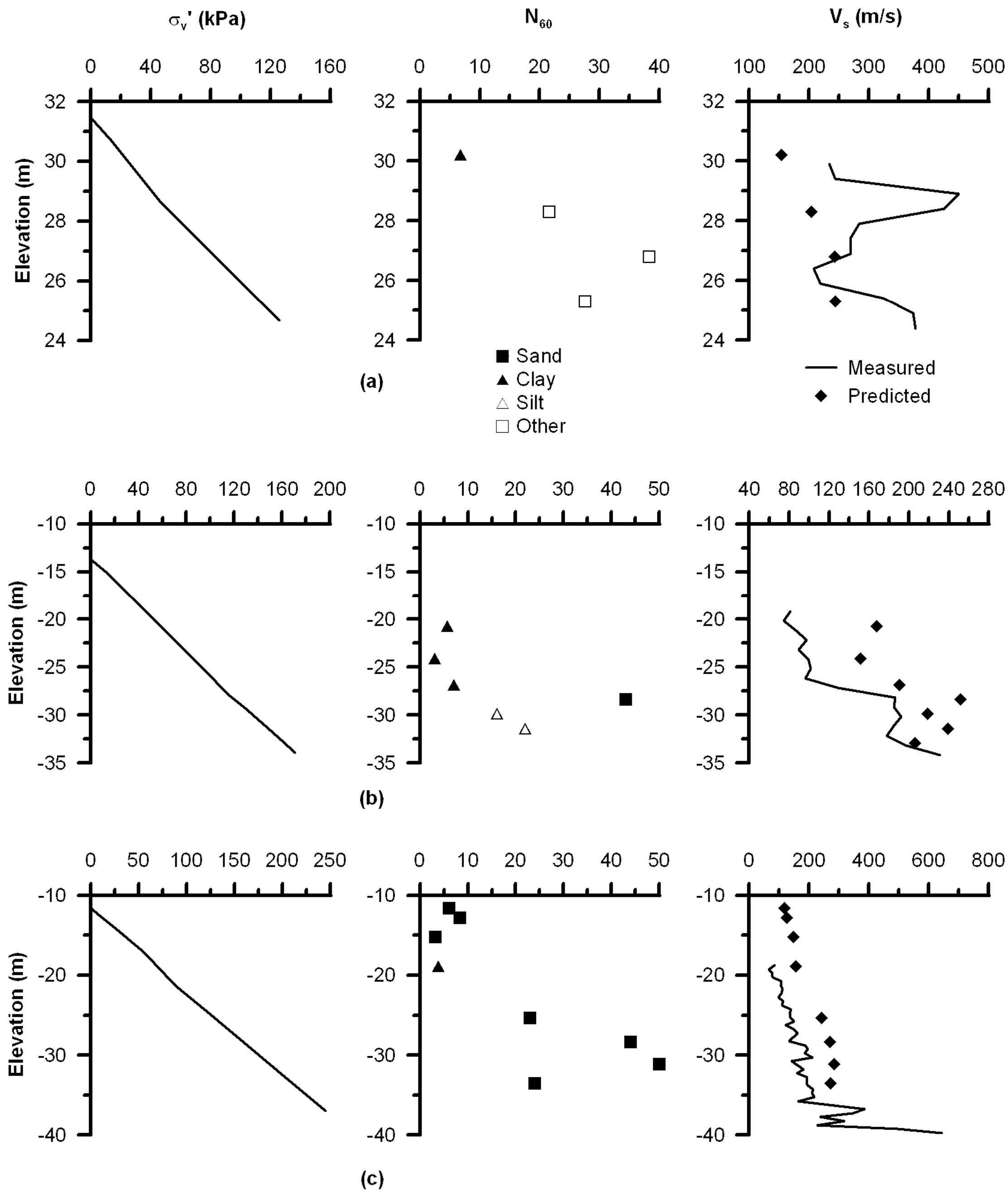

Fig. A.2 (a) Bridge no. 10-0298, boring no. 98-10 (abut 1) (b) Bridge no. 28-0253R, boring no. 94B1R (Pier 9) (c) Bridge no. 28-0153R, boring no. 96-5 (Pier 8).

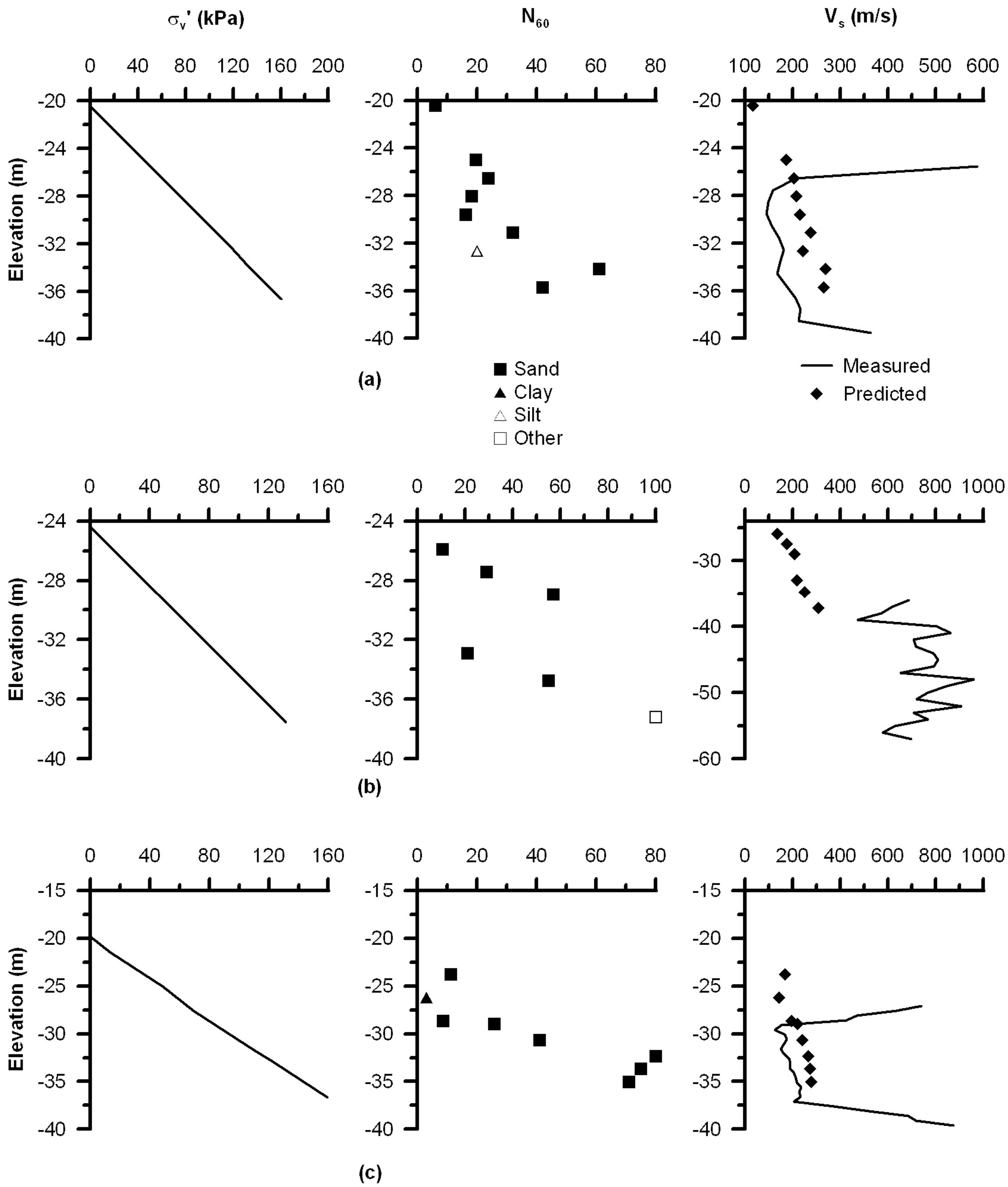

Fig. A.3 (a) Bridge no. 28-1053R, boring no. 95B13R (Pier 7) (b) Bridge no. 28-1053R, boring no. 96-4 (Pier 7) (c) Bridge no. 28-1053R, boring no. 95-12 (Pier 5).

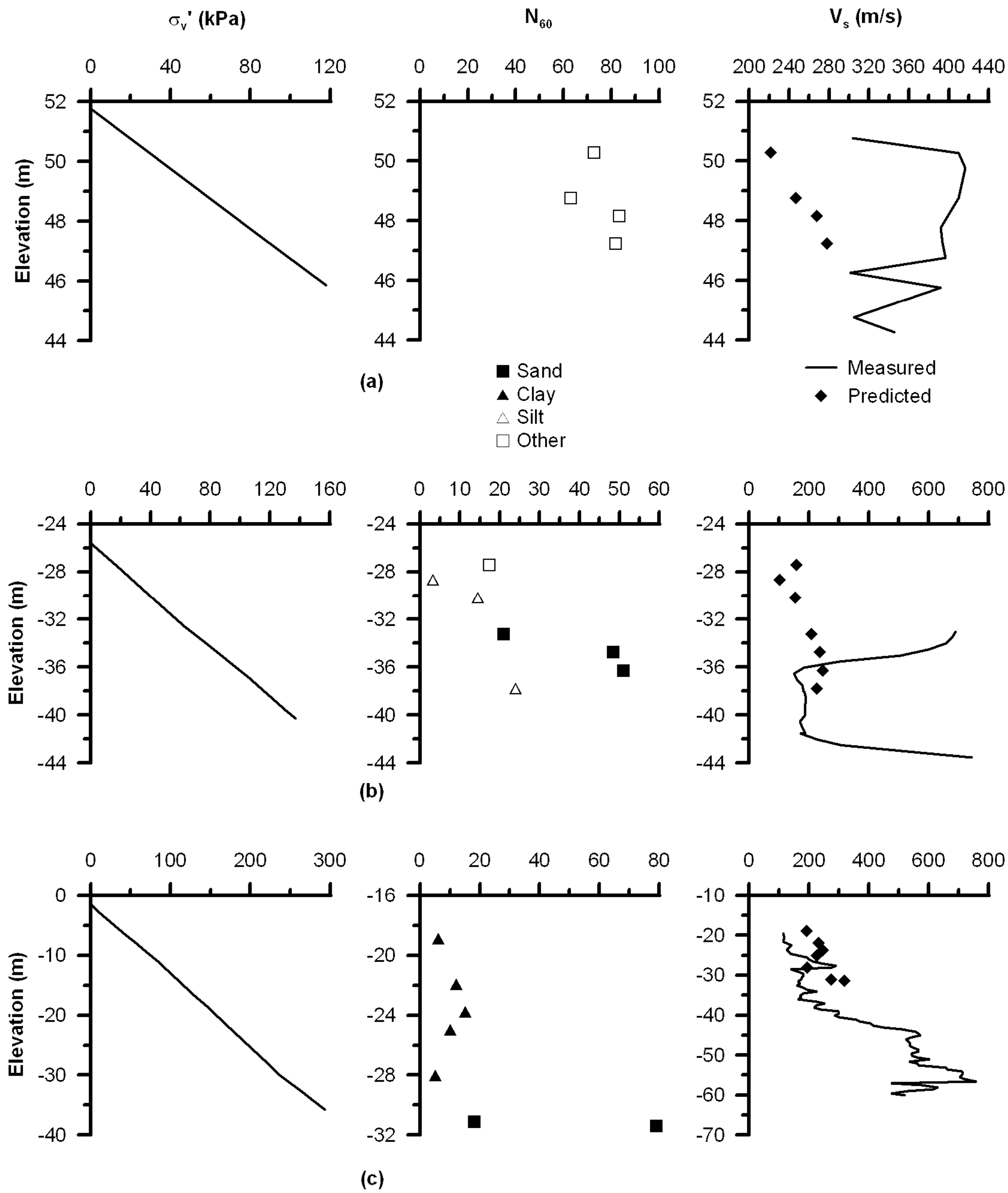

Fig. A.4 (a) Bridge no. 28-0352L, boring no. 96B-29 (b) Bridge no. 28-0352L, boring no. 95-2 (Pier 3) (c) Bridge no. 28-0352L, boring no. 95-1 (Pier 4).

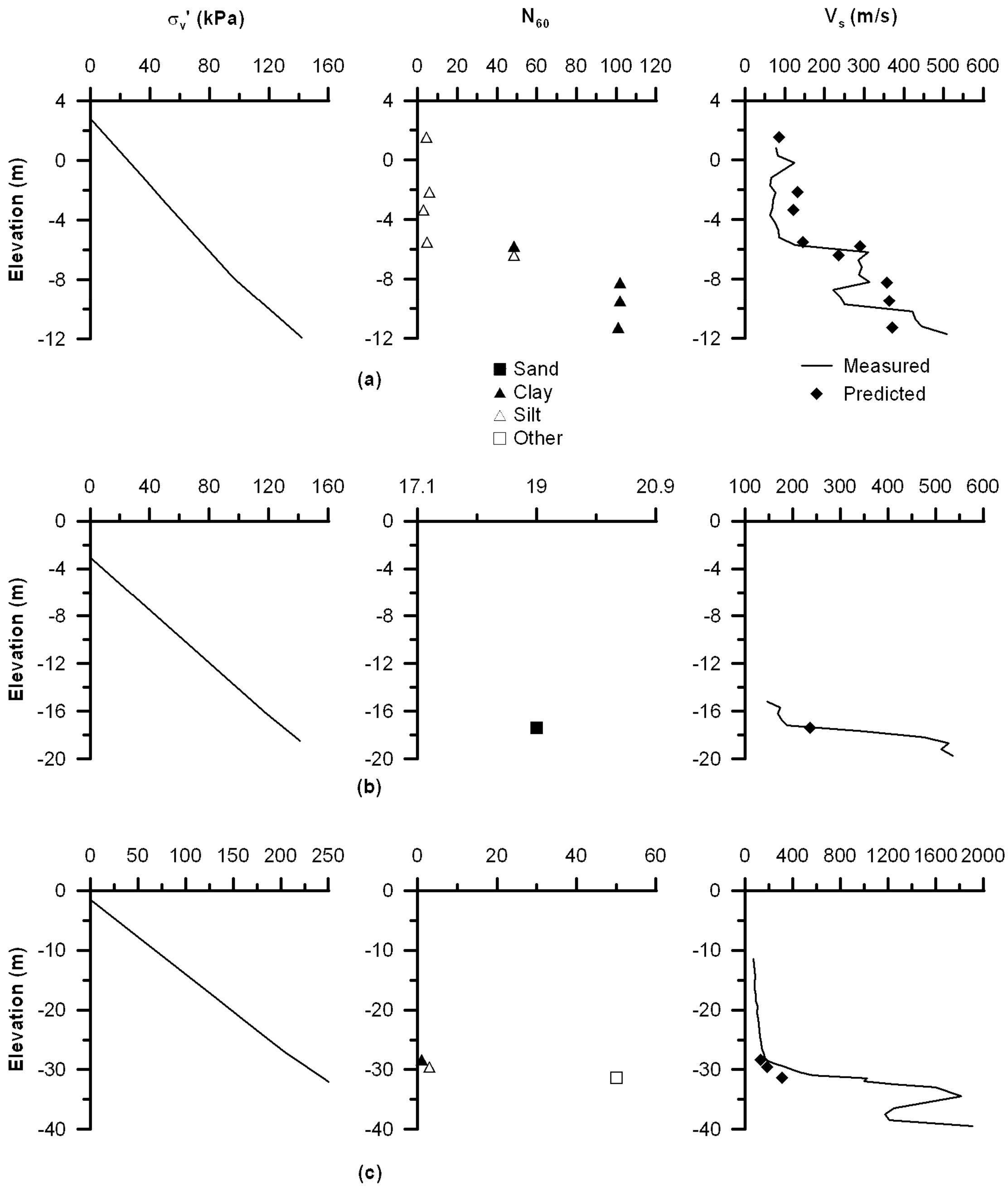

Fig. A.5 **(a) Bridge no. 28-0352L, boring no. 96B-37 (b) Bridge no. 28-0100, boring no. 96-2 (Piers 10 and 11) (c) Bridge no. 28-0100, boring no. 96-5 (Piers 31/32).**

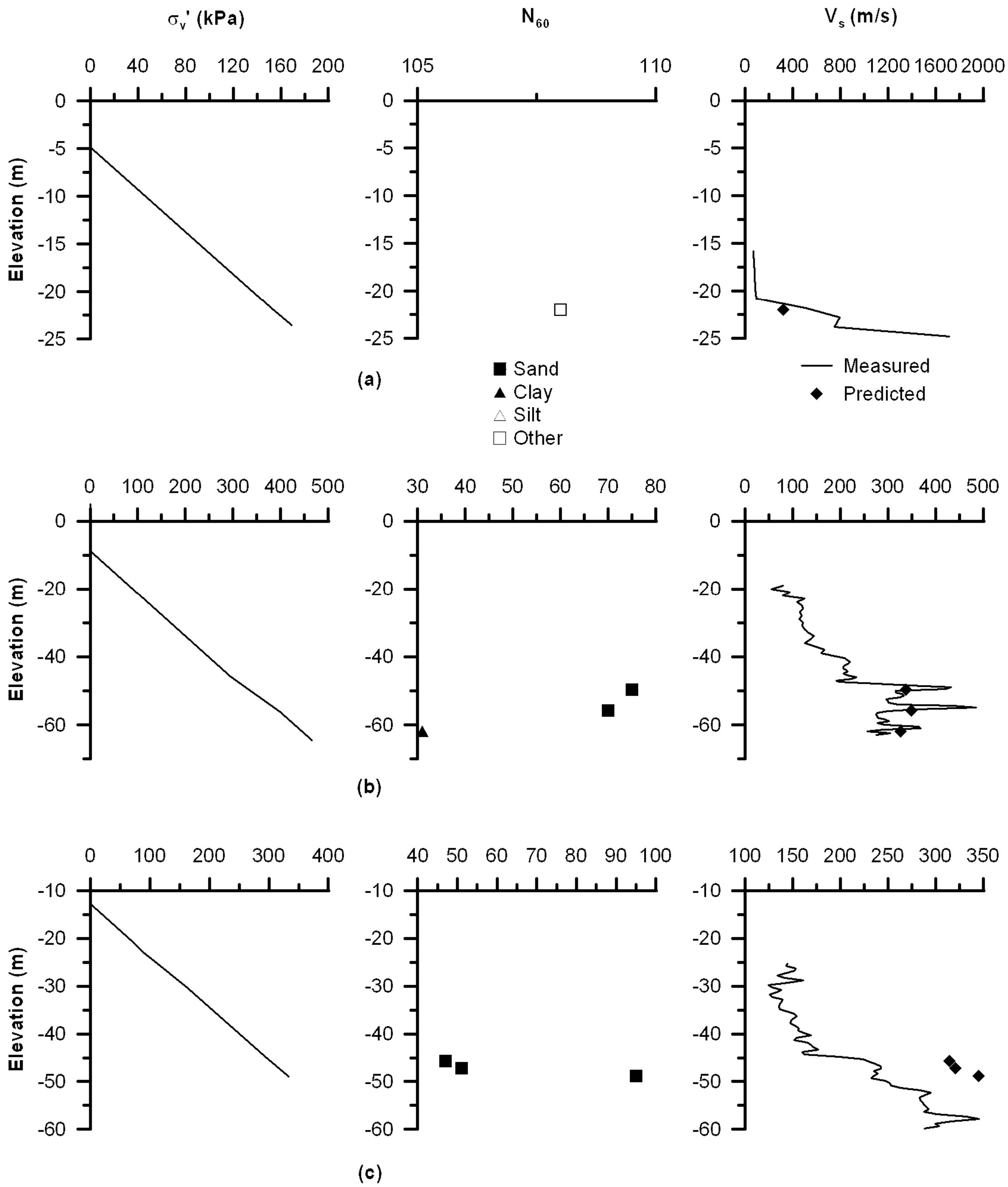

Fig. A.6 (a) Bridge no. 28-0100, boring no. 96-7 (Pier 8) (b) Bridge no. 28-0100, 95-7 (Pier 21) (c) Bridge no. 28-0100, boring no. 95B4R (Pier 25).

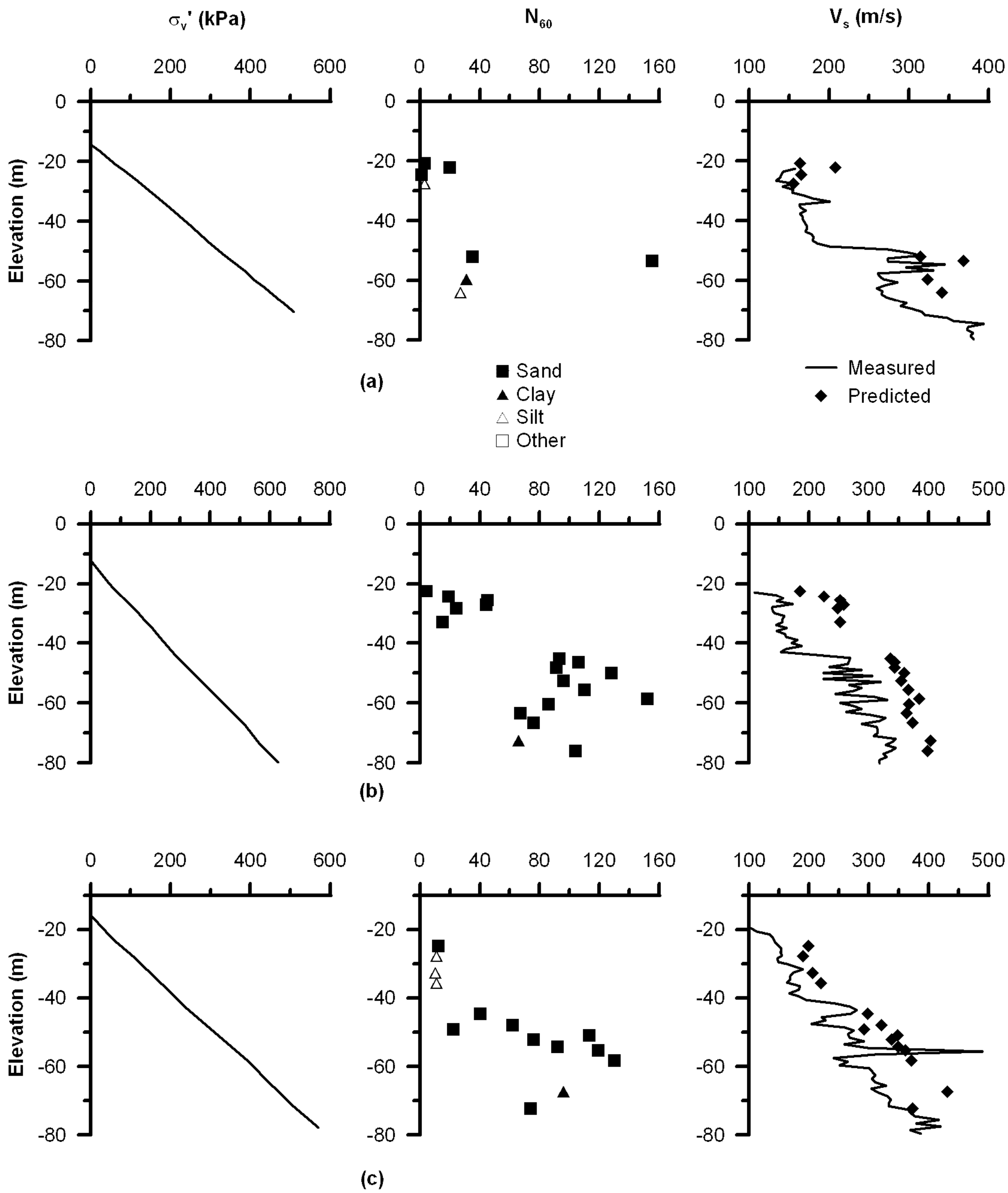

Fig. A.7 (a) Bridge no. 28-0100, boring no. 95B5R (Pier 35) (b) Bridge no. 28-0100, boring no. 95B2R (Pier 32/33) (c) Bridge no. 28-0100, boring no. 95B3R/95B9R (Pier 34).

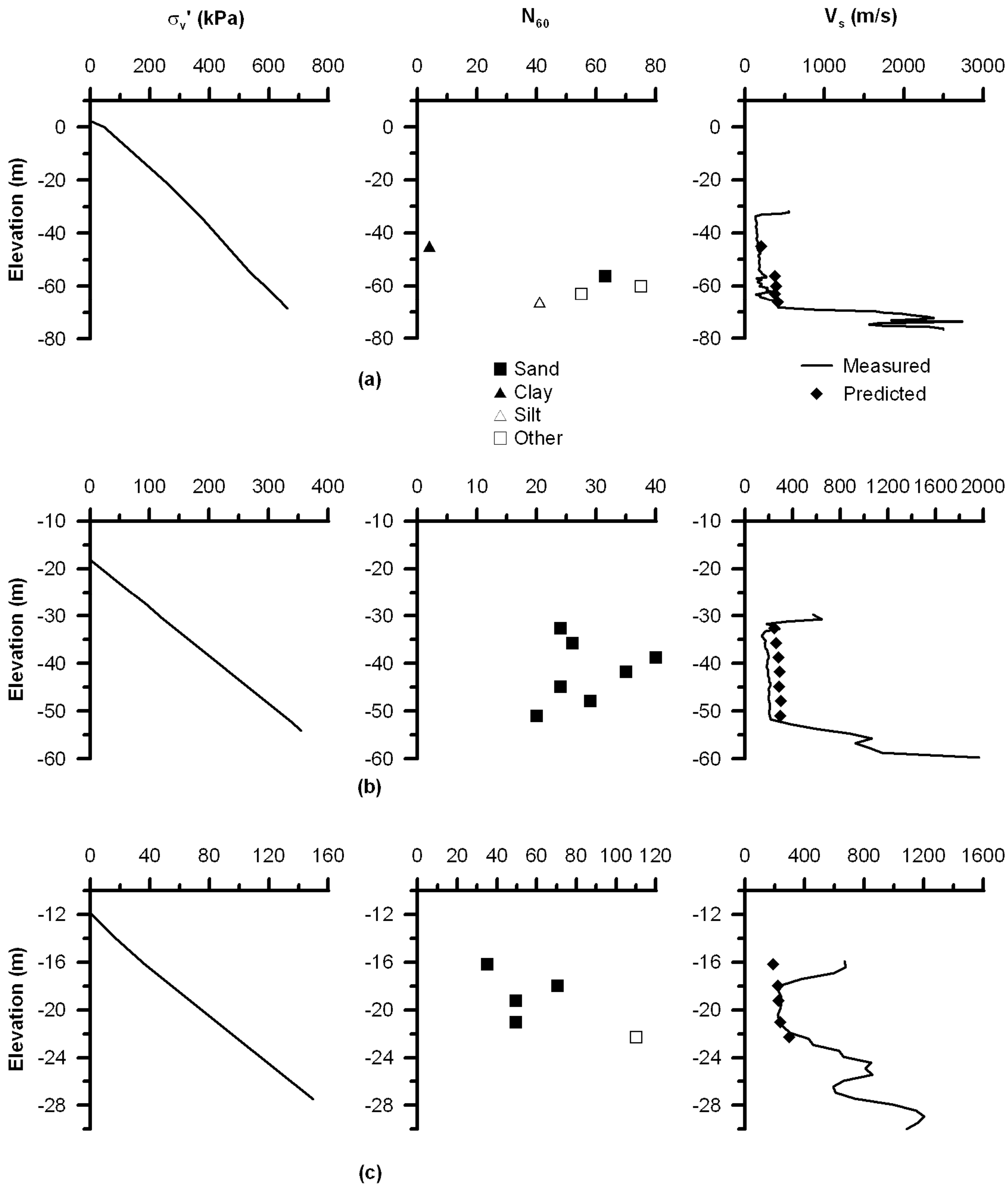

Fig. A.8 (a) Bridge no. 28-0100, boring no. 95-10 (Pier 47) (b) Bridge no. 28-0100, boring no. 95-11 (Pier 48) (c) Bridge no. 28-0100, boring no. 95B1R (Pier 58).

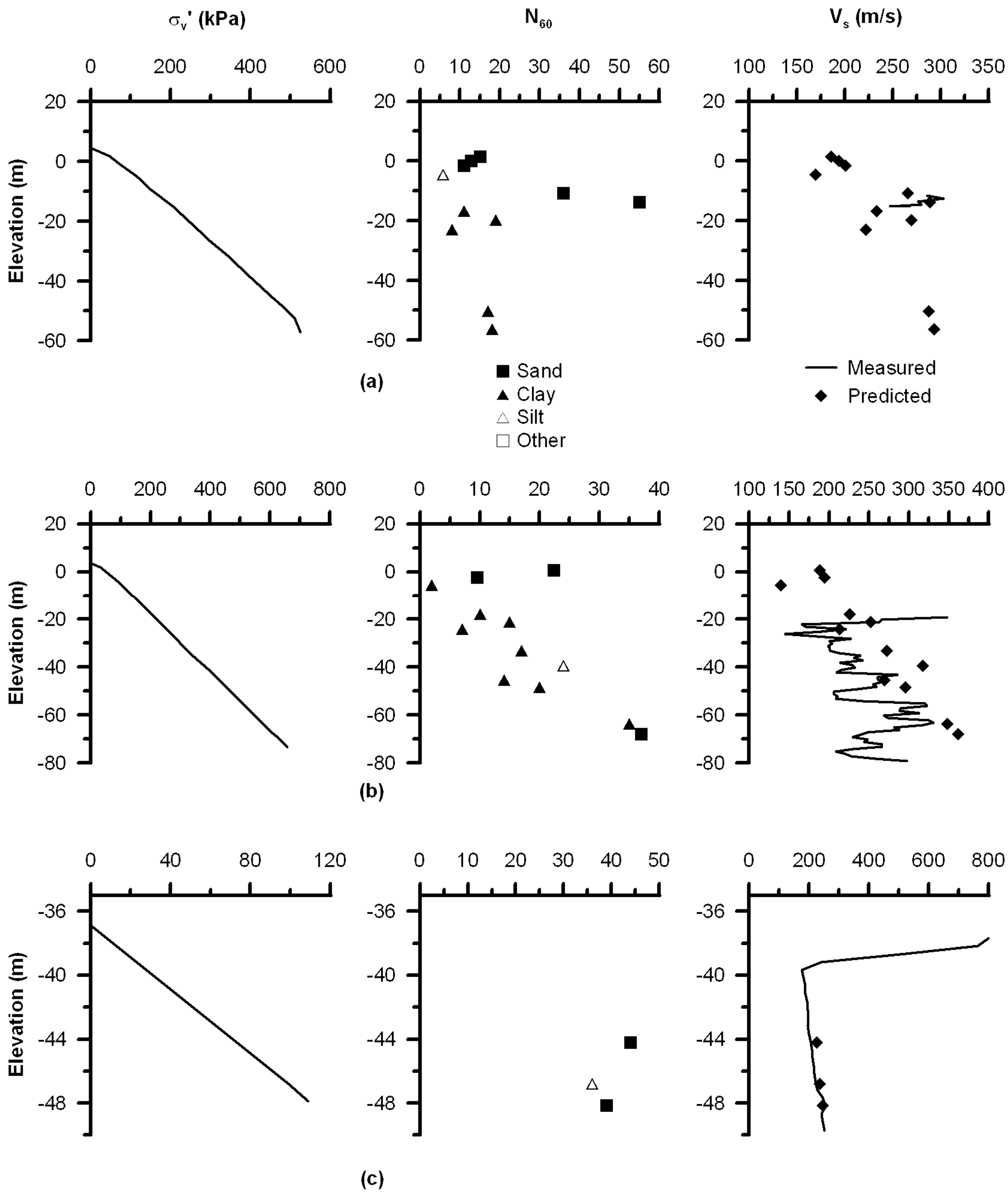

Fig. A.9 (a) Bridge no. 33-0025, boring no. B6 (Pier E19) (b) Bridge no. 33-0025, boring no. B-7 (Pier E10) (c) Bridge no. 34-0003, boring no. 95-14 (Pier W6).

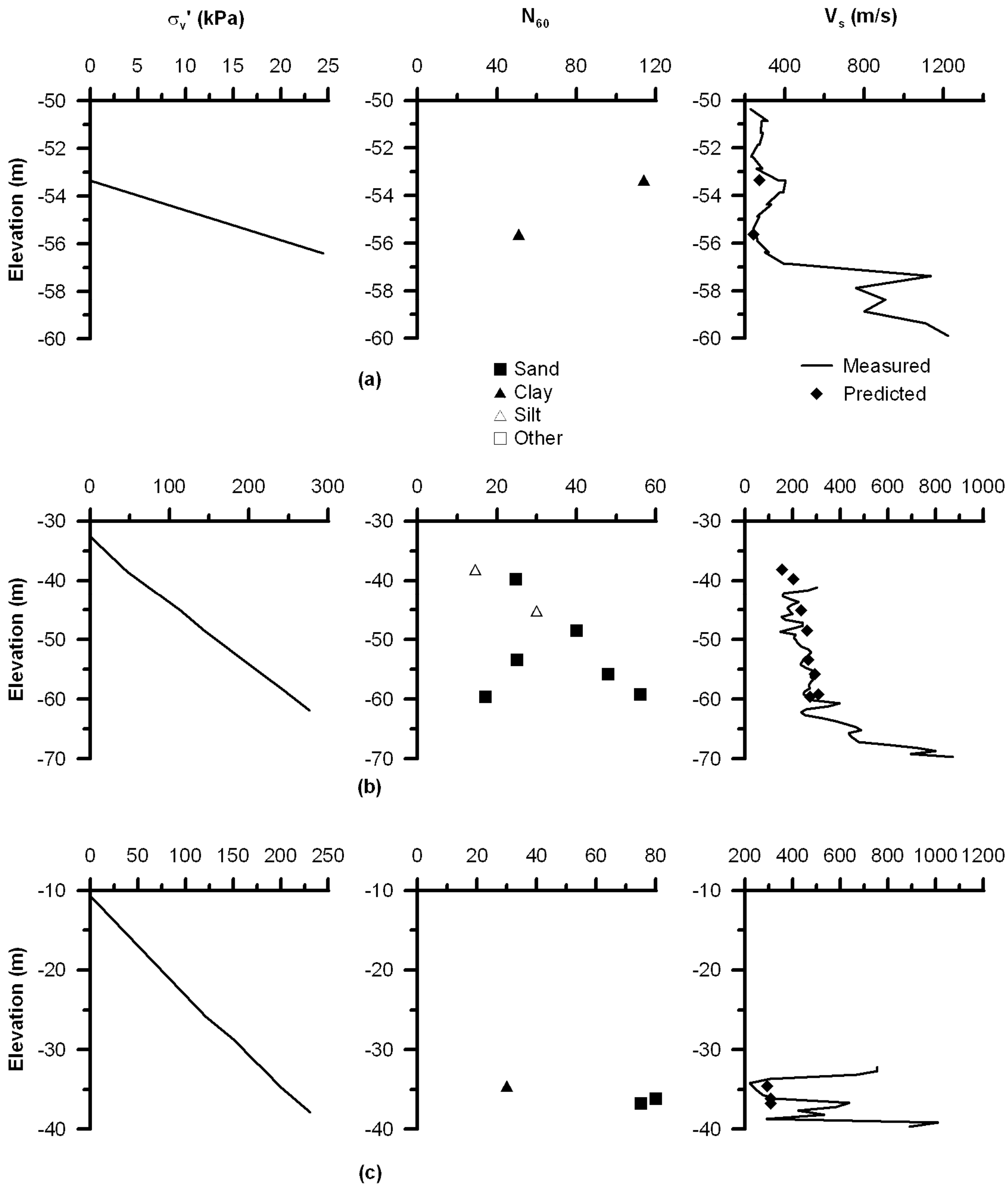

Fig. A.10 (a) Bridge no. 34-0003, boring no. 95-12 (Pier W4) (b) Bridge no. 34-0003, boring no. 95-11 (Pier W3) (c) Bridge no. 34-0003, boring no. 95-10 (Pier W2).

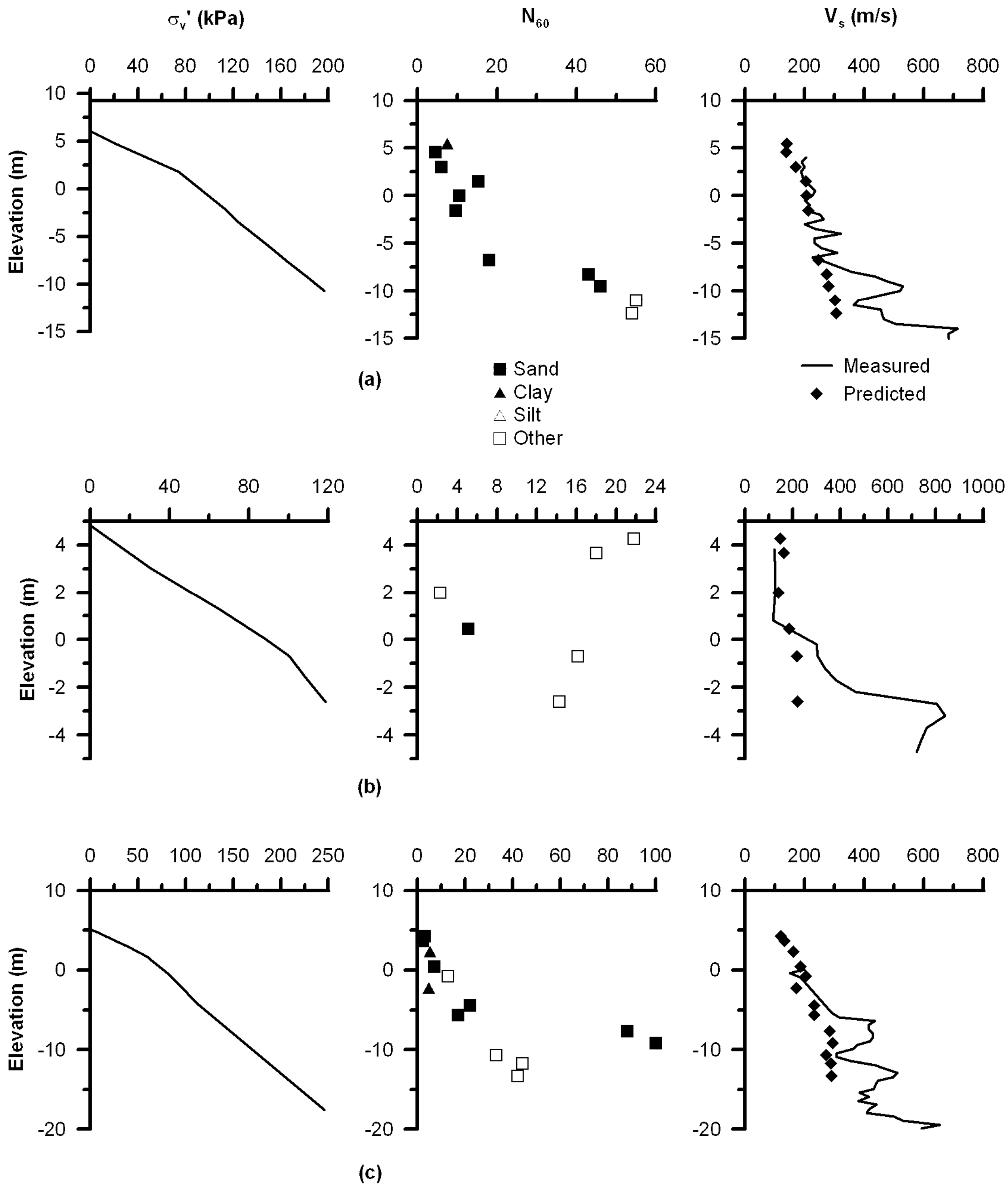

Fig. A.11 (a) Bridge no. 34-0003, boring no. 95-5 (Pier A) (b) Bridge no. 34-0003, boring no. 95-4 (c) Bridge no. 34-0003, boring no. 95-6.

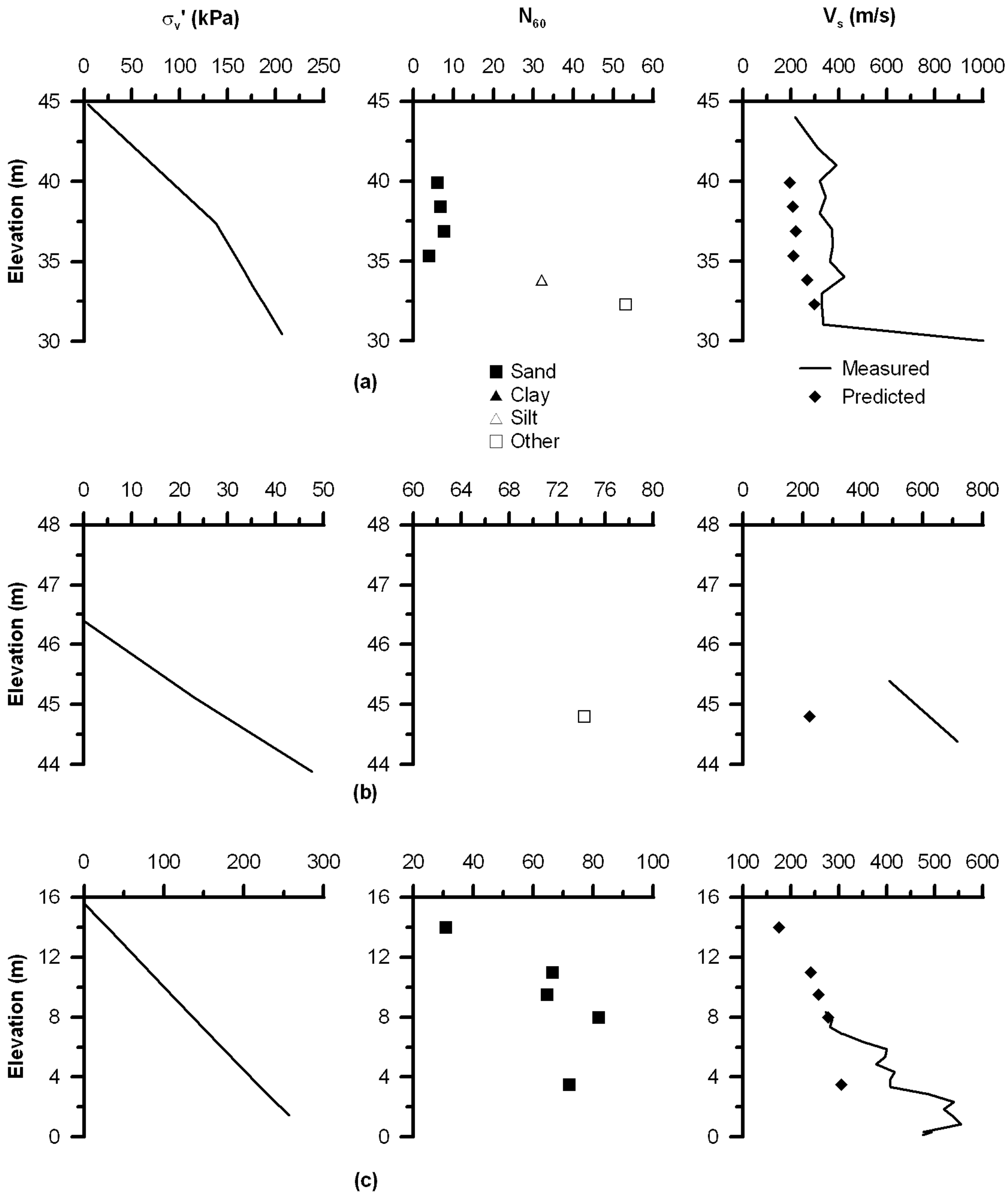

Fig. A.12 (a) Bridge no. 34-0004, boring no. B95-2 (b) Bridge no. 34-0004, boring no. B95-3 (c) Bridge no. 34-0077, boring no. 01-B2.

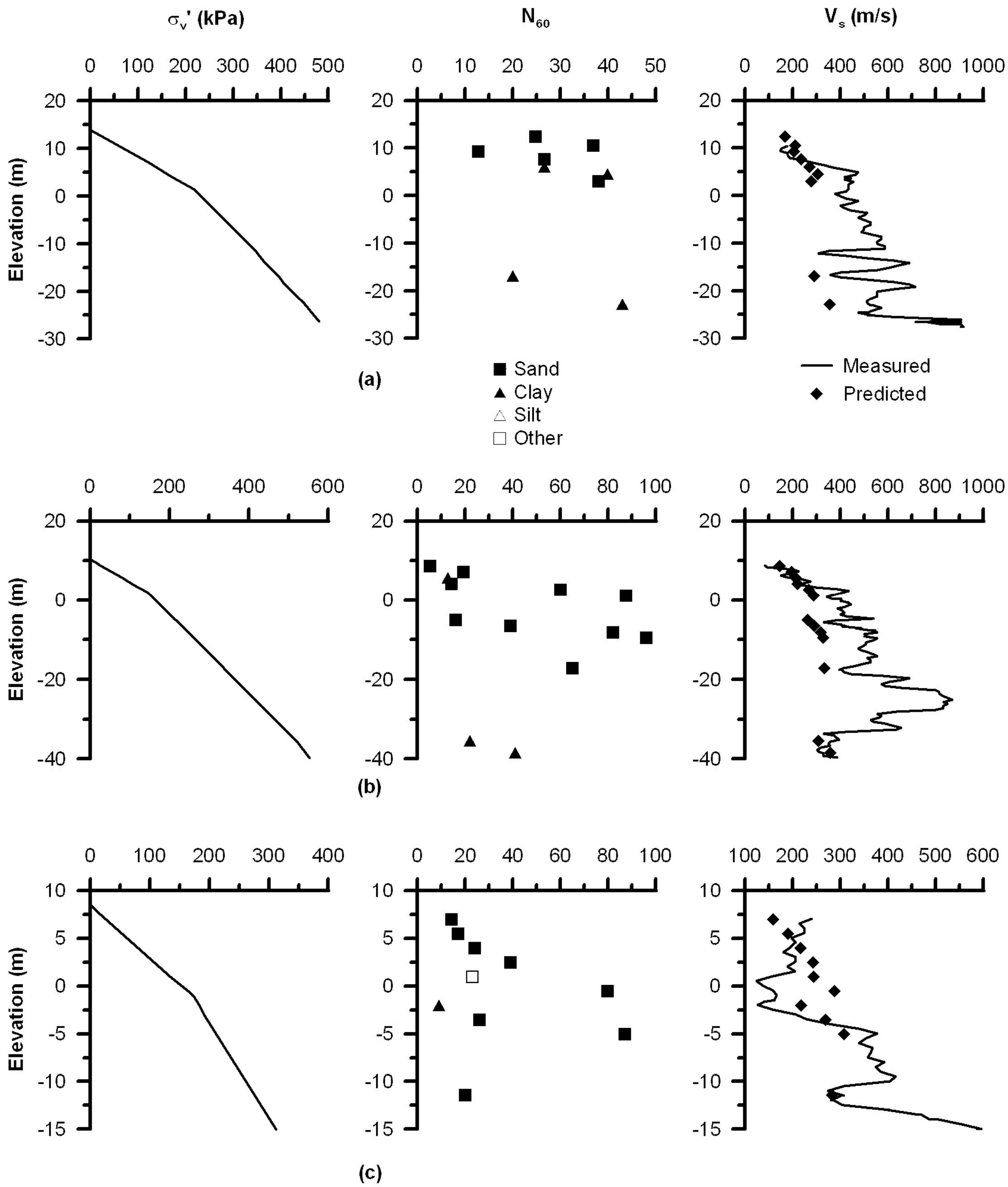

Fig. A.13 (a) Bridge no. 34-0077, boring no. 01-05 (b) Bridge no. 34-0077, boring no. 01-08 (c) Bridge no. 34-0077, boring no. 01-11.

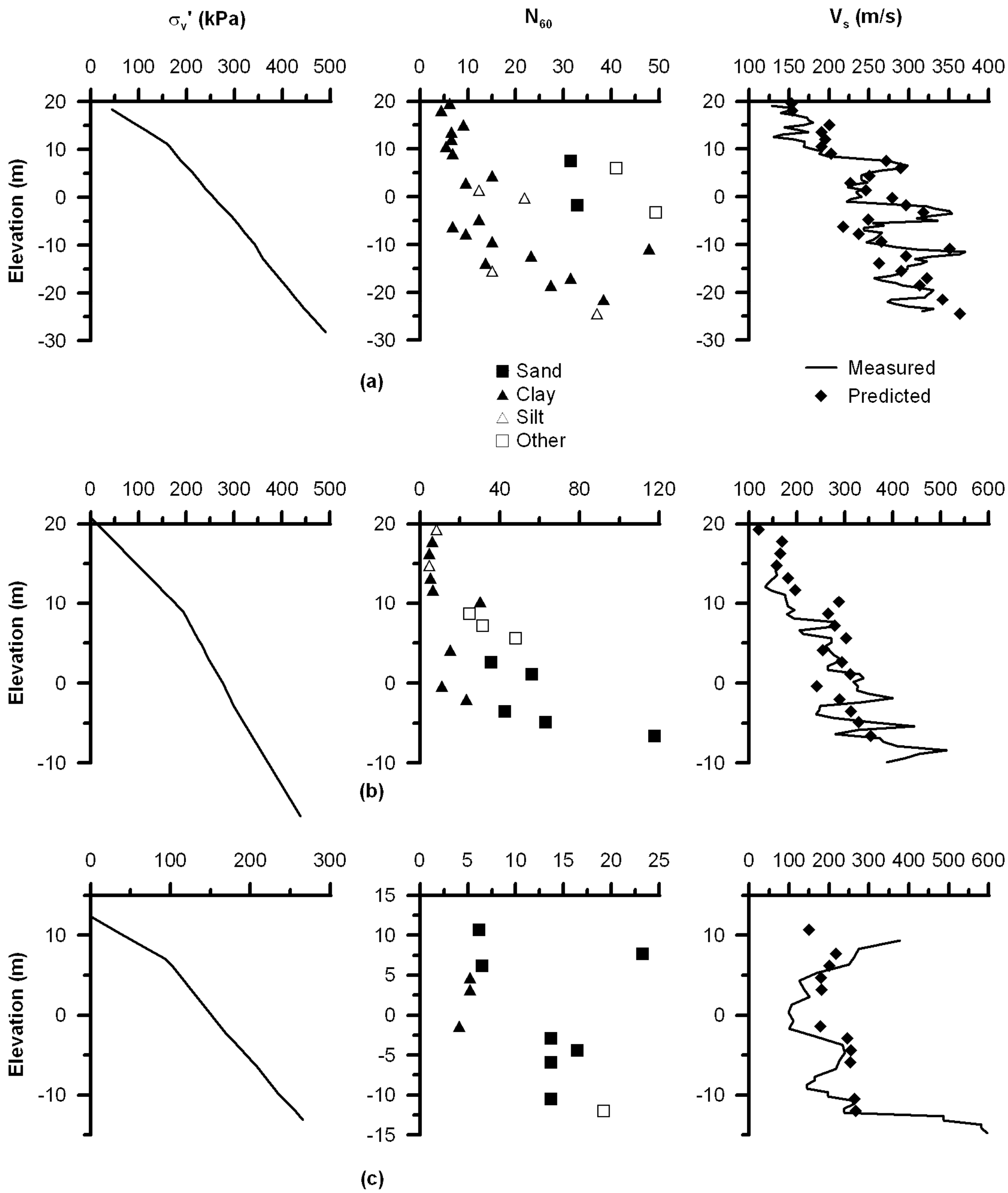

Fig. A.14 (a) Bridge no. 37-0853, boring no.98-1 (Pier 4) (b) Bridge no. 38-0583, boring no. 98-4 (Bent 7) (c) Bridge no. 49-0014L, boring no.98-1 (Abut 1).

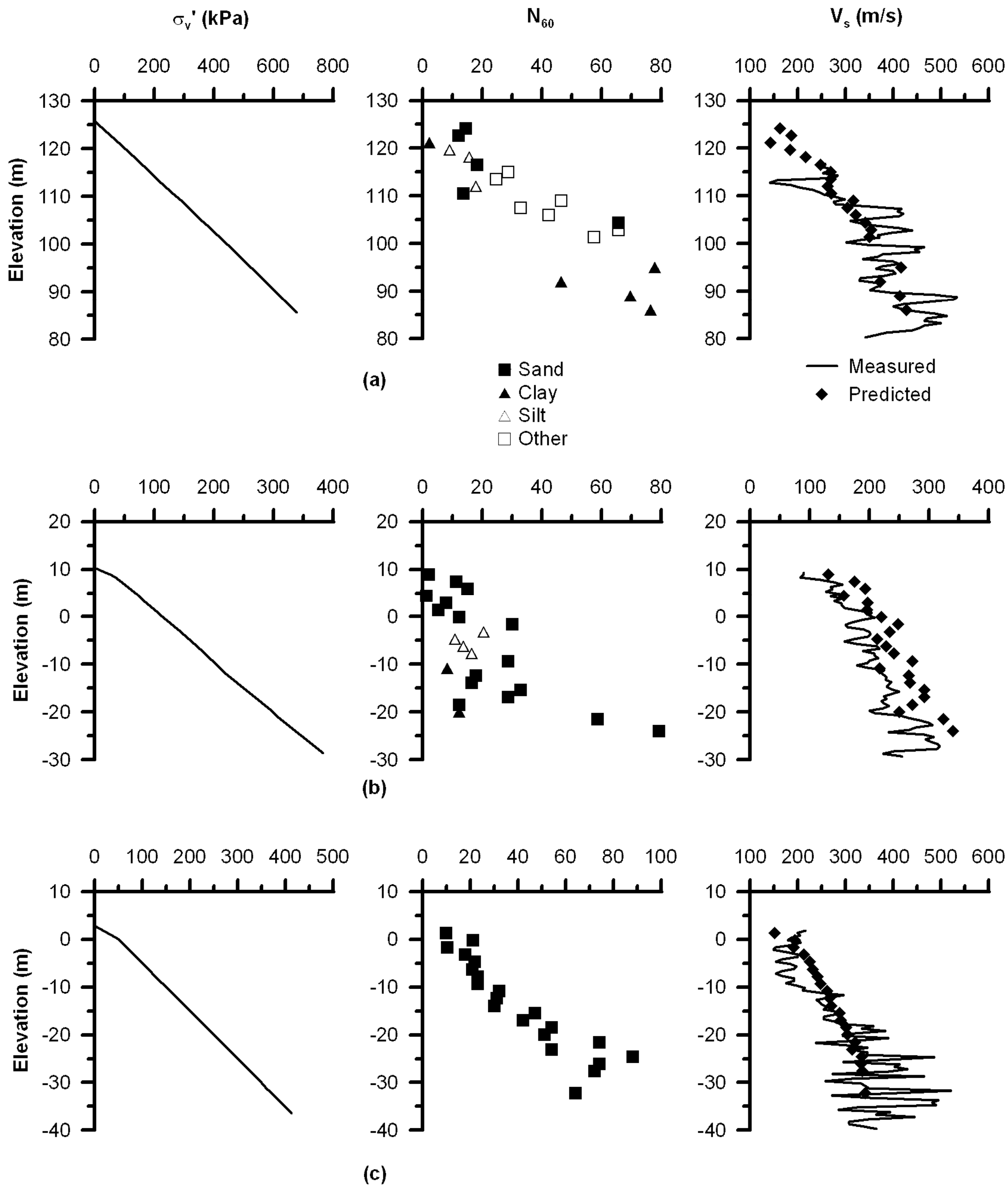

Fig. A.15 (a) Bridge no. 51-0139, boring no. 98-1 (Abut 1) (b) Bridge no. 52-0443, boring no. 99-1 (c) Bridge no. 53-1471, boring no. 95B5R.

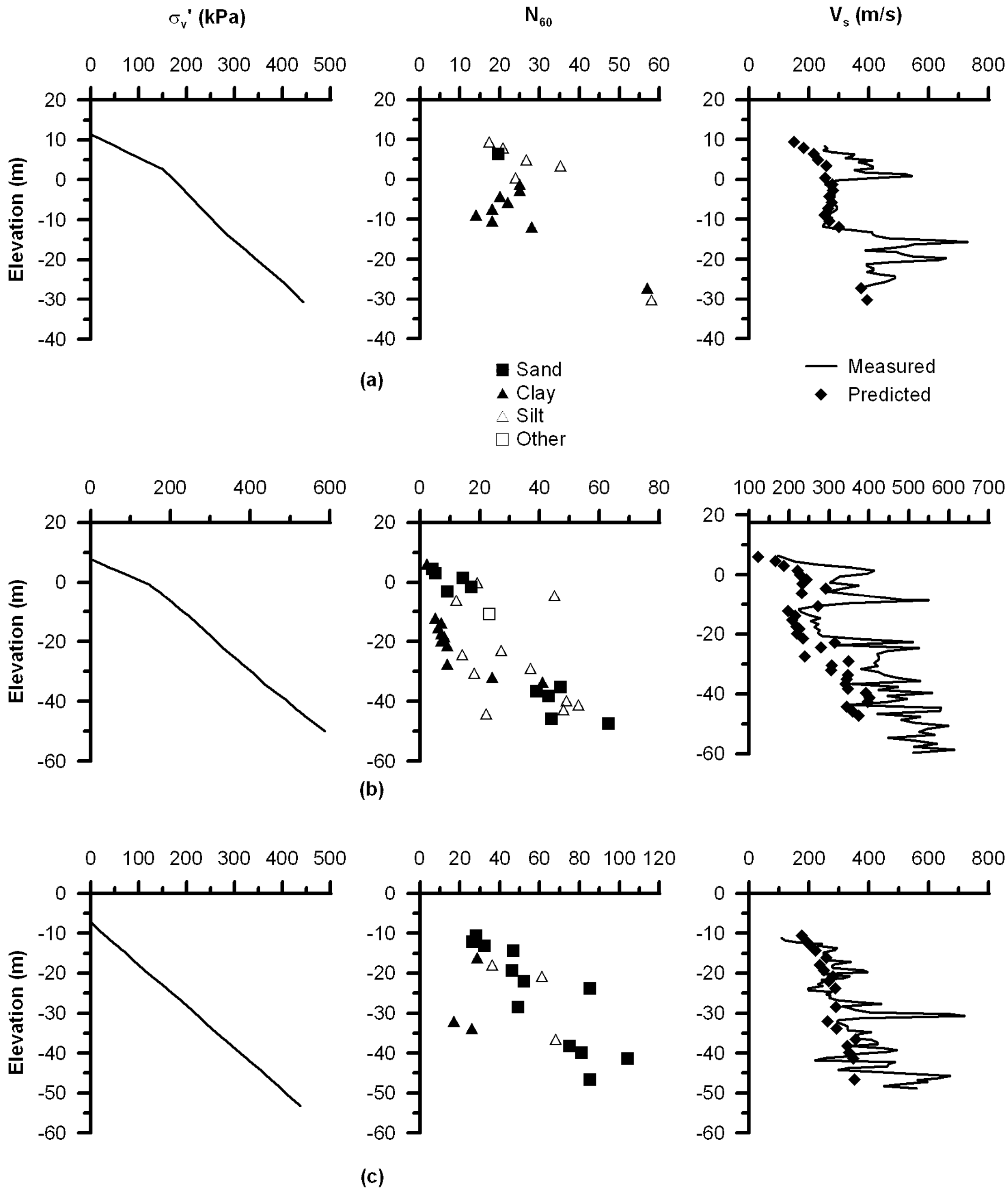

Fig. A.16 (a) Bridge no. 53-1471, boring no. 95B4R (b) Bridge no. 53-1471, boring no. 95B1R (c) Bridge no. 53-1471, boring no. 95B2R.

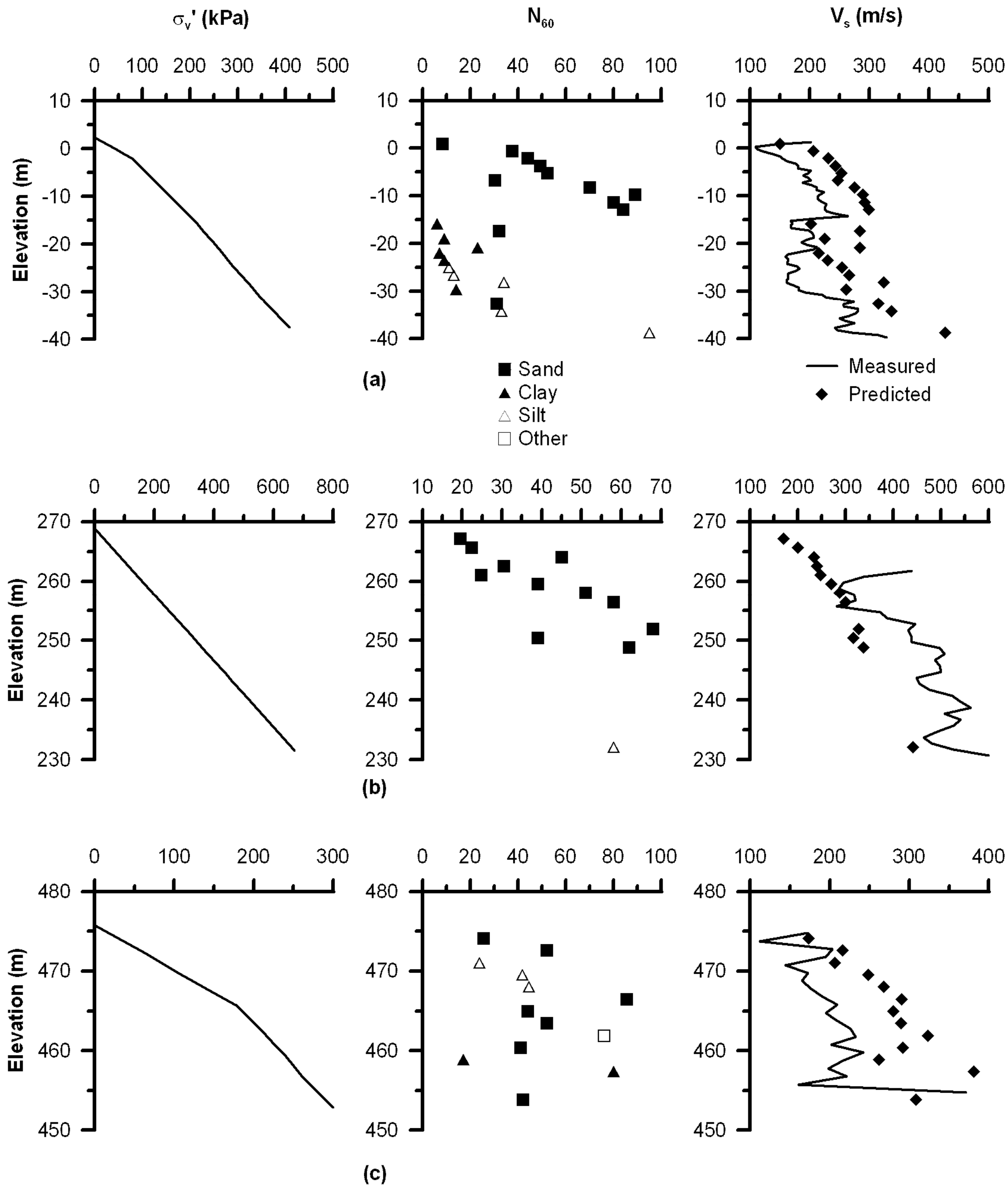

Fig. A.17 (a) Bridge no. 53-1471, boring no. 95B3R (b) Bridge no. 53-2272, boring no. B-1 (c) Bridge no. 53-2790R, boring no. B-6.

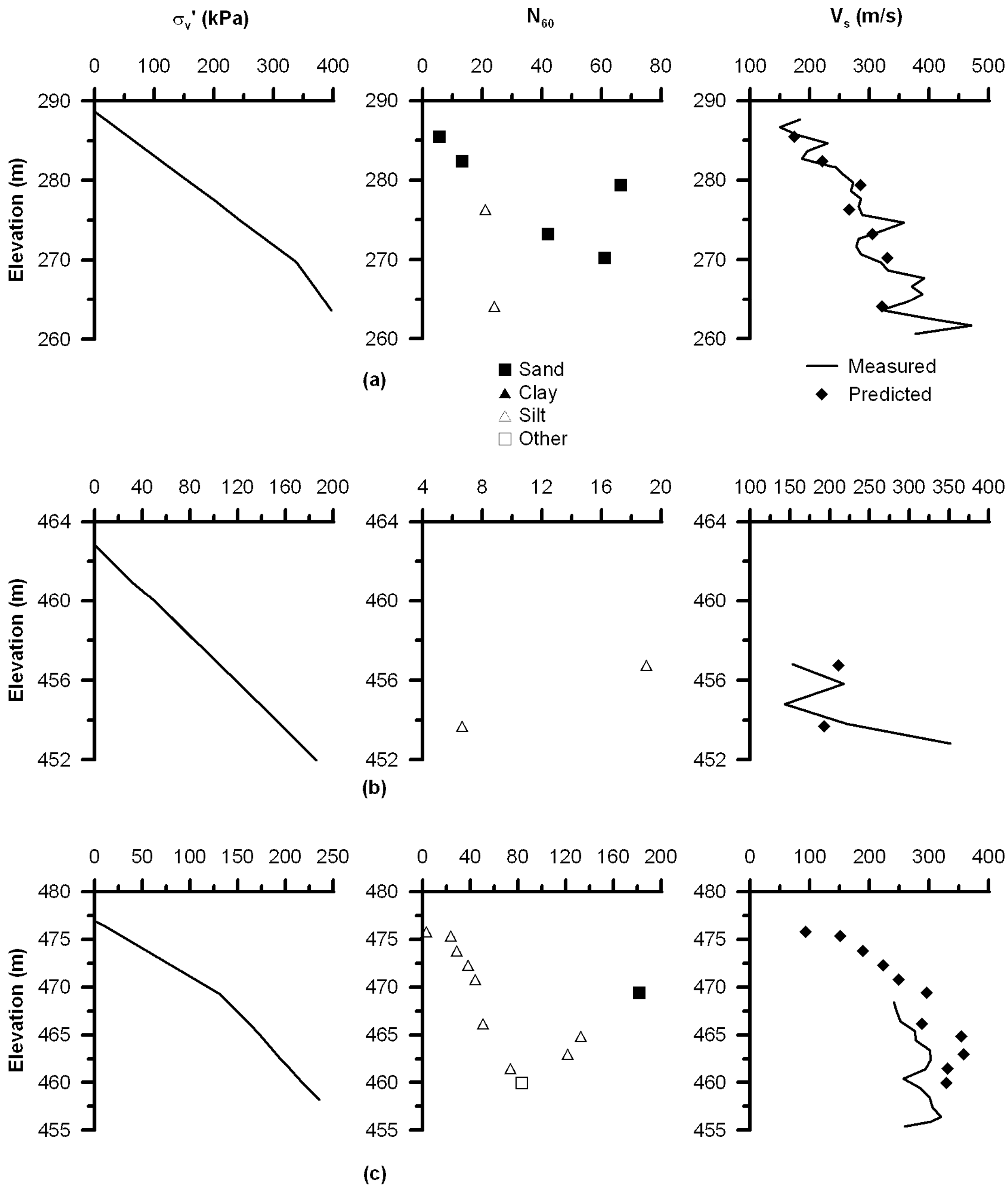

Fig. A.18 (a) Bridge no. 53-2794R, boring no. B-1 (b) Bridge no. 53-2795F, boring no. 94-21 (c) Bridge no. 53-2796F, boring no. 94-30.

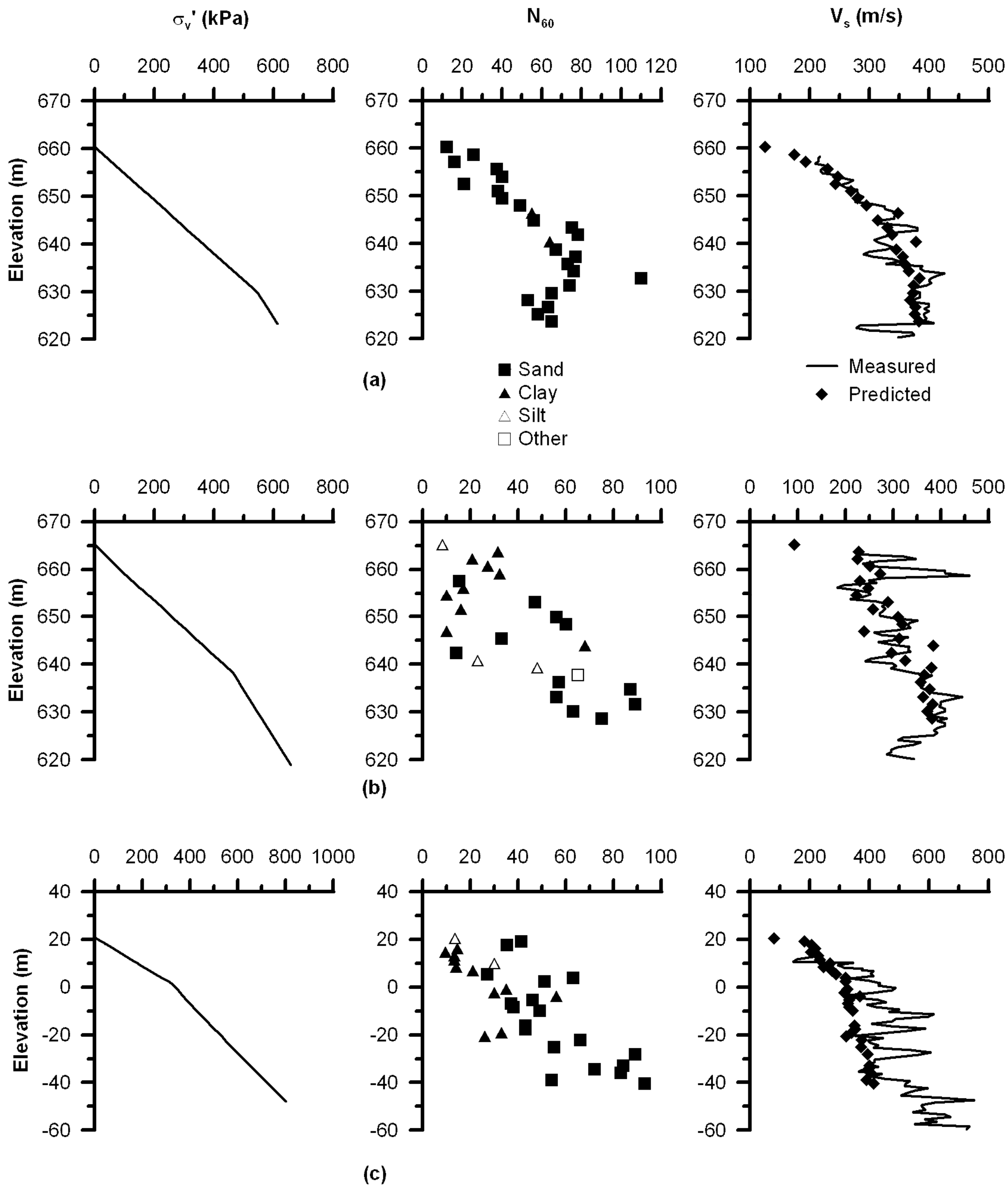

Fig. A.19 (a) Bridge no. 54-1110R, boring no. 98-1 (Abut 1) (b) Bridge no. 54-1110R, boring no. 98-6 (Abut 8) (c) Bridge no. 57-0857, boring no. 96-52 (Bents R48 and 49).

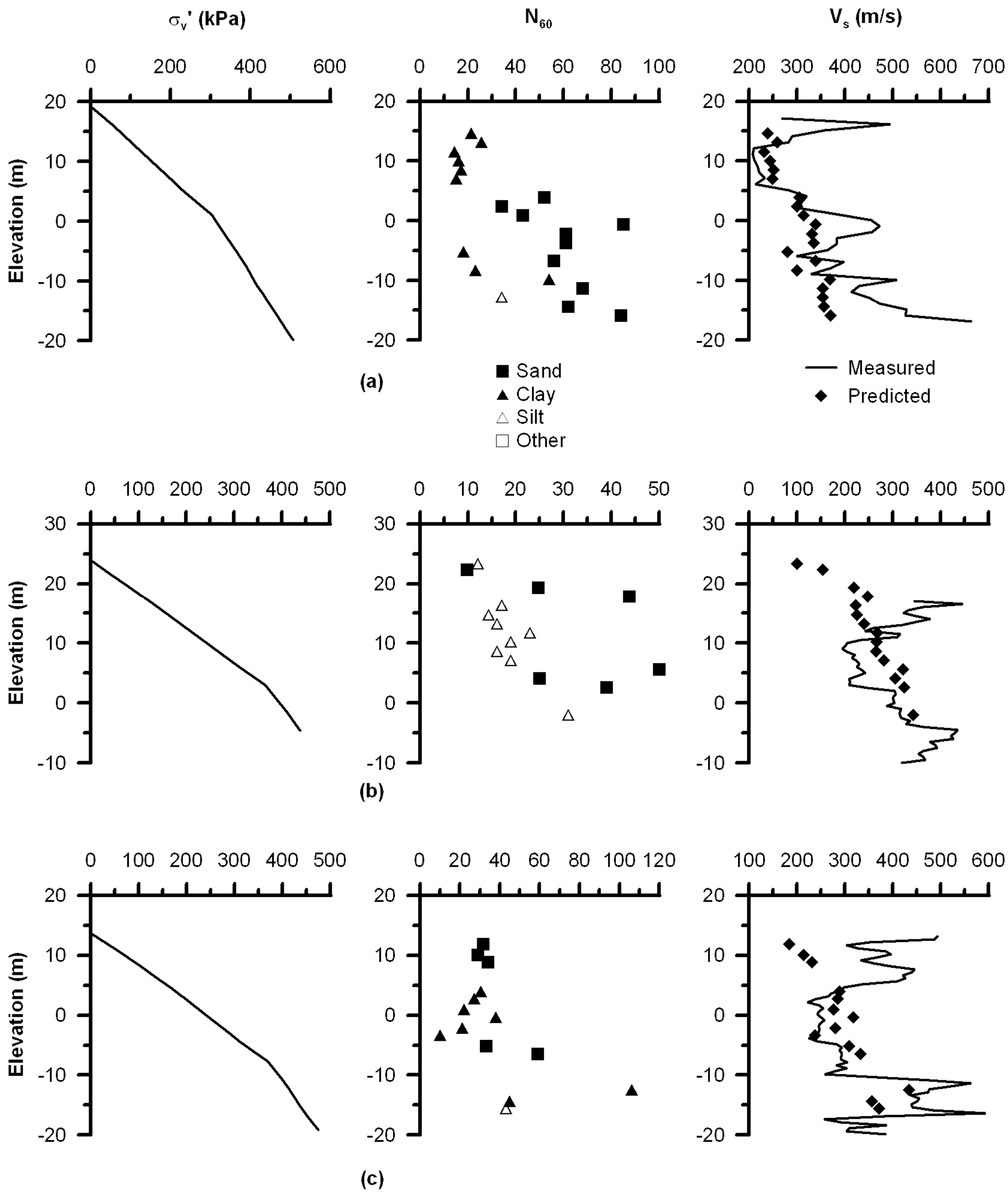

Fig. A.20 (a) Bridge no. 57-0857, boring no. 96-17 (Abut S48) (b) Bridge no. 57-0857, boring no. 95-2 (Pier 33) (c) Bridge no. 57-0857, boring no. 96-16 (Bent 41F,R).

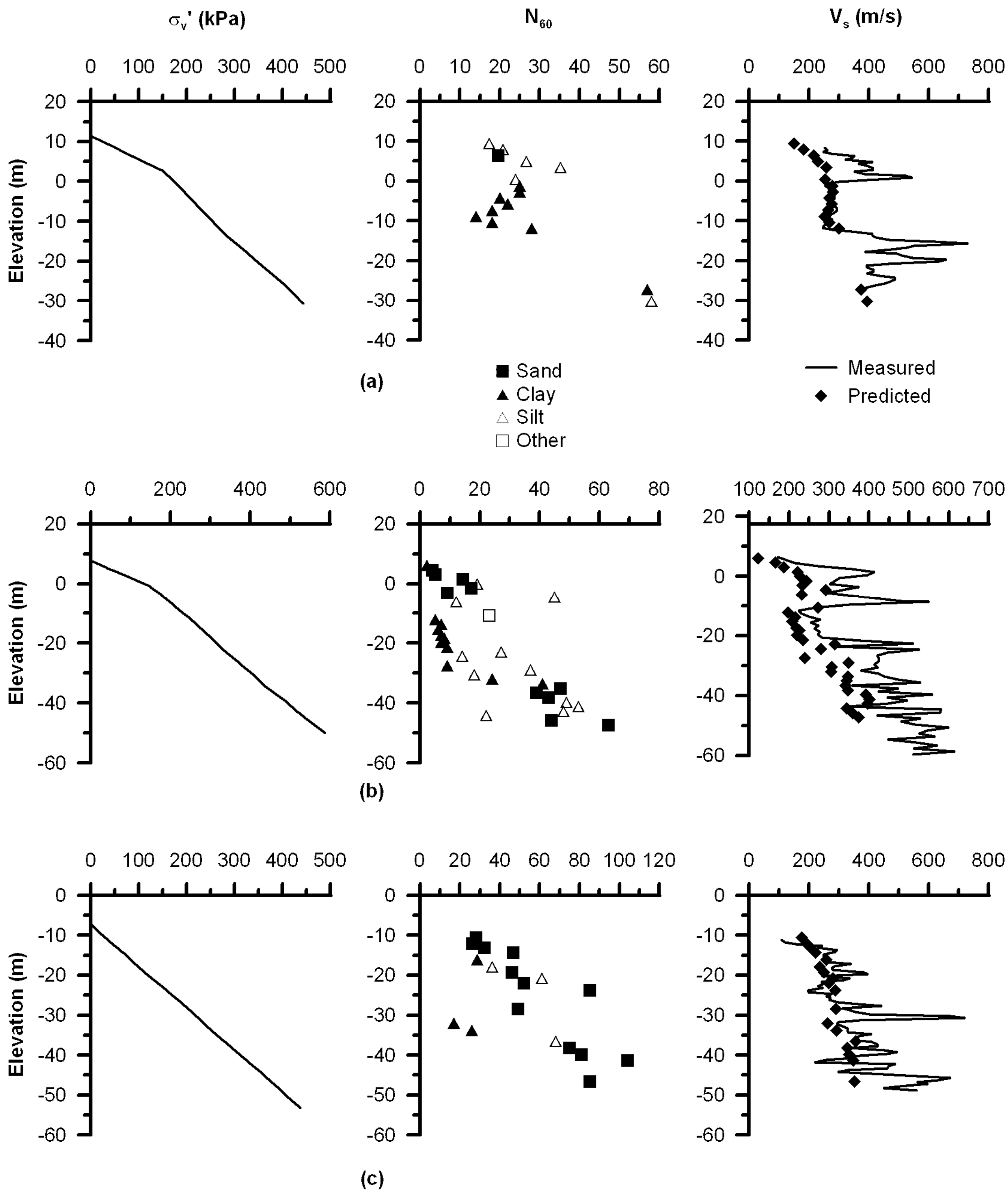

Fig. A.21 **(a) Bridge no. 57-0857, boring no. 96-29 (b) Bridge no. 57-0857, boring no. 96-53R (c) Bridge no. 57-0857, boring no. 96-66.**

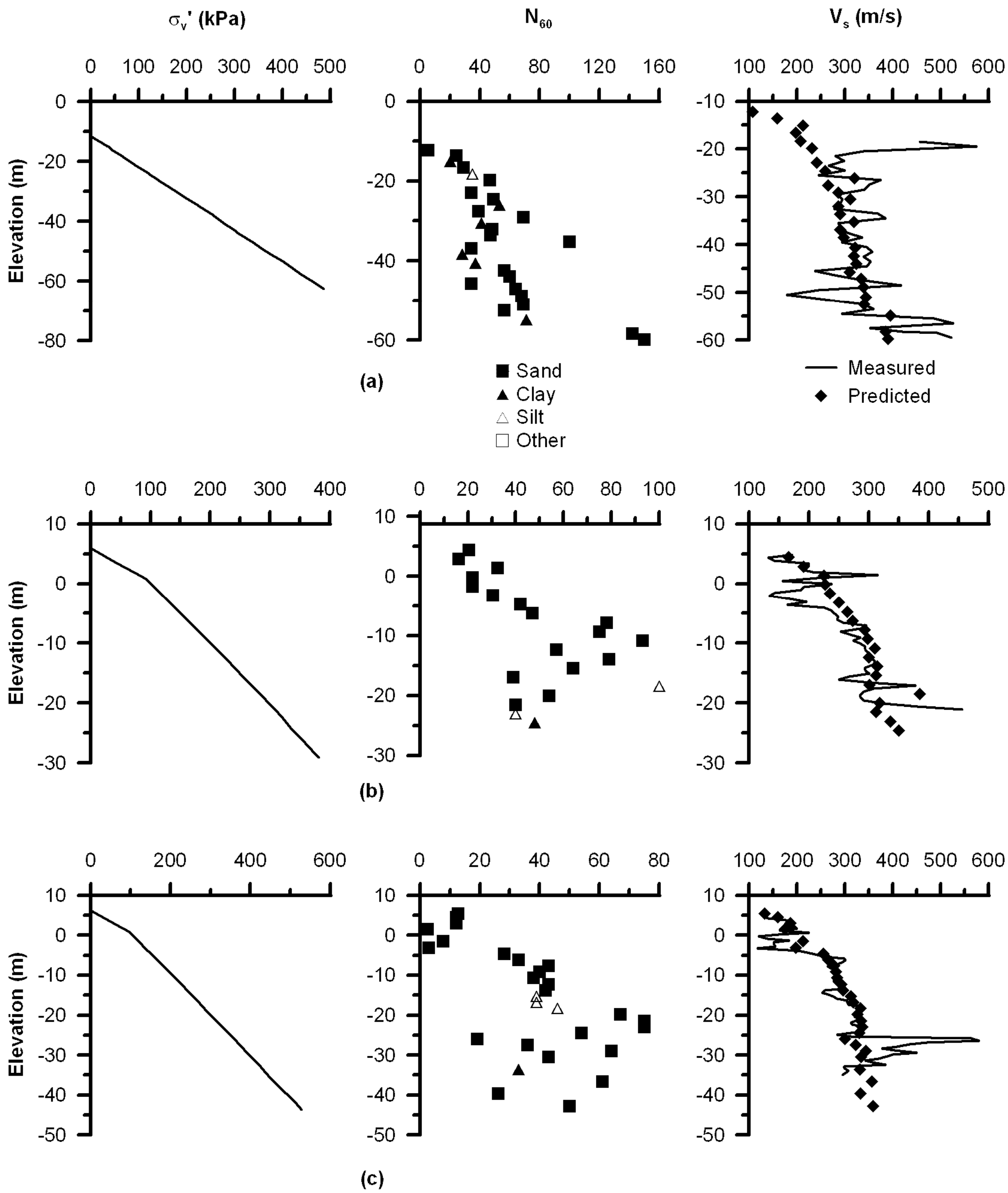

Fig. A.22 (a) Bridge no. 57-0857, boring no. 96-65 (b) Bridge no. 57-0857, boring no. 96-35 (Toll Plaza North West) (c) Bridge no. 57-0857, boring no. 96-34 (Toll Plaza South East).

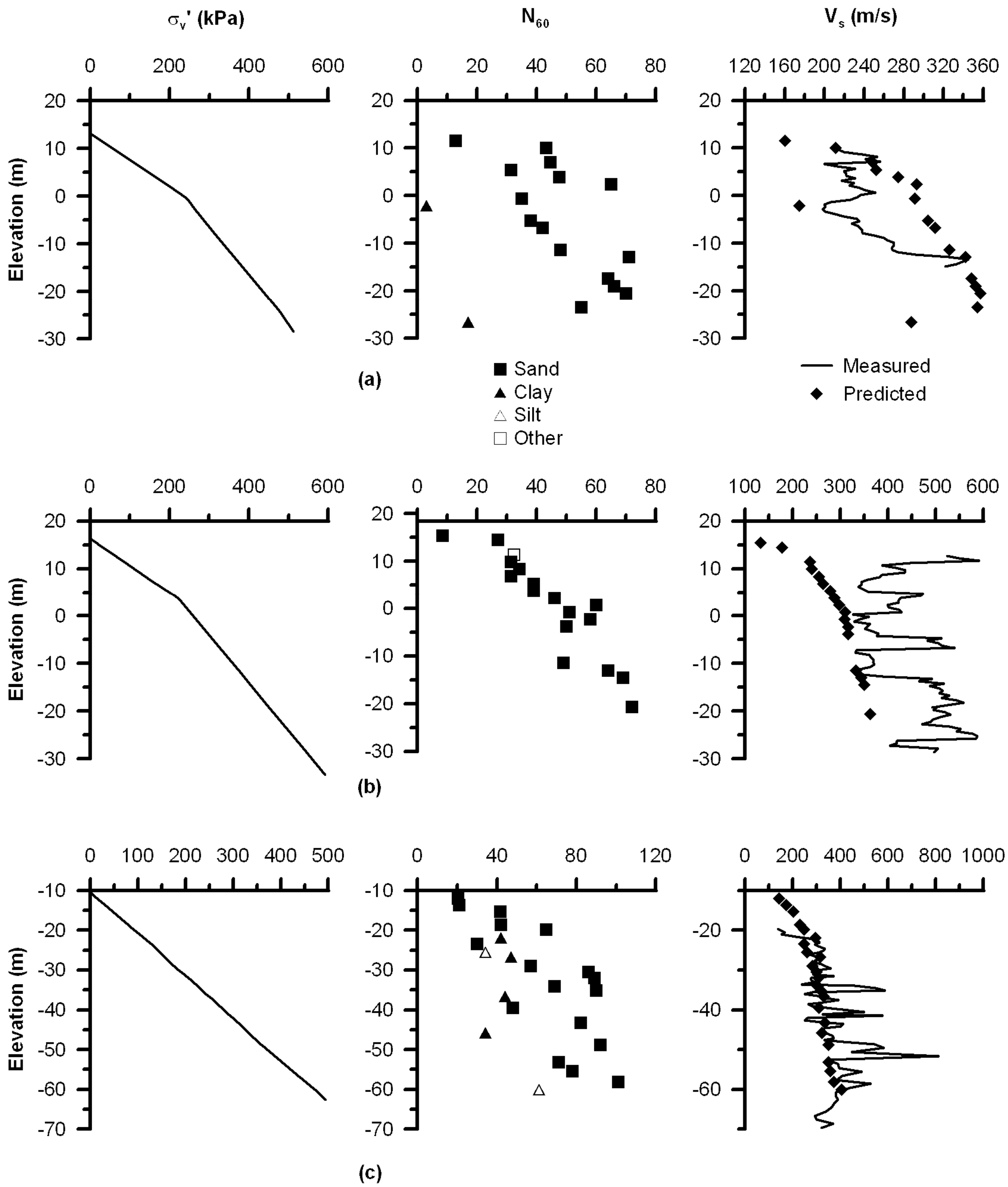

Fig. A.23 (a) Bridge no. 57-0857, boring no. 96-21 (b) Bridge no. 57-0857, boring no. 96-28 (c) Bridge no. 57-0857, boring no. 96-60.

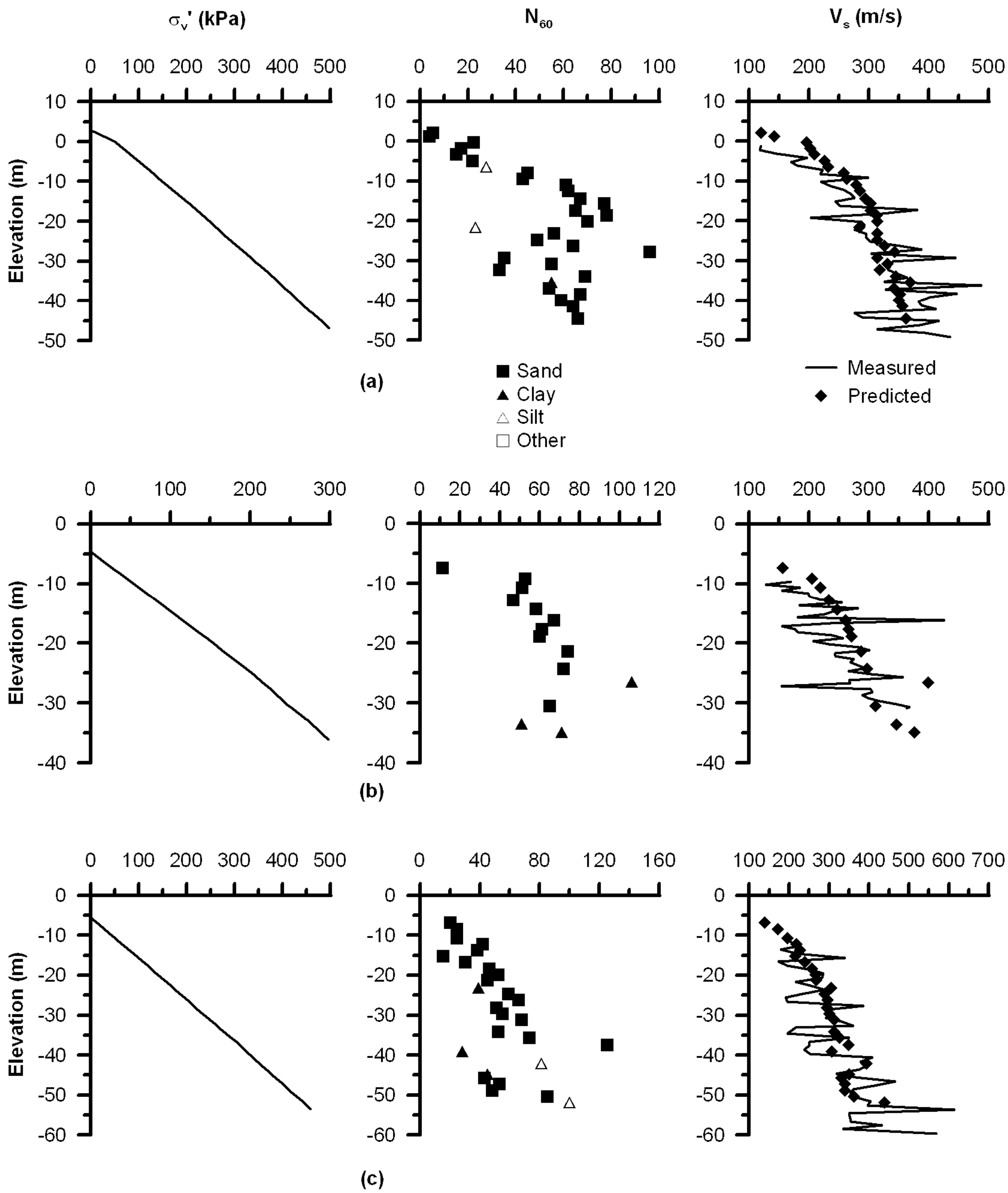

Fig. A.24 (a) Bridge no. 57-0857, boring no. 96-68R (b) Bridge no. 57-0857, boring no. 96-56 (c) Bridge no. 57-0857, boring no. 96-67.

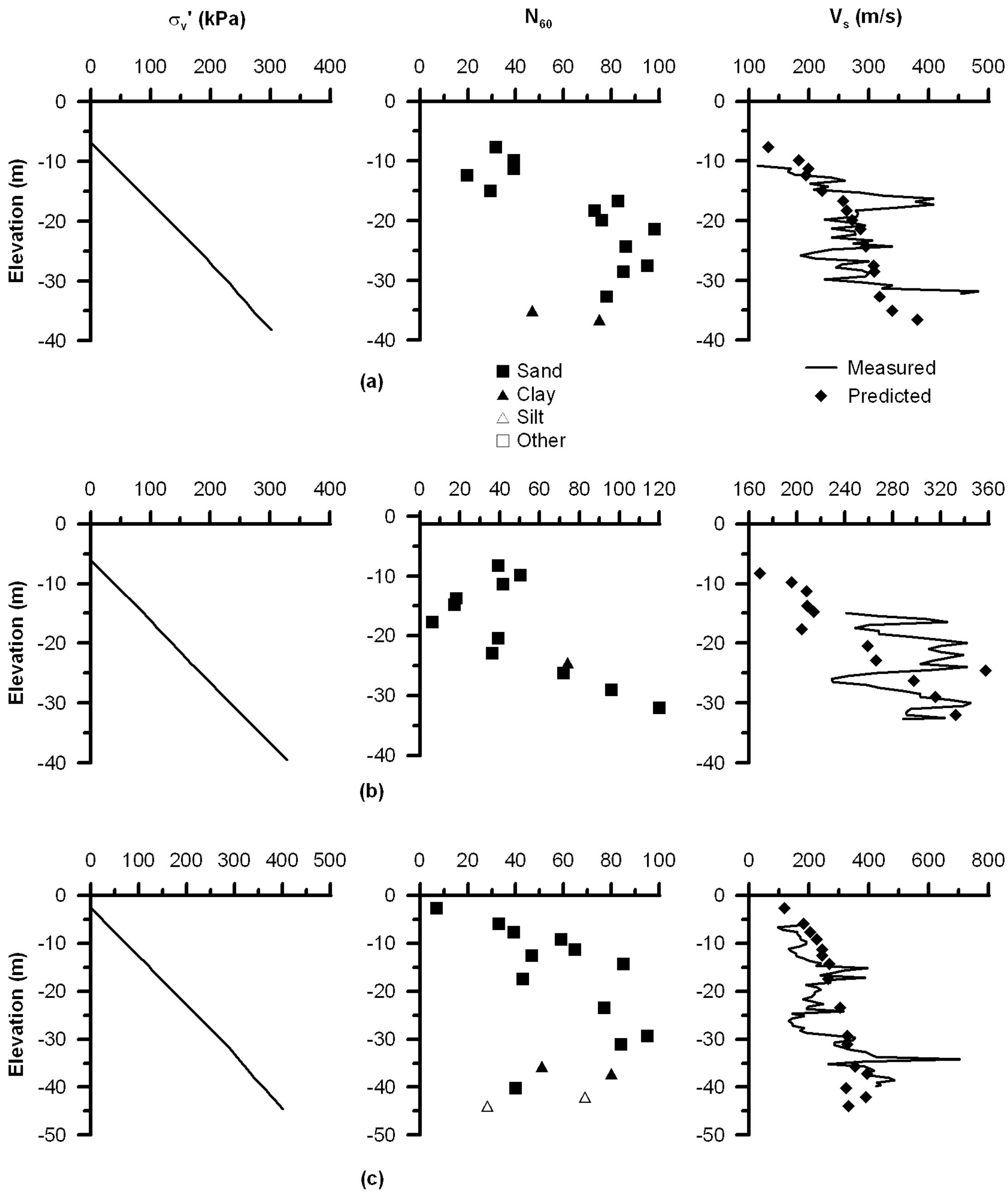

Fig. A.25 (a) Bridge no. 57-0857, boring no. 96-54 (b) Bridge no. 57-0857, boring no. 96-55 (c) Bridge no. 57-0857, boring no. 96-59.

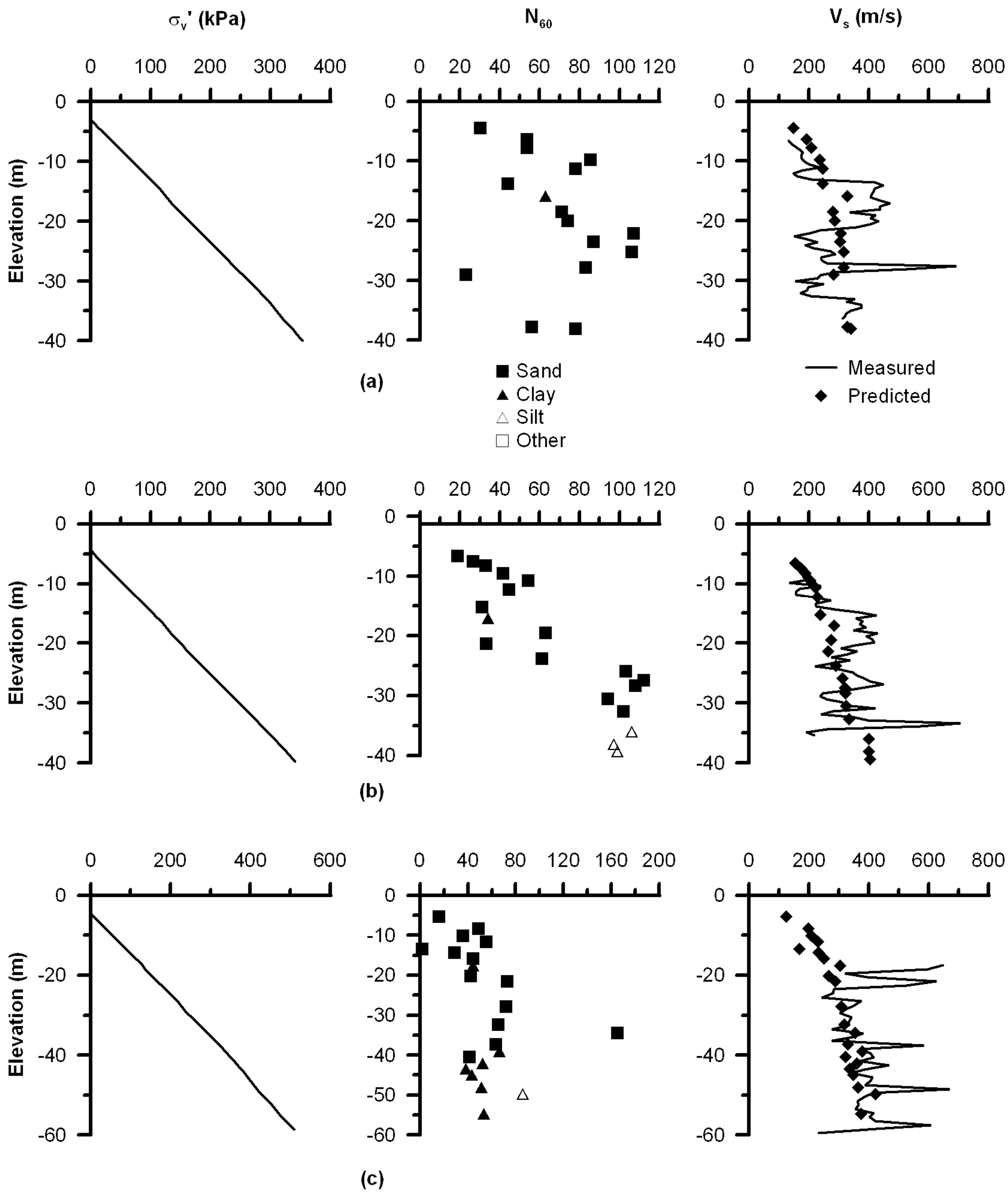

Fig. A.26 (a) Bridge no. 57-0857, boring no. 96-58 (b) Bridge no. 57-0857, boring no. 96-57 (c) Bridge no. 57-0857, boring no. 96-64.

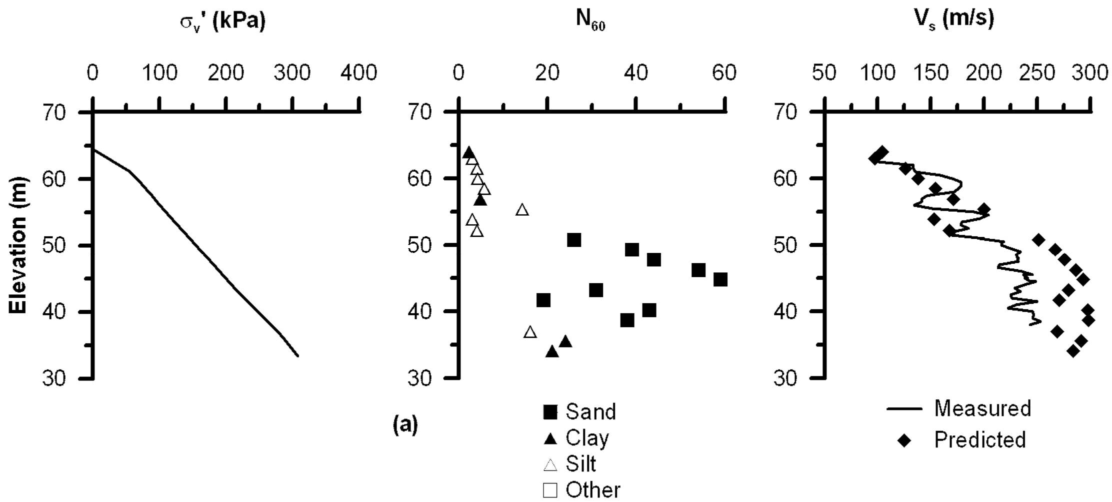

Fig. A.27 (a) Bridge no. 58-0335RL, boring no. B5-01.

PEER REPORTS

PEER reports are available individually or by yearly subscription. PEER reports can be ordered at http://peer.berkeley.edu/publications/peer_reports.html or by contacting the Pacific Earthquake Engineering Research Center, 1301 South 46th Street, Richmond, CA 94804-4698. Tel.: (510) 665-3448; Fax: (510) 665-3456; Email: peer_editor@berkeley.edu

PEER 2010/03 *Shear Wave Velocity as a Statistical Function of Standard Penetration Test Resistance and Vertical Effective Stress at Caltrans Bridge Sites.* Scott J. Brandenberg, Naresh Bellana, and Thomas Shantz. June 2010.

PEER 2010/02 *Stochastic Modeling and Simulation of Ground Motions for Performance-Based Earthquake Engineering.* Sanaz Rezaeian and Armen Der Kiureghian. June 2010.

PEER 2010/01 *Structural Response and Cost Characterization of Bridge Construction Using Seismic Performance Enhancement Strategies.* Ady Aviram, Božidar Stojadinović, Gustavo J. Parra-Montesinos, and Kevin R. Mackie. March 2010.

PEER 2009/03 *The Integration of Experimental and Simulation Data in the Study of Reinforced Concrete Bridge Systems Including Soil-Foundation-Structure Interaction.* Matthew Dryden and Gregory L. Fenves. November 2009.

PEER 2009/02 *Improving Earthquake Mitigation through Innovations and Applications in Seismic Science, Engineering, Communication, and Response. Proceedings of a U.S.-Iran Seismic Workshop.* October 2009.

PEER 2009/01 *Evaluation of Ground Motion Selection and Modification Methods: Predicting Median Interstory Drift Response of Buildings.* Curt B. Haselton, Ed. June 2009.

PEER 2008/10 *Technical Manual for Strata.* Albert R. Kottke and Ellen M. Rathje. February 2009.

PEER 2008/09 *NGA Model for Average Horizontal Component of Peak Ground Motion and Response Spectra.* Brian S.-J. Chiou and Robert R. Youngs. November 2008.

PEER 2008/08 *Toward Earthquake-Resistant Design of Concentrically Braced Steel Structures.* Patxi Uriz and Stephen A. Mahin. November 2008.

PEER 2008/07 *Using OpenSees for Performance-Based Evaluation of Bridges on Liquefiable Soils.* Stephen L. Kramer, Pedro Arduino, and HyungSuk Shin. November 2008.

PEER 2008/06 *Shaking Table Tests and Numerical Investigation of Self-Centering Reinforced Concrete Bridge Columns.* Hyung IL Jeong, Junichi Sakai, and Stephen A. Mahin. September 2008.

PEER 2008/05 *Performance-Based Earthquake Engineering Design Evaluation Procedure for Bridge Foundations Undergoing Liquefaction-Induced Lateral Ground Displacement.* Christian A. Ledezma and Jonathan D. Bray. August 2008.

PEER 2008/04 *Benchmarking of Nonlinear Geotechnical Ground Response Analysis Procedures.* Jonathan P. Stewart, Annie On-Lei Kwok, Yousseff M. A. Hashash, Neven Matasovic, Robert Pyke, Zhiliang Wang, and Zhaohui Yang. August 2008.

PEER 2008/03 *Guidelines for Nonlinear Analysis of Bridge Structures in California.* Ady Aviram, Kevin R. Mackie, and Božidar Stojadinović. August 2008.

PEER 2008/02 *Treatment of Uncertainties in Seismic-Risk Analysis of Transportation Systems.* Evangelos Stergiou and Anne S. Kiremidjian. July 2008.

PEER 2008/01 *Seismic Performance Objectives for Tall Buildings.* William T. Holmes, Charles Kircher, William Petak, and Nabih Youssef. August 2008.

PEER 2007/12 *An Assessment to Benchmark the Seismic Performance of a Code-Conforming Reinforced Concrete Moment-Frame Building.* Curt Haselton, Christine A. Goulet, Judith Mitrani-Reiser, James L. Beck, Gregory G. Deierlein, Keith A. Porter, Jonathan P. Stewart, and Ertugrul Taciroglu. August 2008.

PEER 2007/11 *Bar Buckling in Reinforced Concrete Bridge Columns.* Wayne A. Brown, Dawn E. Lehman, and John F. Stanton. February 2008.

PEER 2007/10 *Computational Modeling of Progressive Collapse in Reinforced Concrete Frame Structures.* Mohamed M. Talaat and Khalid M. Mosalam. May 2008.

PEER 2007/09 *Integrated Probabilistic Performance-Based Evaluation of Benchmark Reinforced Concrete Bridges.* Kevin R. Mackie, John-Michael Wong, and Božidar Stojadinović. January 2008.

PEER 2007/08 *Assessing Seismic Collapse Safety of Modern Reinforced Concrete Moment-Frame Buildings.* Curt B. Haselton and Gregory G. Deierlein. February 2008.

PEER 2007/07 *Performance Modeling Strategies for Modern Reinforced Concrete Bridge Columns.* Michael P. Berry and Marc O. Eberhard. April 2008.

PEER 2007/06 *Development of Improved Procedures for Seismic Design of Buried and Partially Buried Structures.* Linda Al Atik and Nicholas Sitar. June 2007.

PEER 2007/05 *Uncertainty and Correlation in Seismic Risk Assessment of Transportation Systems.* Renee G. Lee and Anne S. Kiremidjian. July 2007.

PEER 2007/04 *Numerical Models for Analysis and Performance-Based Design of Shallow Foundations Subjected to Seismic Loading.* Sivapalan Gajan, Tara C. Hutchinson, Bruce L. Kutter, Prishati Raychowdhury, José A. Ugalde, and Jonathan P. Stewart. May 2008.

PEER 2007/03 *Beam-Column Element Model Calibrated for Predicting Flexural Response Leading to Global Collapse of RC Frame Buildings.* Curt B. Haselton, Abbie B. Liel, Sarah Taylor Lange, and Gregory G. Deierlein. May 2008.

PEER 2007/02 *Campbell-Bozorgnia NGA Ground Motion Relations for the Geometric Mean Horizontal Component of Peak and Spectral Ground Motion Parameters.* Kenneth W. Campbell and Yousef Bozorgnia. May 2007.

PEER 2007/01 *Boore-Atkinson NGA Ground Motion Relations for the Geometric Mean Horizontal Component of Peak and Spectral Ground Motion Parameters.* David M. Boore and Gail M. Atkinson. May. May 2007.

PEER 2006/12 *Societal Implications of Performance-Based Earthquake Engineering.* Peter J. May. May 2007.

PEER 2006/11 *Probabilistic Seismic Demand Analysis Using Advanced Ground Motion Intensity Measures, Attenuation Relationships, and Near-Fault Effects.* Polsak Tothong and C. Allin Cornell. March 2007.

PEER 2006/10 *Application of the PEER PBEE Methodology to the I-880 Viaduct.* Sashi Kunnath. February 2007.

PEER 2006/09 *Quantifying Economic Losses from Travel Forgone Following a Large Metropolitan Earthquake.* James Moore, Sungbin Cho, Yue Yue Fan, and Stuart Werner. November 2006.

PEER 2006/08 *Vector-Valued Ground Motion Intensity Measures for Probabilistic Seismic Demand Analysis*. Jack W. Baker and C. Allin Cornell. October 2006.

PEER 2006/07 *Analytical Modeling of Reinforced Concrete Walls for Predicting Flexural and Coupled–Shear-Flexural Responses.* Kutay Orakcal, Leonardo M. Massone, and John W. Wallace. October 2006.

PEER 2006/06 *Nonlinear Analysis of a Soil-Drilled Pier System under Static and Dynamic Axial Loading.* Gang Wang and Nicholas Sitar. November 2006.

PEER 2006/05 *Advanced Seismic Assessment Guidelines.* Paolo Bazzurro, C. Allin Cornell, Charles Menun, Maziar Motahari, and Nicolas Luco. September 2006.

PEER 2006/04 *Probabilistic Seismic Evaluation of Reinforced Concrete Structural Components and Systems.* Tae Hyung Lee and Khalid M. Mosalam. August 2006.

PEER 2006/03 *Performance of Lifelines Subjected to Lateral Spreading.* Scott A. Ashford and Teerawut Juirnarongrit. July 2006.

PEER 2006/02 *Pacific Earthquake Engineering Research Center Highway Demonstration Project.* Anne Kiremidjian, James Moore, Yue Yue Fan, Nesrin Basoz, Ozgur Yazali, and Meredith Williams. April 2006.

PEER 2006/01 *Bracing Berkeley. A Guide to Seismic Safety on the UC Berkeley Campus.* Mary C. Comerio, Stephen Tobriner, and Ariane Fehrenkamp. January 2006.

PEER 2005/16 *Seismic Response and Reliability of Electrical Substation Equipment and Systems.* Junho Song, Armen Der Kiureghian, and Jerome L. Sackman. April 2006.

PEER 2005/15 *CPT-Based Probabilistic Assessment of Seismic Soil Liquefaction Initiation.* R. E. S. Moss, R. B. Seed, R. E. Kayen, J. P. Stewart, and A. Der Kiureghian. April 2006.

PEER 2005/14 *Workshop on Modeling of Nonlinear Cyclic Load-Deformation Behavior of Shallow Foundations.* Bruce L. Kutter, Geoffrey Martin, Tara Hutchinson, Chad Harden, Sivapalan Gajan, and Justin Phalen. March 2006.

PEER 2005/13 *Stochastic Characterization and Decision Bases under Time-Dependent Aftershock Risk in Performance-Based Earthquake Engineering.* Gee Liek Yeo and C. Allin Cornell. July 2005.

PEER 2005/12 *PEER Testbed Study on a Laboratory Building: Exercising Seismic Performance Assessment.* Mary C. Comerio, editor. November 2005.

PEER 2005/11 *Van Nuys Hotel Building Testbed Report: Exercising Seismic Performance Assessment.* Helmut Krawinkler, editor. October 2005.

PEER 2005/10 *First NEES/E-Defense Workshop on Collapse Simulation of Reinforced Concrete Building Structures.* September 2005.

PEER 2005/09 *Test Applications of Advanced Seismic Assessment Guidelines.* Joe Maffei, Karl Telleen, Danya Mohr, William Holmes, and Yuki Nakayama. August 2006.

PEER 2005/08 *Damage Accumulation in Lightly Confined Reinforced Concrete Bridge Columns.* R. Tyler Ranf, Jared M. Nelson, Zach Price, Marc O. Eberhard, and John F. Stanton. April 2006.

PEER 2005/07 *Experimental and Analytical Studies on the Seismic Response of Freestanding and Anchored Laboratory Equipment.* Dimitrios Konstantinidis and Nicos Makris. January 2005.

PEER 2005/06 *Global Collapse of Frame Structures under Seismic Excitations*. Luis F. Ibarra and Helmut Krawinkler. September 2005.

PEER 2005//05 *Performance Characterization of Bench- and Shelf-Mounted Equipment.* Samit Ray Chaudhuri and Tara C. Hutchinson. May 2006.

PEER 2005/04 *Numerical Modeling of the Nonlinear Cyclic Response of Shallow Foundations.* Chad Harden, Tara Hutchinson, Geoffrey R. Martin, and Bruce L. Kutter. August 2005.

PEER 2005/03 *A Taxonomy of Building Components for Performance-Based Earthquake Engineering.* Keith A. Porter. September 2005.

PEER 2005/02 *Fragility Basis for California Highway Overpass Bridge Seismic Decision Making*. Kevin R. Mackie and Božidar Stojadinović. June 2005.

PEER 2005/01 *Empirical Characterization of Site Conditions on Strong Ground Motion.* Jonathan P. Stewart, Yoojoong Choi, and Robert W. Graves. June 2005.

PEER 2004/09 *Electrical Substation Equipment Interaction: Experimental Rigid Conductor Studies.* Christopher Stearns and André Filiatrault. February 2005.

PEER 2004/08 *Seismic Qualification and Fragility Testing of Line Break 550-kV Disconnect Switches.* Shakhzod M. Takhirov, Gregory L. Fenves, and Eric Fujisaki. January 2005.

PEER 2004/07 *Ground Motions for Earthquake Simulator Qualification of Electrical Substation Equipment.* Shakhzod M. Takhirov, Gregory L. Fenves, Eric Fujisaki, and Don Clyde. January 2005.

PEER 2004/06 *Performance-Based Regulation and Regulatory Regimes.* Peter J. May and Chris Koski. September 2004.

PEER 2004/05 *Performance-Based Seismic Design Concepts and Implementation: Proceedings of an International Workshop.* Peter Fajfar and Helmut Krawinkler, editors. September 2004.

PEER 2004/04 *Seismic Performance of an Instrumented Tilt-up Wall Building.* James C. Anderson and Vitelmo V. Bertero. July 2004.

PEER 2004/03 *Evaluation and Application of Concrete Tilt-up Assessment Methodologies.* Timothy Graf and James O. Malley. October 2004.

PEER 2004/02 *Analytical Investigations of New Methods for Reducing Residual Displacements of Reinforced Concrete Bridge Columns.* Junichi Sakai and Stephen A. Mahin. August 2004.

PEER 2004/01 *Seismic Performance of Masonry Buildings and Design Implications.* Kerri Anne Taeko Tokoro, James C. Anderson, and Vitelmo V. Bertero. February 2004.

PEER 2003/18 *Performance Models for Flexural Damage in Reinforced Concrete Columns.* Michael Berry and Marc Eberhard. August 2003.

PEER 2003/17 *Predicting Earthquake Damage in Older Reinforced Concrete Beam-Column Joints.* Catherine Pagni and Laura Lowes. October 2004.

PEER 2003/16 *Seismic Demands for Performance-Based Design of Bridges.* Kevin Mackie and Božidar Stojadinović. August 2003.

PEER 2003/15 *Seismic Demands for Nondeteriorating Frame Structures and Their Dependence on Ground Motions.* Ricardo Antonio Medina and Helmut Krawinkler. May 2004.

PEER 2003/14 *Finite Element Reliability and Sensitivity Methods for Performance-Based Earthquake Engineering.* Terje Haukaas and Armen Der Kiureghian. April 2004.

PEER 2003/13 *Effects of Connection Hysteretic Degradation on the Seismic Behavior of Steel Moment-Resisting Frames.* Janise E. Rodgers and Stephen A. Mahin. March 2004.

PEER 2003/12 *Implementation Manual for the Seismic Protection of Laboratory Contents: Format and Case Studies.* William T. Holmes and Mary C. Comerio. October 2003.

PEER 2003/11 *Fifth U.S.-Japan Workshop on Performance-Based Earthquake Engineering Methodology for Reinforced Concrete Building Structures.* February 2004.

PEER 2003/10 *A Beam-Column Joint Model for Simulating the Earthquake Response of Reinforced Concrete Frames.* Laura N. Lowes, Nilanjan Mitra, and Arash Altoontash. February 2004.

PEER 2003/09 *Sequencing Repairs after an Earthquake: An Economic Approach.* Marco Casari and Simon J. Wilkie. April 2004.

PEER 2003/08 *A Technical Framework for Probability-Based Demand and Capacity Factor Design (DCFD) Seismic Formats.* Fatemeh Jalayer and C. Allin Cornell. November 2003.

PEER 2003/07 *Uncertainty Specification and Propagation for Loss Estimation Using FOSM Methods.* Jack W. Baker and C. Allin Cornell. September 2003.

PEER 2003/06 *Performance of Circular Reinforced Concrete Bridge Columns under Bidirectional Earthquake Loading*. Mahmoud M. Hachem, Stephen A. Mahin, and Jack P. Moehle. February 2003.

PEER 2003/05 *Response Assessment for Building-Specific Loss Estimation.* Eduardo Miranda and Shahram Taghavi. September 2003.

PEER 2003/04 *Experimental Assessment of Columns with Short Lap Splices Subjected to Cyclic Loads*. Murat Melek, John W. Wallace, and Joel Conte. April 2003.

PEER 2003/03 *Probabilistic Response Assessment for Building-Specific Loss Estimation.* Eduardo Miranda and Hesameddin Aslani. September 2003.

PEER 2003/02 *Software Framework for Collaborative Development of Nonlinear Dynamic Analysis Program.* Jun Peng and Kincho H. Law. September 2003.

PEER 2003/01 *Shake Table Tests and Analytical Studies on the Gravity Load Collapse of Reinforced Concrete Frames.* Kenneth John Elwood and Jack P. Moehle. November 2003.

PEER 2002/24 *Performance of Beam to Column Bridge Joints Subjected to a Large Velocity Pulse.* Natalie Gibson, André Filiatrault, and Scott A. Ashford. April 2002.

PEER 2002/23 *Effects of Large Velocity Pulses on Reinforced Concrete Bridge Columns.* Greg L. Orozco and Scott A. Ashford. April 2002.

PEER 2002/22 *Characterization of Large Velocity Pulses for Laboratory Testing.* Kenneth E. Cox and Scott A. Ashford. April 2002.

PEER 2002/21 *Fourth U.S.-Japan Workshop on Performance-Based Earthquake Engineering Methodology for Reinforced Concrete Building Structures*. December 2002.

PEER 2002/20 *Barriers to Adoption and Implementation of PBEE Innovations.* Peter J. May. August 2002.

PEER 2002/19 *Economic-Engineered Integrated Models for Earthquakes: Socioeconomic Impacts.* Peter Gordon, James E. Moore II, and Harry W. Richardson. July 2002.

PEER 2002/18 *Assessment of Reinforced Concrete Building Exterior Joints with Substandard Details.* Chris P. Pantelides, Jon Hansen, Justin Nadauld, and Lawrence D. Reaveley. May 2002.

PEER 2002/17 *Structural Characterization and Seismic Response Analysis of a Highway Overcrossing Equipped with Elastomeric Bearings and Fluid Dampers: A Case Study.* Nicos Makris and Jian Zhang. November 2002.

PEER 2002/16 *Estimation of Uncertainty in Geotechnical Properties for Performance-Based Earthquake Engineering.* Allen L. Jones, Steven L. Kramer, and Pedro Arduino. December 2002.

PEER 2002/15 *Seismic Behavior of Bridge Columns Subjected to Various Loading Patterns.* Asadollah Esmaeily-Gh. and Yan Xiao. December 2002.

PEER 2002/14 *Inelastic Seismic Response of Extended Pile Shaft Supported Bridge Structures.* T.C. Hutchinson, R.W. Boulanger, Y.H. Chai, and I.M. Idriss. December 2002.

PEER 2002/13 *Probabilistic Models and Fragility Estimates for Bridge Components and Systems.* Paolo Gardoni, Armen Der Kiureghian, and Khalid M. Mosalam. June 2002.

PEER 2002/12 *Effects of Fault Dip and Slip Rake on Near-Source Ground Motions: Why Chi-Chi Was a Relatively Mild M7.6 Earthquake.* Brad T. Aagaard, John F. Hall, and Thomas H. Heaton. December 2002.

PEER 2002/11 *Analytical and Experimental Study of Fiber-Reinforced Strip Isolators*. James M. Kelly and Shakhzod M. Takhirov. September 2002.

PEER 2002/10 *Centrifuge Modeling of Settlement and Lateral Spreading with Comparisons to Numerical Analyses***.** Sivapalan Gajan and Bruce L. Kutter. January 2003.

PEER 2002/09 *Documentation and Analysis of Field Case Histories of Seismic Compression during the 1994 Northridge, California, Earthquake.* Jonathan P. Stewart, Patrick M. Smith, Daniel H. Whang, and Jonathan D. Bray. October 2002.

PEER 2002/08 *Component Testing, Stability Analysis and Characterization of Buckling-Restrained Unbonded Braces™.* Cameron Black, Nicos Makris, and Ian Aiken. September 2002.

PEER 2002/07 *Seismic Performance of Pile-Wharf Connections.* Charles W. Roeder, Robert Graff, Jennifer Soderstrom, and Jun Han Yoo. December 2001.

PEER 2002/06 *The Use of Benefit-Cost Analysis for Evaluation of Performance-Based Earthquake Engineering Decisions*. Richard O. Zerbe and Anthony Falit-Baiamonte. September 2001.

PEER 2002/05 *Guidelines, Specifications, and Seismic Performance Characterization of Nonstructural Building Components and Equipment*. André Filiatrault, Constantin Christopoulos, and Christopher Stearns. September 2001.

PEER 2002/04 *Consortium of Organizations for Strong-Motion Observation Systems and the Pacific Earthquake Engineering Research Center Lifelines Program: Invited Workshop on Archiving and Web Dissemination of Geotechnical Data, 4–5 October 2001*. September 2002.

PEER 2002/03 *Investigation of Sensitivity of Building Loss Estimates to Major Uncertain Variables for the Van Nuys Testbed.* Keith A. Porter, James L. Beck, and Rustem V. Shaikhutdinov. August 2002.

PEER 2002/02 *The Third U.S.-Japan Workshop on Performance-Based Earthquake Engineering Methodology for Reinforced Concrete Building Structures*. July 2002.

PEER 2002/01 *Nonstructural Loss Estimation: The UC Berkeley Case Study.* Mary C. Comerio and John C. Stallmeyer. December 2001.

PEER 2001/16 *Statistics of SDF-System Estimate of Roof Displacement for Pushover Analysis of Buildings.* Anil K. Chopra, Rakesh K. Goel, and Chatpan Chintanapakdee. December 2001.

PEER 2001/15 *Damage to Bridges during the 2001 Nisqually Earthquake.* R. Tyler Ranf, Marc O. Eberhard, and Michael P. Berry. November 2001.

PEER 2001/14 *Rocking Response of Equipment Anchored to a Base Foundation.* Nicos Makris and Cameron J. Black. September 2001.

PEER 2001/13 *Modeling Soil Liquefaction Hazards for Performance-Based Earthquake Engineering.* Steven L. Kramer and Ahmed-W. Elgamal. February 2001.

PEER 2001/12 *Development of Geotechnical Capabilities in OpenSees.* Boris Jeremi . September 2001.

PEER 2001/11 *Analytical and Experimental Study of Fiber-Reinforced Elastomeric Isolators*. James M. Kelly and Shakhzod M. Takhirov. September 2001.

PEER 2001/10 *Amplification Factors for Spectral Acceleration in Active Regions.* Jonathan P. Stewart, Andrew H. Liu, Yoojoong Choi, and Mehmet B. Baturay. December 2001.

PEER 2001/09 *Ground Motion Evaluation Procedures for Performance-Based Design.* Jonathan P. Stewart, Shyh-Jeng Chiou, Jonathan D. Bray, Robert W. Graves, Paul G. Somerville, and Norman A. Abrahamson. September 2001.

PEER 2001/08 *Experimental and Computational Evaluation of Reinforced Concrete Bridge Beam-Column Connections for Seismic Performance*. Clay J. Naito, Jack P. Moehle, and Khalid M. Mosalam. November 2001.

PEER 2001/07 *The Rocking Spectrum and the Shortcomings of Design Guidelines.* Nicos Makris and Dimitrios Konstantinidis. August 2001.

PEER 2001/06 *Development of an Electrical Substation Equipment Performance Database for Evaluation of Equipment Fragilities.* Thalia Agnanos. April 1999.

PEER 2001/05 *Stiffness Analysis of Fiber-Reinforced Elastomeric Isolators.* Hsiang-Chuan Tsai and James M. Kelly. May 2001.

PEER 2001/04 *Organizational and Societal Considerations for Performance-Based Earthquake Engineering.* Peter J. May. April 2001.

PEER 2001/03 *A Modal Pushover Analysis Procedure to Estimate Seismic Demands for Buildings: Theory and Preliminary Evaluation.* Anil K. Chopra and Rakesh K. Goel. January 2001.

PEER 2001/02 *Seismic Response Analysis of Highway Overcrossings Including Soil-Structure Interaction.* Jian Zhang and Nicos Makris. March 2001.

PEER 2001/01 *Experimental Study of Large Seismic Steel Beam-to-Column Connections.* Egor P. Popov and Shakhzod M. Takhirov. November 2000.

PEER 2000/10 *The Second U.S.-Japan Workshop on Performance-Based Earthquake Engineering Methodology for Reinforced Concrete Building Structures.* March 2000.

PEER 2000/09 *Structural Engineering Reconnaissance of the August 17, 1999 Earthquake: Kocaeli (Izmit), Turkey.* Halil Sezen, Kenneth J. Elwood, Andrew S. Whittaker, Khalid Mosalam, John J. Wallace, and John F. Stanton. December 2000.

PEER 2000/08 *Behavior of Reinforced Concrete Bridge Columns Having Varying Aspect Ratios and Varying Lengths of Confinement.* Anthony J. Calderone, Dawn E. Lehman, and Jack P. Moehle. January 2001.

PEER 2000/07 *Cover-Plate and Flange-Plate Reinforced Steel Moment-Resisting Connections.* Taejin Kim, Andrew S. Whittaker, Amir S. Gilani, Vitelmo V. Bertero, and Shakhzod M. Takhirov. September 2000.

PEER 2000/06 *Seismic Evaluation and Analysis of 230-kV Disconnect Switches.* Amir S. J. Gilani, Andrew S. Whittaker, Gregory L. Fenves, Chun-Hao Chen, Henry Ho, and Eric Fujisaki. July 2000.

PEER 2000/05 *Performance-Based Evaluation of Exterior Reinforced Concrete Building Joints for Seismic Excitation.* Chandra Clyde, Chris P. Pantelides, and Lawrence D. Reaveley. July 2000.

PEER 2000/04 *An Evaluation of Seismic Energy Demand: An Attenuation Approach.* Chung-Che Chou and Chia-Ming Uang. July 1999.

PEER 2000/03 *Framing Earthquake Retrofitting Decisions: The Case of Hillside Homes in Los Angeles.* Detlof von Winterfeldt, Nels Roselund, and Alicia Kitsuse. March 2000.

PEER 2000/02 *U.S.-Japan Workshop on the Effects of Near-Field Earthquake Shaking.* Andrew Whittaker, ed. July 2000.

PEER 2000/01 *Further Studies on Seismic Interaction in Interconnected Electrical Substation Equipment.* Armen Der Kiureghian, Kee-Jeung Hong, and Jerome L. Sackman. November 1999.

PEER 1999/14 *Seismic Evaluation and Retrofit of 230-kV Porcelain Transformer Bushings*. Amir S. Gilani, Andrew S. Whittaker, Gregory L. Fenves, and Eric Fujisaki. December 1999.

PEER 1999/13 *Building Vulnerability Studies: Modeling and Evaluation of Tilt-up and Steel Reinforced Concrete Buildings.* John W. Wallace, Jonathan P. Stewart, and Andrew S. Whittaker, editors. December 1999.

PEER 1999/12 *Rehabilitation of Nonductile RC Frame Building Using Encasement Plates and Energy-Dissipating Devices.* Mehrdad Sasani, Vitelmo V. Bertero, James C. Anderson. December 1999.

PEER 1999/11 *Performance Evaluation Database for Concrete Bridge Components and Systems under Simulated Seismic Loads.* Yael D. Hose and Frieder Seible. November 1999.

PEER 1999/10 *U.S.-Japan Workshop on Performance-Based Earthquake Engineering Methodology for Reinforced Concrete Building Structures.* December 1999.

PEER 1999/09 *Performance Improvement of Long Period Building Structures Subjected to Severe Pulse-Type Ground Motions*. James C. Anderson, Vitelmo V. Bertero, and Raul Bertero. October 1999.

PEER 1999/08 *Envelopes for Seismic Response Vectors.* Charles Menun and Armen Der Kiureghian. July 1999.

PEER 1999/07 *Documentation of Strengths and Weaknesses of Current Computer Analysis Methods for Seismic Performance of Reinforced Concrete Members.* William F. Cofer. November 1999.

PEER 1999/06 *Rocking Response and Overturning of Anchored Equipment under Seismic Excitations.* Nicos Makris and Jian Zhang. November 1999.

PEER 1999/05 *Seismic Evaluation of 550 kV Porcelain Transformer Bushings.* Amir S. Gilani, Andrew S. Whittaker, Gregory L. Fenves, and Eric Fujisaki. October 1999.

PEER 1999/04 *Adoption and Enforcement of Earthquake Risk-Reduction Measures.* Peter J. May, Raymond J. Burby, T. Jens Feeley, and Robert Wood.

PEER 1999/03 *Task 3 Characterization of Site Response General Site Categories*. Adrian Rodriguez-Marek, Jonathan D. Bray, and Norman Abrahamson. February 1999.

PEER 1999/02 *Capacity-Demand-Diagram Methods for Estimating Seismic Deformation of Inelastic Structures: SDF Systems*. Anil K. Chopra and Rakesh Goel. April 1999.

PEER 1999/01 *Interaction in Interconnected Electrical Substation Equipment Subjected to Earthquake Ground Motions.* Armen Der Kiureghian, Jerome L. Sackman, and Kee-Jeung Hong. February 1999.

PEER 1998/08 *Behavior and Failure Analysis of a Multiple-Frame Highway Bridge in the 1994 Northridge Earthquake.* Gregory L. Fenves and Michael Ellery. December 1998.

PEER 1998/07 *Empirical Evaluation of Inertial Soil-Structure Interaction Effects.* Jonathan P. Stewart, Raymond B. Seed, and Gregory L. Fenves. November 1998.

PEER 1998/06 *Effect of Damping Mechanisms on the Response of Seismic Isolated Structures.* Nicos Makris and Shih-Po Chang. November 1998.

PEER 1998/05 *Rocking Response and Overturning of Equipment under Horizontal Pulse-Type Motions.* Nicos Makris and Yiannis Roussos. October 1998.

PEER 1998/04 *Pacific Earthquake Engineering Research Invitational Workshop Proceedings, May 14–15, 1998: Defining the Links between Planning, Policy Analysis, Economics and Earthquake Engineering.* Mary Comerio and Peter Gordon. September 1998.

PEER 1998/03 *Repair/Upgrade Procedures for Welded Beam to Column Connections.* James C. Anderson and Xiaojing Duan. May 1998.

PEER 1998/02 *Seismic Evaluation of 196 kV Porcelain Transformer Bushings*. Amir S. Gilani, Juan W. Chavez, Gregory L. Fenves, and Andrew S. Whittaker. May 1998.

PEER 1998/01 *Seismic Performance of Well-Confined Concrete Bridge Columns.* Dawn E. Lehman and Jack P. Moehle. December 2000.

ONLINE REPORTS

The following PEER reports are available by Internet only at http://peer.berkeley.edu/publications/peer_reports.html

PEER 2010/106 *Verification of Probabilistic Seismic Hazard Analysis Computer Programs.* Patricia Thomas, Ivan Wong, and Norman Abrahamson. May 2010.

PEER 2010/105 *Structural Engineering Reconnaissance of the April 6, 2009, Abruzzo, Italy, Earthquake, and Lessons Learned.* M. Selim Günay and Khalid M. Mosalam. April 2010.

PEER 2010/104 *Simulating the Inelastic Seismic Behavior of Steel Braced Frames, Including the Effects of Low-Cycle Fatigue.* Yuli Huang and Stephen A. Mahin. April 2010.

PEER 2010/103 *Post-Earthquake Traffic Capacity of Modern Bridges in California.* Vesna Terzic and Božidar Stojadinović. March 2010.

PEER 2010/102 *Analysis of Cumulative Absolute Velocity (CAV) and JMA Instrumental Seismic Intensity (I_{JMA}) Using the PEER–NGA Strong Motion Database.* Kenneth W. Campbell and Yousef Bozorgnia. February 2010.

PEER 2010/101 *Rocking Response of Bridges on Shallow Foundations.* Jose A. Ugalde, Bruce L. Kutter, Boris Jeremic

PEER 2009/109 *Simulation and Performance-Based Earthquake Engineering Assessment of Self-Centering Post-Tensioned Concrete Bridge Systems.* Won K. Lee and Sarah L. Billington. December 2009.

PEER 2009/108 *PEER Lifelines Geotechnical Virtual Data Center.* J. Carl Stepp, Daniel J. Ponti, Loren L. Turner, Jennifer N. Swift, Sean Devlin, Yang Zhu, Jean Benoit, and John Bobbitt. September 2009.

PEER 2009/107 *Experimental and Computational Evaluation of Current and Innovative In-Span Hinge Details in Reinforced Concrete Box-Girder Bridges: Part 2: Post-Test Analysis and Design Recommendations.* Matias A. Hube and Khalid M. Mosalam. December 2009.

PEER 2009/106 *Shear Strength Models of Exterior Beam-Column Joints without Transverse Reinforcement.* Sangjoon Park and Khalid M. Mosalam. November 2009.

PEER 2009/105 *Reduced Uncertainty of Ground Motion Prediction Equations through Bayesian Variance Analysis.* Robb Eric S. Moss. November 2009.

PEER 2009/104 *Advanced Implementation of Hybrid Simulation.* Andreas H. Schellenberg, Stephen A. Mahin, Gregory L. Fenves. November 2009.

PEER 2009/103 *Performance Evaluation of Innovative Steel Braced Frames.* T. Y. Yang, Jack P. Moehle, and Božidar Stojadinovic. August 2009.

PEER 2009/102 *Reinvestigation of Liquefaction and Nonliquefaction Case Histories from the 1976 Tangshan Earthquake.* Robb Eric Moss, Robert E. Kayen, Liyuan Tong, Songyu Liu, Guojun Cai, and Jiaer Wu. August 2009.

PEER 2009/101 *Report of the First Joint Planning Meeting for the Second Phase of NEES/E-Defense Collaborative Research on Earthquake Engineering.* Stephen A. Mahin et al. July 2009.

PEER 2008/104 *Experimental and Analytical Study of the Seismic Performance of Retaining Structures.* Linda Al Atik and Nicholas Sitar. January 2009.

PEER 2008/103 *Experimental and Computational Evaluation of Current and Innovative In-Span Hinge Details in Reinforced Concrete Box-Girder Bridges. Part 1: Experimental Findings and Pre-Test Analysis.* Matias A. Hube and Khalid M. Mosalam. January 2009.

PEER 2008/102 *Modeling of Unreinforced Masonry Infill Walls Considering In-Plane and Out-of-Plane Interaction.* Stephen Kadysiewski and Khalid M. Mosalam. January 2009.

PEER 2008/101 *Seismic Performance Objectives for Tall Buildings.* William T. Holmes, Charles Kircher, William Petak, and Nabih Youssef. August 2008.

PEER 2007/101 *Generalized Hybrid Simulation Framework for Structural Systems Subjected to Seismic Loading.* Tarek Elkhoraibi and Khalid M. Mosalam. July 2007.

PEER 2007/100 *Seismic Evaluation of Reinforced Concrete Buildings Including Effects of Masonry Infill Walls.* Alidad Hashemi and Khalid M. Mosalam. July 2007.